

Design and Control of a 6 DOF Biped Robot

By: Fuhai Gu

Supervised by: Dr. Xiaoping Liu

A THESIS SUBMITTED IN PARTIAL FULFILLMENT OF THE
REQUIREMENTS OF MScEng DEGREE IN CONTROL
ENGINEERING FACULTY OF ENGINEERING
LAKEHEAD UNIVERSITY
THUNDER BAY, ONTARIO

P7B 5E1

June, 2006



Library and
Archives Canada

Bibliothèque et
Archives Canada

Published Heritage
Branch

Direction du
Patrimoine de l'édition

395 Wellington Street
Ottawa ON K1A 0N4
Canada

395, rue Wellington
Ottawa ON K1A 0N4
Canada

Your file *Votre référence*
ISBN: 978-0-494-21511-1
Our file *Notre référence*
ISBN: 978-0-494-21511-1

NOTICE:

The author has granted a non-exclusive license allowing Library and Archives Canada to reproduce, publish, archive, preserve, conserve, communicate to the public by telecommunication or on the Internet, loan, distribute and sell theses worldwide, for commercial or non-commercial purposes, in microform, paper, electronic and/or any other formats.

The author retains copyright ownership and moral rights in this thesis. Neither the thesis nor substantial extracts from it may be printed or otherwise reproduced without the author's permission.

AVIS:

L'auteur a accordé une licence non exclusive permettant à la Bibliothèque et Archives Canada de reproduire, publier, archiver, sauvegarder, conserver, transmettre au public par télécommunication ou par l'Internet, prêter, distribuer et vendre des thèses partout dans le monde, à des fins commerciales ou autres, sur support microforme, papier, électronique et/ou autres formats.

L'auteur conserve la propriété du droit d'auteur et des droits moraux qui protègent cette thèse. Ni la thèse ni des extraits substantiels de celle-ci ne doivent être imprimés ou autrement reproduits sans son autorisation.

In compliance with the Canadian Privacy Act some supporting forms may have been removed from this thesis.

Conformément à la loi canadienne sur la protection de la vie privée, quelques formulaires secondaires ont été enlevés de cette thèse.

While these forms may be included in the document page count, their removal does not represent any loss of content from the thesis.

Bien que ces formulaires aient inclus dans la pagination, il n'y aura aucun contenu manquant.


Canada

Abstract

This thesis is composed of the following five parts: construction of a 6 Degrees of Freedom (DOF) biped robot, control system design, analysis of forward kinematics and inverse kinematics, walking pattern planning, and PID control implementation.

The 6 DOF biped robot is built with aluminum plates, aluminum angles, wood, and rubber materials. It has two legs, two feet, and one trunk, each leg having three joints: hip, knee, and ankle. All joints are actuated by gear head DC motors with built-in encoders.

A microcontroller-and-PC-computer-based control system is designed for the biped robot. The control system consists of actuators, sensors, controllers, and a PC computer. The actuators are the gear head DC motors with H-bridge circuits as drivers and the sensors are incremental encoders built in the DC motors. The controllers used are two microcontrollers, one for each leg. The microprocessors read and process joint angle measurements from the encoders and then transmit them to the PC computer. At the same time, the microcontrollers receive control signals from the PC computer and transfer them to the H-bridge circuits to control the robot joints. Data transfer between the microcontrollers and the PC computer is implemented by two RS232 serial communication channels. A control algorithm and walking pattern planning are carried out on the PC computer.

Both forward kinematics and inverse kinematics are analyzed based on the D-H representation for the biped robot.

Foot trajectories and hip trajectory are calculated by using the 3rd order spline interpolation method. Desired trajectories for joint angles are determined by the inverse kinematics. Simulation is performed to demonstrate the walking pattern.

PID controllers are designed for controlling the biped robot to walk according to the designed walking pattern. The proposed PID controllers are implemented on the biped robot.

Acknowledgements

During my studying, I have been accompanied and supported by many people and I have a desire to express my appreciation to them. And now, the thesis has been finished and I have the opportunity to express my gratitude to them.

I would like to express my deepest gratitude to my supervisor, Dr. Xiaoping. Liu, whose support made it possible to realize this thesis. Without his guidance and mentorship, this thesis would not have come into existence.

I am very grateful for my co-supervisor, Dr. Xiaoli (Lucy) Yang, for her suggestions and help in my research.

I also express my sincere thanks to Dr. Abdelhamid Tayebi and Dr. Krishnamoorthy Natarajan for their great lectures in my academic studies.

I would like to thank for Manfred Klein, Warren Paju, and Kailash Bhatia, who gave me a lot of help for building the PCB circuits.

I also would like to thank graduate students Wenguang Li and Zhirui Huang for helping me in my experiments.

I would like to thank my fellow graduate students for their advice and discussions related to this thesis, and for the good times we have had working together.

Finally, I extend my thanks to my family that supported me to accomplish this work.

Contents

| | |
|--|----|
| Chapter 1 | 1 |
| Introduction | 1 |
| 1.1 Motivation | 1 |
| 1.2 Literature Review | 2 |
| 1.3 Outline | 7 |
| Chapter 2 | 9 |
| Hardware and Software Design | 9 |
| 2.1 Mechanical Design | 9 |
| 2.2 Hardware Design | 10 |
| 2.2.1 Motor Drivers | 11 |
| 2.2.2 Microcontrollers | 12 |
| 2.2.3 Communication Circuits | 13 |
| 2.3 Software Design | 14 |
| 2.3.1 Communication Program | 14 |
| 2.3.2 Control Program | 16 |
| Chapter 3 | 19 |
| Forward Kinematics of the Biped Robot | 19 |
| 3.1 Denavit-Hartenberg Representation | 20 |
| 3.2 Forward Kinematics for the Biped Robot | 23 |
| 3.3 Inverse Kinematics for the Biped Robot | 26 |
| Chapter 4 | 31 |
| Design of Walking Trajectories | 32 |
| 4.1 Third-Order Spline Interpolation | 32 |

| | |
|--|----|
| 4.2 Walking Patterns of Biped Robot | 38 |
| 4.3 Foot Trajectories | 43 |
| 4.4 Hip Trajectory | 47 |
| 4.5 Joint Trajectories | 48 |
| 4.6 Simulation Results | 49 |
| Chapter 5 | 58 |
| PID Controller Design | 58 |
| 5.1 PID Control Theory | 58 |
| 5.2 Control Design | 60 |
| Chapter 6 | 62 |
| Experimental Results | 62 |
| 6.1 Experiment with PD Controllers | 63 |
| 6.2 Experiment with PID Controllers | 71 |
| 6.3 Analysis of Experimental Results | 78 |
| Chapter 7 | 80 |
| Conclusions and Future work | 80 |
| 7.1 Conclusions | 80 |
| 7.2 Future work | 81 |
| References | 82 |
| Appendix | 86 |

List of Figures

| | |
|---|----|
| 2.1 Prototype of the biped robot | 10 |
| 2.2 Structure of the biped robot control system | 11 |
| 2.3 PWM | 12 |
| 2.4 The structure of communication circuit | 13 |
| 2.5 Flowchart of the communication program | 16 |
| 2.6 Flowchart of the control program | 18 |
| 3.1 The frame for a biped robot | 20 |
| 3.2 Denavit-Hartenberg frame assignments | 21 |
| 3.3 The reference frames of a biped robot | 23 |
| 4.1. Walking cycle: single and double support phases..... | 40 |
| 4.2 Trajectories of the biped robot..... | 42 |
| 4.3 Right and left foot trajectories in x axis..... | 51 |
| 4.4 Right and left foot velocities in x axis..... | 51 |
| 4.5 Right and left foot trajectories in z axis..... | 51 |
| 4.6 Right and left foot velocities in z axis..... | 52 |
| 4.7 Right and left foot angles..... | 52 |
| 4.8 Right and left foot angular velocities | 52 |
| 4.9 Hip trajectory in x axis | 53 |
| 4.10 Hip velocity in x axis..... | 53 |
| 4.11 Foot angular trajectories..... | 53 |
| 4.12 Foot angular velocities..... | 54 |
| 4.13 Knee joint trajectories..... | 54 |
| 4.14 Knee joint velocities..... | 54 |
| 4.15 Hip joint trajectories..... | 55 |
| 4.16 Hip joint velocities..... | 55 |
| 4.17 Ankle joint trajectories..... | 55 |
| 4.18 Ankle joint velocities..... | 56 |
| 4.19 $\beta_4\beta'$ and $\beta_2\beta$ trajectories..... | 56 |

| | |
|--|----|
| 4.20 β_4 and β_2 trajectories..... | 56 |
| 4.21 β and β_2 trajectories..... | 57 |
| 4.22 β' and β_4 trajectories..... | 57 |
| 6.1 The biped robot experiment..... | 62 |
| 6.2 Tracking performance for the right ankle (Parameter I) | 64 |
| 6.3 Tracking performance for the right ankle (Parameter II) | 64 |
| 6.4 Tracking performance for the right knee (Parameter I) | 64 |
| 6.5 Tracking performance for the right knee (Parameter II) | 64 |
| 6.6 Tracking performance for the right hip (Parameter I) | 65 |
| 6.7 Tracking performance for the right hip (Parameter II) | 65 |
| 6.8 Tracking performance for the left ankle (Parameter I) | 65 |
| 6.9 Tracking performance for the left ankle (Parameter II) | 65 |
| 6.10 Tracking performance for the left knee (Parameter I) | 66 |
| 6.11 Tracking performance for the left knee (Parameter II) | 66 |
| 6.12 Tracking performance for the left hip (Parameter I) | 66 |
| 6.13 Tracking performance for the left hip (Parameter II) | 66 |
| 6.14 Tracking error for the right ankle (Parameter I) | 67 |
| 6.15 Tracking error for the right ankle (Parameter II) | 67 |
| 6.16 Tracking error for the right knee (Parameter I) | 67 |
| 6.17 Tracking error for the right knee (Parameter II) | 67 |
| 6.18 Tracking error for the right hip (Parameter I) | 68 |
| 6.19 Tracking error for the right hip (Parameter II) | 68 |
| 6.20 Tracking error for the left ankle (Parameter I) | 68 |
| 6.21 Tracking error for the left ankle (Parameter II) | 68 |
| 6.22 Tracking error for the left knee (Parameter I) | 69 |
| 6.23 Tracking error for the left knee (Parameter II) | 69 |
| 6.24 Tracking error for the left hip (Parameter I) | 69 |
| 6.25 Tracking error for the left hip (Parameter II) | 69 |
| 6.26 Tracking performance for the right ankle (Parameter I) | 72 |
| 6.27 Tracking performance for the right ankle (Parameter II) | 72 |
| 6.28 Tracking performance for the right knee (Parameter I) | 72 |

| | |
|---|----|
| 6.29 Tracking performance for the right knee (Parameter II) | 72 |
| 6.30 Tracking performance for the right hip (Parameter I) | 73 |
| 6.31 Tracking performance for the right hip (Parameter II) | 73 |
| 6.32 Tracking performance for the left ankle (Parameter I)..... | 73 |
| 6.33 Tracking performance for the left ankle (Parameter II)..... | 73 |
| 6.34 Tracking performance for the left knee (Parameter I) | 74 |
| 6.35 Tracking performance for the left knee (Parameter II) | 74 |
| 6.36 Tracking performance for the left hip (Parameter I) | 74 |
| 6.37 Tracking performance for the left hip (Parameter II) | 74 |
| 6.38 Tracking error for the right ankle (Parameter I) | 75 |
| 6.39 Tracking error for the right ankle (Parameter II) | 75 |
| 6.40 Tracking error for the right knee (Parameter I) | 75 |
| 6.41 Tracking error for the right knee (Parameter II) | 75 |
| 6.42 Tracking error for the right hip (Parameter I) | 76 |
| 6.43 Tracking error for the right hip (Parameter II) | 76 |
| 6.44 Tracking error for the left ankle (Parameter I) | 76 |
| 6.45 Tracking error for the left ankle (Parameter II) | 76 |
| 6.46 Tracking error for the left knee (Parameter I) | 77 |
| 6.47 Tracking error for the left knee (Parameter II) | 77 |
| 6.48 Tracking error for the left hip (Parameter I) | 77 |
| 6.49 Tracking error for the left hip (Parameter II) | 77 |

Chapter 1

Introduction

1.1 Motivation

Locomotion is defined as the ability for an object to move from one place to another. In the natural setting, locomotion takes on many forms, such as legs, wings, fins. While in an artificial setting, locomotion can be achieved by wheels, wings, and legs. When the research on mobile robots began, the first obvious choice to achieve mobility was the adoption of the wheel. Wheeled robots are simple, easy to build, and can be used in a great variety of applications. Even though wheels provide a convenient and efficient method for mobile robots to move on sufficiently smooth grounds, wheeled vehicles in general are not suitable for unstructured environments, such as rough terrain and steep stairs. Therefore, more universal locomotion ability is needed. This is why legged robots came into play. By observing activities of human beings and legged animals, it is obvious that legs can adapt to a great variety of situations. Many legged robot prototypes have been produced. There is no doubt that humanoid robots can serve in a very wide range of applications: from dangerous tasks such as working in harmful environments to entertainment purposes, from house caring to invalid people assistance.

1.2 Literature Review

In the past years, many biped robot prototypes have been made. Research on humanoid robots has been very active and many famous walking robots have been made in Japan. Weighing 7kg and standing 50cm tall, the HOAP-2 is made by Fujitsu Automation Co., Ltd. It is a genuine humanoid robot with a complete, open architecture, enabling anyone to develop his own software algorithms. The humanoid robot SDR-4X II made by SONY is about 580X190X270mm in size and weighs about 7kg. This robot can carry on simple conversations with its 60,000-word vocabulary, recognize color, dodge obstacles in its path and even sing. The biped robot ASIMO made by Honda is 130mm tall and 54kg in weight. The ASIMO can move carts and other objects around and can deliver drinks on a tray.

Some prototypes were also developed in other countries. Weighing 2.6kg, and with dimension 402X200X110mm, RBP-DLX02, the biped humanoid robot, made by Dajin Robot Co., Ltd, Korea, can walk autonomously. It can be generally used in robotics laboratories and robotics classes based on direction change available (forward, backward, side walk to left or right, left & right rotation, diagonal step). The humanoid robot ROBOTA is made by Computational Learning and Motor Control Lab, USA. It is an artificial intelligence doll that offers multiple means of interaction, which provide adaptive and learning abilities. The humanoid robot JOHNNIE made by the Technical University of Munich, Germany, weighs about 49kg and is 1.80m high. This robot can realize an anthropomorphic

walking machine with a human-like, dynamically stable gait, and walk on even and uneven ground and around curves.

The biped robot is better than the wheeled robot in mobility. It can move in a variety of environments, such as rough terrain, up and down slopes, or with obstacles. Therefore, biped robots have been in the research and development phase since early 1970s. Many related issues, such as mechanical design, electrical design, dynamics analysis, static and dynamic balancing, walking pattern planning, and control algorithms, have been studied.

Walking pattern planning is crucial for legged robots. Walking pattern synthesis has been investigated intensively. Walking patterns for the biped robot have been investigated [1] [2] [3]. A third-order spline interpolation is presented for trajectory planning. In order to achieve a smooth trajectory for the swing leg, the instant velocity change should be decreased, which occurs at the time of collision of the swing leg with the ground. Basically, trajectories for the swing foot and hip are generated by using third order spline interpolation, which guarantees that the objective locomotion parameters attain certain prescribed values. Then a continuous trajectory can be determined by using the concept of the spline interpolation and zero moment points (ZMP).

Considering walking parameters under the various environments, a method is proposed to generate walking patterns for the biped robot in [4]. The algorithm derives the optimal hip height and uses cubic polynomials to generate the hip and foot trajectory. The control of initial and final speeds in a walking cycle achieves continuous walking up and down stairs. Then, the walking motion

of the biped can be determined by the hip and foot trajectory, and cubic polynomials are used to generate the hip and swing foot trajectory. In order to achieve stable walking, both the swing foot motion and whole body motion are required to control. Stable walking can be achieved by Center of Gravity (COG) control and ZMP control.

Two trajectories (center of gravity and tip trajectory of swing leg) are obtained by using the method, which can make a biped robot walk in various terrains [5][6]. A COG trajectory is determined based on walking stability. The tip trajectory of the swing leg is determined based on environmental information. The line inverted pendulum model can be used to generate the COG trajectory. The tip trajectory of the swing leg is obtained by using 5th-order spline interpolation based on environmental information. It can achieve a smooth walking pattern for the biped robot.

In order to walk stably in various environments such as rough terrain, up and down slopes, it is desirable to adapt to such ground conditions with a suitable foot motion, and maintain the stability of the robot by a smooth hip motion [7][8]. A method is proposed to plan a walking pattern. By setting the values of constraint parameters, it is easy to produce different types of foot motion. On the other hand, in order to develop a humanoid biped robot, the selection of suitable joint actuators is an important point. To select suitable actuators and effectively utilize the selected actuators, the relationship between walking patterns and the specifications of each joint actuator must be clarified. A

smooth biped robot swing leg trajectory can be achieved by reducing the instant velocity change.

Based on cubic polynomial interpolation of the initial conditions for the robot's position, velocity, and acceleration, an algorithm to control a biped robot is proposed in [9] and [10]. For the biped robot, the main features include variable length legs and a translatable balance weight in the body. The walking of the biped robot is a mixture of both statically stable and dynamically stable modes, and relies on some degrees of static stability provided by large feet and by carefully controlling the COG position.

A method to generate the specified positions of the body and feet is proposed in [11] and [12]. By fixing both the position and the orientation, the configuration of the biped robot is established. On a large scale, the biped robot must be able to walk in many types of terrain. So, a walking pattern was thus developed that allows for the stride length, the single-support balance point, turning angle, and the maximum height of the swing foot to be modified dynamically.

Virtual model control is another control scheme for the biped robot [13]. It can imagine mechanical components to create forces, which are applied through real joint torque, thereby creating the illusion that the virtual components are connected to the robot. For generating a straight legged walking pattern for a biped robot, a new methodology is presented in [14], which includes the knee stretch index and the knee torque index. By stretching the knee joints, human-like natural walking motion is obtained. Moreover, energy efficiency is improved since

required torque and energy consumption to support the body weight become small at knee joints. The model is designed to simulate human walking by modulating joint moment and stiffness while using limited feedback control [15]. It is intended that this model be a development tool for walking controllers. Therefore, an important feature of the model is that no prior limitations are placed on joint angle trajectories. First the knee joint angles are determined by using the inverse kinematics; and then, by stretching the knee joints, human-like natural walking motion is obtained. In order to minimize tracking errors to achieve smooth motion, two genetic-algorithm-based tuning methods were developed in [16].

The biped is constrained to the sagittal plane, and the motion generation is reduced to a problem of controlling the position and velocity of the robot's center of gravity. In many approaches to ensure the stable movement of the robot's center of gravity [17], the model of the robot's single leg support phase is reduced to the model of an inverted pendulum so as to control the robot's center of gravity based on a simple robot model. To maintain the stable walking gait, the timing of switching the support leg must be determined strictly.

To guarantee stable walking of the robot and decrease impact with floor [18][19], the general rule of designing walking pattern is to make the foot land onto the floor with zero velocity with respect to the floor.

By utilizing the zero moment point (ZMP) and equivalent force-moment, the physical admissibility of the biped walking is characterized in [20] and [21].

The trajectory of the ZMP on the floor must be inside the stable region of the supporting sole for physically realizable walking during the single support phase.

1.3 Outline

This section outlines the overall structure of the thesis, and provides a brief description for each chapter.

Chapter 2 gives the mechanical structure of the biped robot built for this thesis.

On the other hand, it presents the hardware and software design procedure. In the hardware aspect, the basic knowledge of H-Bridge, microcontroller, and communication circuit is introduced. In the software aspect, both communication programs and control programs are introduced.

Chapter 3 provides some basic knowledge about robots and describes the procedure by which the forward kinematics and inverse kinematics are derived. All joint angles can be calculated based on inverse kinematics, when positions and orientations of the hip and ankle are given.

Chapter 4 explains the walking pattern design theoretically with a walking cycle (a single-support phase and a double-support phase) and discusses how to use third-order spline interpolation functions to generate foot trajectories and hip trajectory. The joint trajectories for the biped robot are generated by using the inverse kinematics.

Chapter 5 introduces the design of PD controllers and PID controllers for the biped robot manipulator to track the desired trajectories.

Chapter 6 shows experimental results for the PD controllers and PID controllers

Lakehead University

Comparison is made between the PD and PID controllers.

Chapter 7 summarizes the outcomes of the project and discusses the future work.

Chapter 2

Hardware and Software Design

2.1 Mechanical Design

The philosophy behind the biped robot design is that it should be as simple as possible, but complex enough to exhibit the basic behaviors that human beings have. To this end, a 6 degree-of-freedom biped robot was built. It has two legs, two feet, and one trunk. Each leg has three joints: hip, knee, and ankle. To reduce the weight, the legs are made with aluminum plates and the ankles and hips are built with aluminum plates. Two hips are connected together by a wood hip bridge. The control circuits are placed on the trunk, which was made with thin aluminum plates. The feet are built with aluminum plates and rubber materials. The rubber materials are used to increase the traction between the foot and the floor. The structure of the biped robot is shown in Figure 2.1.

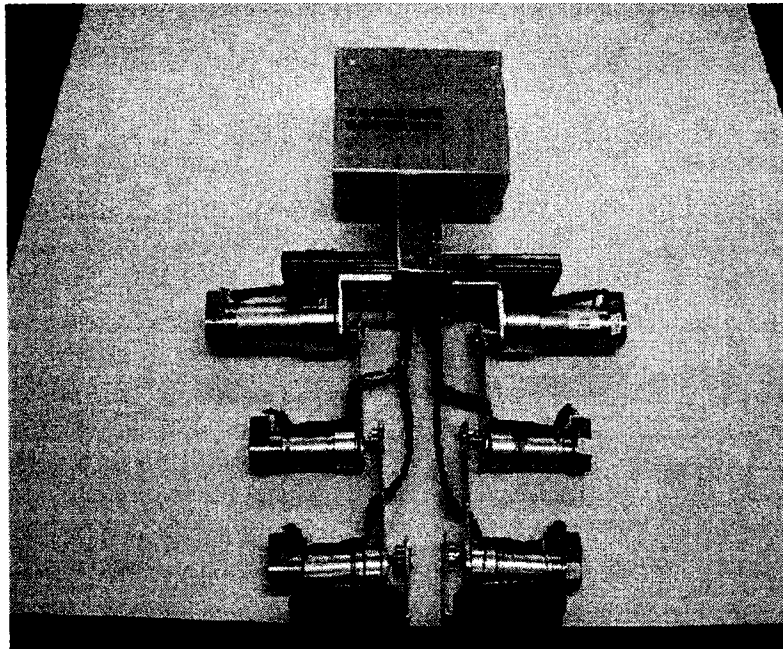


Figure2.1 Prototype of the biped robot

2.2 Hardware Design

The biped robot control system is composed of actuators, sensors, and controllers, as shown in Figure 2.2. The actuators used in the biped robot are gear-head DC motors. The two hips are driven by GM9236S019 gear head motors with a transmission ratio of 19:1 while the ankles and knees are controlled by GM8724S015 gear head motors with a transmission ratio of 19.5:1. The sensors used in the biped robot are incremental encoders built in the gear-head DC motors. The encoders need a 5V power supply and the encoder resolution is 500 pulses per revolution. The controller consists of six motor drivers, two microcontrollers, two communication circuits, and one PC computer.

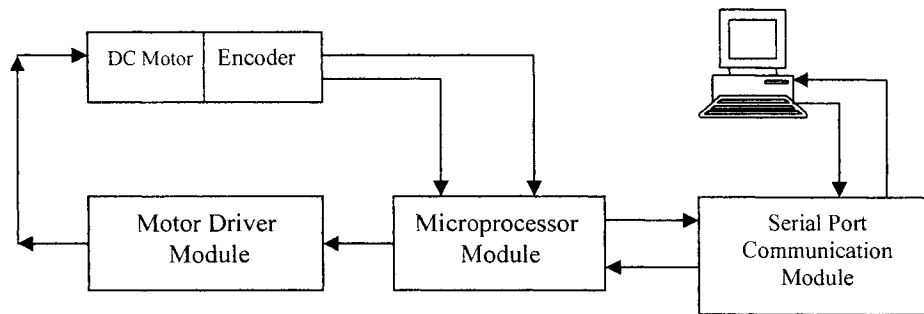


Figure 2.2 Structure of the biped robot control system

2.2.1 Motor Drivers

There are six identical motor drivers in the biped robot. Each motor driver is implemented by a LMD18200T H-Bridge circuit (see Appendix).

The LMD18200T H-Bridge operates at a 12V power supply and can supply a 3A continuous current. The output voltage from **Output1** and **Output2** are controlled by a PWM signal applied to **Direction Input** with **PWM input** connected to 5V. The output voltage is 0V for a PWM signal of a 50% duty cycle. As shown in Figure 2.3. A PWM signal with a less than 50% duty cycle makes the motor rotate in one direction and the lower the duty cycle, the higher the output voltage. The higher the motor speed whereas more than 50% duty cycle makes the motor rotate in the opposite direction and the higher the duty cycle the higher the output voltage and the higher the motor speed. A logic high signal is used to break the motor through **Break Input**.

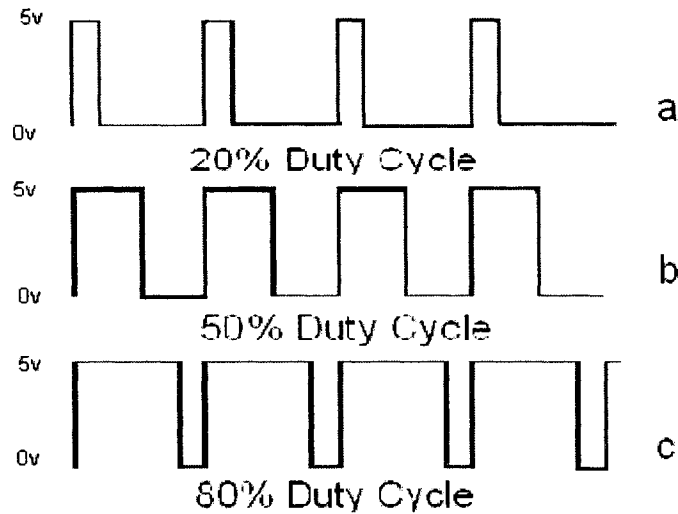


Figure 2.3 PWM

2.2.2 Microcontrollers

Two Atmega 16 microcontrollers are used in the biped control system [22]. Each leg is controlled by one Atmega16. The pinouts of the microcontroller Atmega 16 are shown in Appendix.

Three external interrupts are used to count pulses from **Channel A** of the encoders for joint position measurements. **Channel B** of the encoders is used to produce signals for testing the direction of rotation of motors. **INT2**, **INT0**, and **INT1** of Atmega16 are connected to **Channel A** of the encoder on the first, second, and third motor, respectively. **PB2**, **PB7**, and **PD4** are connected to **Channel B** of the encoder on the first, second, and third motor, respectively.

Three PWM channels are used to generate PWM signals for three motors. **OCR1B**, **OCR1A**, and **OCR2** are connected to **Direction Input** of the H-Bridge for the first, second, and third motor, respectively.

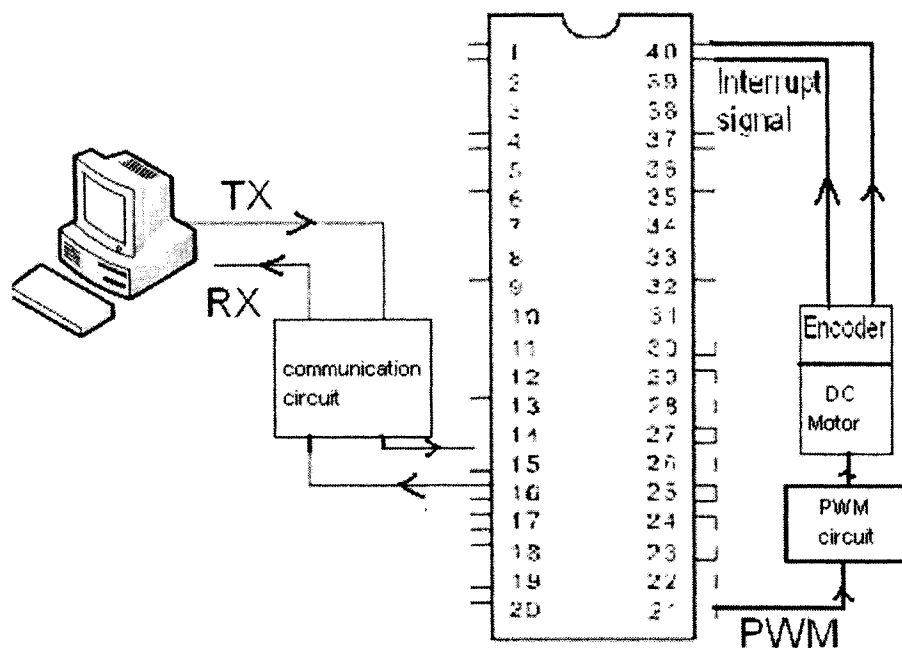


Figure 2.4 The structure of communication circuit

2.2.3 Communication Circuits

Two identical communication circuits are used to transfer data between the microcontrollers and the PC computer, as shown in Figure 2.4. Data communication is implemented by two MAX232 serial channels. Serial transfer is chosen because it simplifies cabling and is supported by a wide range of commercial products. Although serial communication does not offer high speed, it is satisfactory for the control system with a sampling rate of 100Hz with 9600 bps.

The circuit for the control system of the biped robot is shown in Appendix.

2.3 Software Design

Two programs are designed for the biped robot. The first program, communication program, is used for the microcontroller to process data from or to the robot and PC computer. The second program, control program, is designed for the PC computer to achieve the walking pattern planning and to implement control algorithm.

2.3.1 Communication Program

The communication program is designed for reading the encoder signals, transferring data between the microcontroller and PC computer, and sending the PWM signals to the motor drivers. It is written in assembly language. The communication program is composed of the following modules.

- Initialization module

The initialization module includes the following parts:

1. Ports initialization.
2. USART initialization.
3. PWM initialization.
4. Register initialization.

- Counter module

The counter module is responsible for counting the sample data from the encoders. It is comprised of three parts as follows:

1. Counting pulses from external interrupt, INT0.
2. Counting pulses from external interrupt, INT1.

3. Counting pulses from external interrupt, INT2.

- Data processing module

The data processing module is responsible for processing the data from the encoders and PC computer. The contents of this module are as follows:

1. Process data from the counter module and send them to the communication module.
2. Process PWM data from the communication module and send them to the PWM module.

- Communication module

The communication module is comprised of two parts. The first part receives data from the data processing module and sends them to the PC computer. The second part reads PWM data from the PC computer and sends them to the data processing module.

- PWM module

It is responsible for generating PWM signals for the motor driver circuits.

The flowchart for the communication program is shown in Figure 2.5

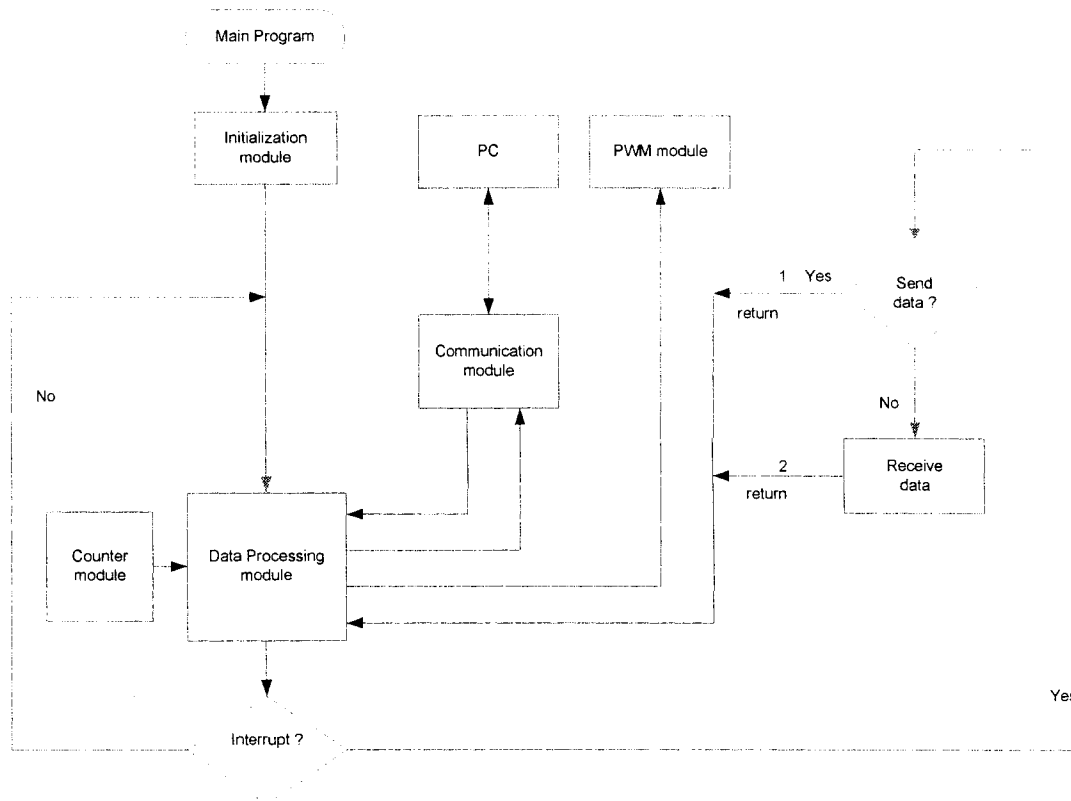


Figure 2.5 Flowchart of the communication program

2.3.2 Control Program

The control program is designed to control the speed and position of the biped robot. The control program is written in C/C++. The function of the control program is given as follows:

- Generate and correct the desired trajectories for the biped robot.
- Generate the duty cycles for the PWM signals.
- Save the data.
- Control the walking pattern for the biped robot.

The control program is comprised of the following modules.

1. Initialization module

2. Interrupt module

Interrupt module is responsible for checking interrupt signals from the microcontroller. If it has an interrupt signal, the data is received. In the meantime, the PWM data are sent to the microcontroller after receiving the data from the microcontroller.

3. Desired trajectory design module

In this module, the walking style is designed, which generates all desired joint angles for the biped robot. The module is responsible for generating the desired trajectories for the biped robot. The desired trajectories of the ankles, knees, and hips are determined by using the combination of the inverse kinematics and third order spline interpolation.

4. Pattern module

Pattern module ensures the stability of the robot during the walking cycle.

This part is comprised of the following three parts:

- PD controller implementation.
- PID controller implementation.
- PWM data generation

The flowchart of the control program is shown in Figure 2.6.

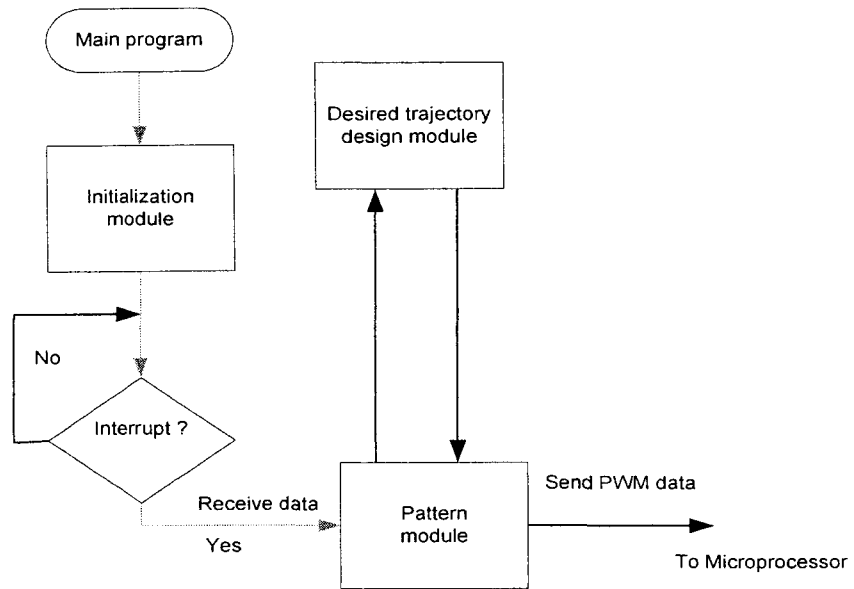


Figure 2.6 Flowchart of the control program

Chapter 3

Forward Kinematics of the Biped

Robot

The forward kinematics model is presented for the biped robot built for the experiments. The biped robot consists of seven rigid links, one link for the upper body (Link 4), two links for the thighs (Link 3 and Link 5), two links for the shanks (Link 2 and Link 6), and two links for the feet (Link 1 and Link 7), as shown in Figure 3.1.

These links are connected with each other by six purely rotational joints, two joints at the hips, two joints at the knees, and two joints at the ankles. These rotational joints are driven by independent motors. For simplicity, it is assumed that all the joints are frictionless.

Reference frames are defined first using a Denavit-Hartenberg convention. Then, the model for the forward kinematics is derived. Finally, the inverse kinematics is discussed.

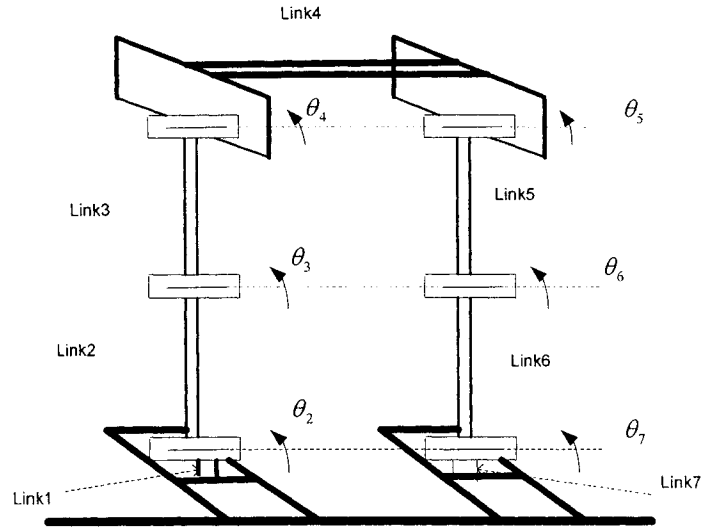


Figure 3.1 The frame for a biped robot

3.1 Denavit-Hartenberg Representation

A commonly used convention for selecting reference frames in robotic applications is the Denavit-Hartenberg (D-H) convention. In the D-H convention, a homogeneous transformation ${}^{i+1}T_i$ from Frame i to Frame $i+1$ can be represented by a product of four basic transformations [23]:

$$\begin{aligned}
 {}^{i+1}T_i &= Rot_{z,\theta_i} Trans_{z,d_i} Trans_{x,a_i} Rot_{x,\alpha_i} \\
 &= \begin{bmatrix} \cos \theta_i & -\sin \theta_i & 0 & 0 \\ \sin \theta_i & \cos \theta_i & 0 & 0 \\ 0 & 0 & 1 & 0 \\ 0 & 0 & 0 & 1 \end{bmatrix} \begin{bmatrix} 1 & 0 & 0 & 0 \\ 0 & 1 & 0 & 0 \\ 0 & 0 & 1 & d_i \\ 0 & 0 & 0 & 1 \end{bmatrix} \begin{bmatrix} 1 & 0 & 0 & a_i \\ 0 & 1 & 0 & 0 \\ 0 & 0 & 1 & 0 \\ 0 & 0 & 0 & 1 \end{bmatrix} \begin{bmatrix} 1 & 0 & 0 & 0 \\ 0 & \cos \alpha_i & -\sin \alpha_i & 0 \\ 0 & \sin \alpha_i & \cos \alpha_i & 0 \\ 0 & 0 & 0 & 1 \end{bmatrix} \\
 &= \begin{bmatrix} \cos \theta_i & -\sin \theta_i \cos \alpha_i & \sin \theta_i \sin \alpha_i & a_i \cos \theta_i \\ \sin \theta_i & \cos \theta_i \cos \alpha_i & -\cos \theta_i \sin \alpha_i & a_i \sin \theta_i \\ 0 & \sin \alpha_i & \cos \alpha_i & d_i \\ 0 & 0 & 0 & 1 \end{bmatrix}
 \end{aligned} \tag{3.1}$$

where θ_i is the angle between x_{i-1} and x_i measured about z_{i-1} , a_i is the distance along x_i from o_i to the intersection of the x_i and z_{i-1} axes, d_i is the distance along z_{i-1} from o_{i-1} to the intersection of the x_i and z_{i-1} axes, and α_i is the angle between z_{i-1} and z_i measured about x_i . (See Figure 3.2)

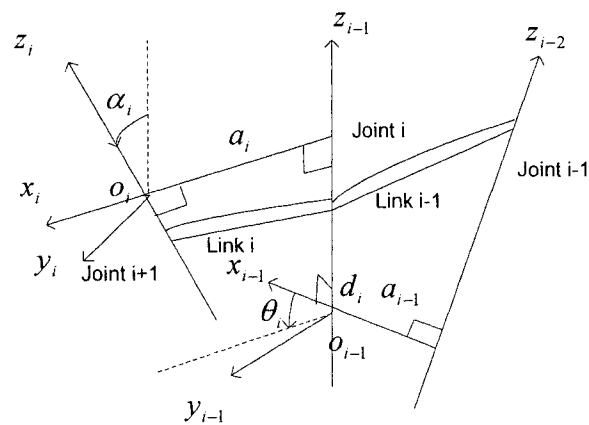


Figure 3.2 Denavit-Hartenberg frame assignments

With the homogeneous transformation ${}^{i+1}_i T$ from Frame i to Frame $i+1$, any vector p_i in Frame i can be expressed by

$$\begin{bmatrix} p_{i+1} \\ 1 \end{bmatrix} = {}^{i+1}_i T \begin{bmatrix} p_i \\ 1 \end{bmatrix} \quad (3.2)$$

where p_{i+1} is the same vector written in Frame $i+1$.

For the biped robot, the reference frames are defined as shown in Figure 3.3. Frame r , o_r, x_r, y_r, z_r , is chosen as a fixed frame. Frame i , o_i, x_i, y_i, z_i , is generally oriented as follows: the origin of Frame i is located as shown in Figure 3.3, z_i points into the page along the direction of the axis of rotation of the joint i , x_i points from the origin of Frame $i-1$ to the origin of Frame i , y_i points to the

direction determined by a right-hand rule for the Cartesian frame, θ_i is the angle of rotation of link i with respect to link $i-1$ about the z_i axis.

It is worth noting that Frame 0, $o_0x_0y_0z_0$, is chosen as follows: the origin of Frame 0 is located at the tip of the toe of the right foot, z_0 points into the page with the intersection between the sole and the ground as the axis of rotation, x_0 points from the origin of Frame r to the origin of Frame 0, y_0 points to the direction determined by a right-hand rule for the Cartesian frame, θ_1 is the angle of the sole of the right foot with the ground. Note that $\theta_1 = 0$ corresponds to the situation when the right foot fully touches the ground.

The parameters in D-H representation are shown in Table 3.1.

Table 3.1 D-H parameters for the biped robot

| link | a_i | α_i | d_i | θ_i | ${}^i_{i-1}T$ |
|------|----------|------------|-------|----------------------------------|---------------|
| 0 | x_a | -90 | 0 | 0 | 0_rT |
| 1 | l_0 | 0 | 0 | $-(180 - (\theta_1 + \alpha_r))$ | 1_0T |
| 2 | l_1 | 0 | 0 | θ_2 | 2_1T |
| 3 | l_2 | 0 | 0 | $-\theta_3$ | 3_2T |
| 4 | l_6 | 0 | 0 | $-\theta_4$ | 4_3T |
| 5 | 0 | 0 | l_3 | 180 | 5_4T |
| 6 | l_6 | 0 | 0 | 0 | 6_5T |
| 7 | l_4 | 0 | 0 | $-\theta_5$ | 7_6T |
| 8 | l_5 | 0 | 0 | θ_6 | 8_7T |
| 9 | l_{am} | 0 | 0 | $-\theta_7$ | 9_8T |

3.2 Forward Kinematics for the Biped Robot

For the biped robot, if the joint variables $\theta = (\theta_1, \theta_2, \dots, \theta_7)$, i.e. the angles between the robot links, are given, then the position and orientation of the biped robot can be determined by the forward kinematics.

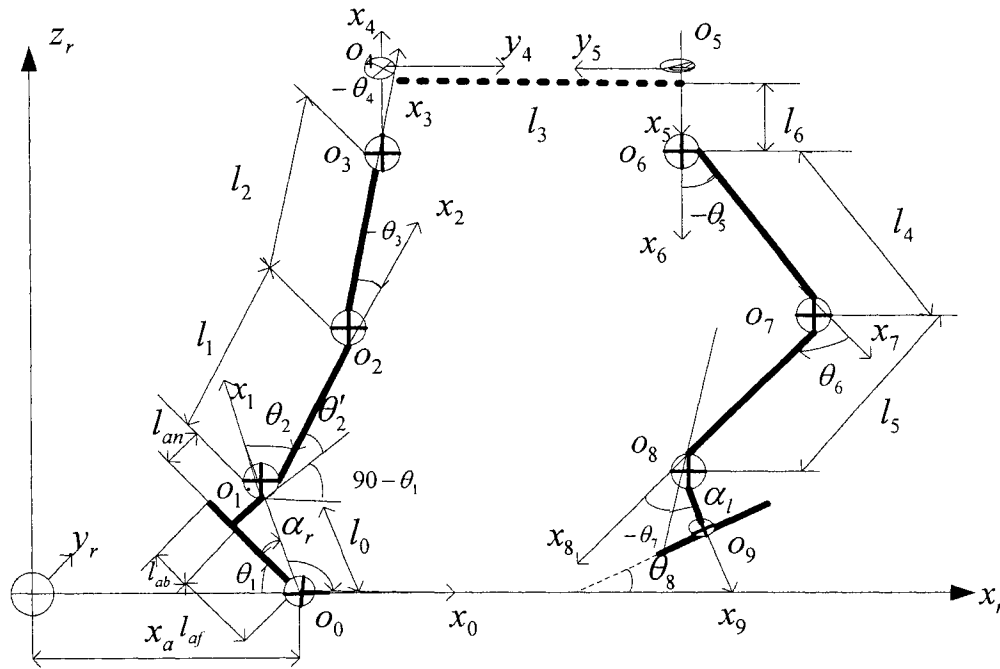


Figure 3.3 The reference frames of a biped robot

According to the walking features of human beings, the angles shown in Figure 3.3 should satisfy the following conditions:

$$0 \leq \theta_1 < 90^\circ, 0 \leq \theta_3 < 90^\circ, 0 < \theta_2 < 90^\circ, -90^\circ < \theta_2' < 90^\circ, \\ -90^\circ < \theta_7 < 90^\circ, 0 \leq \theta_5 < 90^\circ, 0 \leq \theta_6 < 90^\circ, 0 \leq \theta_4 \leq 90^\circ, 0 \leq \theta_5 \leq 90^\circ.$$

The homogenous transformation matrices from Frame i to Frame j is determined by

$${}^i T = {}^{i+1} T_i {}^{i+2} T_{i+1} \dots {}^j T_{j-1}, j > i \quad (3.3)$$

The homogenous transformation matrices from Frame r to Frame j is calculated by

$${}^jT_r = {}^0T_r {}^1T_0 \dots {}^jT_{j-1} \quad (3.4)$$

The matrices ${}^{i-1}T_i, i = 0,1,\dots,9$, ${}^iT_0, i = 0,1,\dots,9$, and ${}^iT_r, i = 0,1,\dots,9$ are given in Appendix.

Let x_{0i} , y_{0i} , and z_{0i} denote the x-coordinate, y-coordinate, and z-coordinate of the origin of Frame i with respect to Frame r, respectively. Then, according to the definition of the homogenous transformation matrix, x_{0i} , y_{0i} , and z_{0i} can be determined by the first three items of the fourth column of the matrix iT_r . Therefore, the following equations can be obtained from Equations (20)-(28) in Appendix.

$$\begin{cases} x_{01} = x_a - l_0 \cos(\theta_1 + \alpha_r) \\ y_{01} = 0 \\ z_{01} = l_0 \sin(\theta_1 + \alpha_r) \end{cases} \quad (3.5)$$

$$\begin{cases} x_{02} = x_a - l_1 \cos(\theta_1 + \theta_2 + \alpha_r) - l_0 \cos(\theta_1 + \alpha_r) \\ y_{02} = 0 \\ z_{02} = l_1 \sin(\theta_1 + \theta_2 + \alpha_r) + l_0 \sin(\theta_1 + \alpha_r) \end{cases} \quad (3.6)$$

$$\begin{cases} x_{03} = x_a - l_2 \cos(\theta_1 + \theta_2 + \alpha_r - \theta_3) - l_1 \cos(\theta_1 + \theta_2 + \alpha_r) - l_0 \cos(\theta_1 + \alpha_r) \\ y_{03} = 0 \\ z_{03} = l_2 \sin(\theta_1 + \theta_2 + \alpha_r - \theta_3) + l_1 \sin(\theta_1 + \theta_2 + \alpha_r) + l_0 \sin(\theta_1 + \alpha_r) \end{cases} \quad (3.7)$$

$$\begin{cases} x_{04} = x_a + DD3 \\ y_{04} = 0 \\ z_{04} = -DD4 \end{cases} \quad (3.8)$$

Lakehead University

$$\begin{cases} x_{05} = DD3 + x_a \\ y_{05} = l_3 \\ z_{05} = -DD4 \end{cases} \quad (3.9)$$

$$\begin{cases} x_{06} = DD5 + x_a \\ y_{06} = l_3 \\ z_{06} = -DD6 \end{cases} \quad (3.10)$$

$$\begin{cases} x_{07} = DD7 + x_a \\ y_{07} = l_3 \\ z_{07} = -DD8 \end{cases} \quad (3.11)$$

$$\begin{cases} x_{08} = DD9 + x_a \\ y_{08} = l_3 \\ z_{08} = -DD10 \end{cases} \quad (3.12)$$

$$\begin{cases} x_{09} = DD11 + x_a \\ y_{09} = l_3 \\ z_{09} = -DD12 \end{cases} \quad (3.13)$$

where

$$DD1 = -l_2 \cos(\theta_1 + \theta_2 - \theta_3 + \alpha_r) - l_1 \cos(\theta_1 + \theta_2 + \alpha_r) - l_0 \cos(\theta_1 + \alpha_r)$$

$$DD2 = -l_2 \sin(\theta_1 + \theta_2 - \theta_3 + \alpha_r) - l_1 \sin(\theta_1 + \theta_2 + \alpha_r) - l_0 \sin(\theta_1 + \alpha_r)$$

$$DD3 = -l_6 \cos(\theta_1 + \theta_2 - \theta_3 - \theta_4 + \alpha_r) + DD1$$

$$DD4 = -l_6 \sin(\theta_1 + \theta_2 - \theta_3 - \theta_4 + \alpha_r) + DD2$$

$$DD5 = l_6 \cos \theta_a + DD3$$

$$DD6 = l_6 \sin \theta_a + DD4$$

$$DD7 = l_4 \cos(\theta_a - \theta_5) + DD5$$

$$DD8 = l_4 \sin(\theta_a - \theta_5) + DD6$$

$$DD9 = l_5 \cos(\theta_a - \theta_5 + \theta_6) + DD7$$

Lakehead University

$$DD10 = l_5 \sin(\theta_a - \theta_5 + \theta_6) + DD8$$

$$DD11 = l_{an} \cos(\theta_a - \theta_5 + \theta_6 - \theta_7) + DD9$$

$$DD12 = l_{an} \sin(\theta_a - \theta_5 + \theta_6 - \theta_7) + DD10$$

$$\theta_a = \theta_1 + \theta_2 - \theta_3 - \theta_4 + \alpha_r$$

$$\alpha_r = \tan^{-1} \frac{l_{an}}{l_{af}}$$

3.3 Inverse Kinematics for the Biped Robot

The problem of Inverse kinematics for the biped robot can be stated as follows.

Given the positions and orientations of both feet and hip, find the joint angles $\theta'_2, \theta_3, \theta_4, \theta_5, \theta_6, \theta_7$.

Note that the position of the ankle of the right leg is determined by (x_{01}, y_{01}, z_{01}) and its orientation is indicated by θ_1 , while for the left leg, the position of the ankle is (x_{08}, y_{08}, z_{08}) and the orientation is determined by the angle between the sole of the left foot and the ground, denoted θ_8 . On the other hand, the position of the hip is given by (x_{03}, y_{03}, z_{03}) and its orientation is determined by the angle between the upper body and the vertical plane, which is always set to zero for the straightforward walking. With the above information, the joint angles $\theta'_2, \theta_3, \theta_4, \theta_5, \theta_6, \theta_7$ can be determined as follows [24].

It follows from Equations (3.5) and (3.7) that

$$x_{03} - x_{01} = -l_2 \cos(\theta_1 + \theta_2 + \alpha_r - \theta_3) - l_1 \cos(\theta_1 + \theta_2 + \alpha_r) \quad (3.14)$$

$$z_{03} - z_{01} = l_2 \sin(\theta_1 + \theta_2 + \alpha_r - \theta_3) + l_1 \sin(\theta_1 + \theta_2 + \alpha_r) \quad (3.15)$$

Adding the square of (3.14) to the square of (3.15) yields

Lakehead University

$$(x_{03} - x_{01})^2 + (z_{03} - z_{01})^2 = l_1^2 + l_2^2 + 2l_1l_2 \cos \theta_3$$

from which, we have

$$\cos \theta_3 = ((x_{03} - x_{01})^2 + (z_{03} - z_{01})^2 - l_1^2 - l_2^2) / 2l_1l_2$$

Considering the mechanical structure of the biped robot, we assume that

$$-90^\circ < \theta_3 < 0, \text{ that is, } -1 < \sin \theta_3 < 0, 0 < \cos \theta_3 < 1.$$

Let

$$D_r = \cos \theta_3 = ((x_{03} - x_{01})^2 + (z_{03} - z_{01})^2 - l_1^2 - l_2^2) / 2l_1l_2$$

Then, $0 < D_r < 1$ and

$$\sin \theta_3 = -\sqrt{1 - \cos^2 \theta_3} = -\sqrt{1 - D_r^2}$$

As a result, θ_3 can be calculated by

$$\theta_3 = \tan^{-1}(-\sqrt{1 - D_r^2}, D_r) \quad (3.16)$$

Equations (3.14) and (3.15) can be rewritten as

$$x_{03} - x_{01} = \cos(\theta_1 + \theta_2 + \alpha_r)(-l_2 \cos \theta_3 - l_1) - l_2 \sin(\theta_1 + \theta_2 + \alpha_r) \sin \theta_3 \quad (3.17)$$

$$z_{03} - z_{01} = \sin(\theta_1 + \theta_2 + \alpha_r)(l_2 \cos \theta_3 + l_1) - l_2 \cos(\theta_1 + \theta_2 + \alpha_r) \sin \theta_3 \quad (3.18)$$

Solving Equations (3.17) and (3.18) for $\sin(\theta_1 + \theta_2 + \alpha_r)$ and $\cos(\theta_1 + \theta_2 + \alpha_r)$

results in

$$\sin(\theta_1 + \theta_2 + \alpha_r) = ((z_{03} - z_{01})(l_2 \cos \theta_3 + l_1) - (x_{03} - x_{01})l_2 \sin \theta_3) / (l_1^2 + l_2^2 + 2l_1l_2 \cos \theta_3) \quad (3.19)$$

$$\cos(\theta_1 + \theta_2 + \alpha_r) = ((z_{01} - z_{03})l_2 \sin \theta_3 - (x_{03} - x_{01})(l_2 \cos \theta_3 + l_1)) / (l_1^2 + l_2^2 + 2l_1l_2 \cos \theta_3) \quad (3.20)$$

from which, it follows that

Lakehead University

$$\tan(\theta_1 + \theta_2 + \alpha_r) = \frac{(z_{03} - z_{01})(l_2 \cos \theta_3 + l_1) - (x_{03} - x_{01})l_2 \sin \theta_3}{(z_{01} - z_{03})l_2 \sin \theta_3 - (x_{03} - x_{01})(l_2 \cos \theta_3 + l_1)}$$

Consequently, θ_2 can be determined by

$$\theta_2 = \tan^{-1} \frac{(z_{03} - z_{01})(l_2 \cos \theta_3 + l_1) - (x_{03} - x_{01})l_2 \sin \theta_3}{(z_{01} - z_{03})l_2 \sin \theta_3 - (x_{03} - x_{01})(l_2 \cos \theta_3 + l_1)} - \theta_1 - \alpha_r \quad (3.21)$$

Note that θ_2 is not the ankle rotation angle. From Figure 3.3, it can be deduced that the ankle rotation angle θ_2' can be determined by

$$\theta_2' = 90 - \alpha_r - \theta_2 \quad (3.22)$$

Substituting Equation (3.21) into Equation (3.22) gives

$$\theta_2' = 90 - \tan^{-1} \frac{(z_{03} - z_{01})(l_2 \cos \theta_3 + l_1) - (x_{03} - x_{01})l_2 \sin \theta_3}{(z_{01} - z_{03})l_2 \sin \theta_3 - (x_{03} - x_{01})(l_2 \cos \theta_3 + l_1)} + \theta_1$$

According to Figure 3.3, it can be verified that $\theta_1, \theta_2', \theta_3$ and θ_4 are related by the following equation

$$-\theta_1 + \theta_2' + \theta_3 + \theta_4 = 0$$

which means that

$$\theta_4 = \theta_1 - \theta_2' - \theta_3 \quad (3.23)$$

Similarly, $\theta_5, \theta_6, \theta_7$ and θ_8 are related by the equation

$$\theta_7 = \theta_6 - \theta_5 + \theta_8 \quad (3.24)$$

Due to the symmetry between the right leg and left leg, θ_5, θ_6 and θ_7 can be derived from Equations (3.10), (3.12) and (3.24) as follows.

$$\theta_6 = \tan^{-1}(-\sqrt{1 - D_l^2}, D_l) \quad (3.25)$$

$$\theta_7 = \tan^{-1} \frac{(z_{08} - z_{06})l_4 \sin \theta_6 + (x_{08} - x_{06})(l_4 \cos \theta_6 + l_5)}{(z_{06} - z_{08})(l_4 \cos \theta_6 + l_5) + (x_{08} - x_{06})l_4 \sin \theta_6} + \theta_8 \quad (3.26)$$

Lakehead University

$$\theta_5 = \theta_6 - \theta_7 + \theta_8 \quad (3.27)$$

with

$$D_i = \cos \theta_6 = ((x_{08} - x_{06})^2 + (z_{08} - z_{06})^2 - l_4^2 - l_5^2) / 2l_4l_5$$

In what follows, the first derivatives of θ_2 , θ_3 and θ_4 are calculated.

According to Equation (3.16), the first derivative of θ_3 can be determined by

$$\dot{\theta}_3 = \frac{1}{\sqrt{1 - D_r^2}} \dot{D}_r, D_r \neq 1 \quad (3.28)$$

where

$$\dot{D}_r = \frac{2(x_{03} - x_{01})(\dot{x}_{03} - \dot{x}_{01}) + 2(z_{03} - z_{01})(\dot{z}_{03} - \dot{z}_{01})}{2l_1l_2}$$

Define

$$\begin{aligned} \beta_1 &= (l_1 + l_2 \cos \theta_3)(x_{01} - x_{03}) + l_2(z_{01} - z_{03}) \sin \theta_3 \\ \beta_2 &= (z_{03} - z_{01})(l_2 \cos \theta_3 + l_1) - (x_{03} - x_{01})l_2 \sin \theta_3 \\ \beta &= l_1^2 + 2l_1l_2 \cos \theta_3 + l_2^2 \end{aligned}$$

Then, (3.19) and (3.20) can be rewritten as

$$\begin{aligned} \cos(\theta_1 + \theta_2 + \alpha_r) &= \beta_1 / \beta \\ \sin(\theta_1 + \theta_2 + \alpha_r) &= \beta_2 / \beta \end{aligned} \quad (3.29)$$

Differentiating the first equation with respect to time produces

$$-\sin(\theta_1 + \theta_2 + \alpha_r)(\dot{\theta}_1 + \dot{\theta}_2 + \dot{\alpha}_r) = \frac{\dot{\beta}_1\beta - \beta_1\dot{\beta}}{\beta^2}, \beta \neq 0 \quad (3.30)$$

with

$$\begin{aligned} \dot{\beta}_1 &= -l_2 \sin \theta_3 \dot{\theta}_3 (x_{01} - x_{03}) + (l_1 + l_2 \cos \theta_3)(\dot{x}_{01} - \dot{x}_{03}) \\ &\quad + l_2 \cos \theta_3 \dot{\theta}_3 (z_{01} - z_{03}) + l_2 \sin \theta_3 (\dot{z}_{01} - \dot{z}_{03}) \\ \dot{\beta} &= -2l_1l_2 \sin \theta_3 \dot{\theta}_3 \end{aligned}$$

It follows from Equation (3.30) that

$$\dot{\theta}_1 + \dot{\theta}_2 + \dot{\alpha}_r = \frac{\dot{\beta}_1\beta - \beta_1\dot{\beta}}{\beta^2} \frac{\beta}{\beta_2} = \frac{\dot{\beta}_1\beta - \beta_1\dot{\beta}}{\beta_2\beta}$$

that is,

$$\dot{\theta}_2 = \frac{\dot{\beta}_1\beta - \beta_1\dot{\beta}}{\beta_2\beta} - \dot{\theta}_1 - \dot{\alpha}_r \quad (3.31)$$

From Equation (3.22), it is easily seen that

$$\dot{\theta}_2' = -\dot{\alpha}_r - \dot{\theta}_2 \quad (3.32)$$

It follows from Equation (3.23) that

$$\dot{\theta}_4 = \dot{\theta}_1 + \dot{\theta}_2 - \dot{\theta}_3 + \dot{\alpha}_r \quad (3.33)$$

By following the same reasoning, the first derivatives of θ_5, θ_6 and θ_7 can be determined as follows:

$$\dot{\theta}_6 = \frac{1}{\sqrt{1-D_l^2}} \dot{D}_l, D_l \neq 1 \quad (3.34)$$

$$\dot{\theta}_7 = \frac{\dot{\beta}_3\beta' - \beta_3\dot{\beta}'}{\beta_4\beta'} + \dot{\theta}_8 \quad (3.35)$$

$$\dot{\theta}_5 = \dot{\theta}_6 - \dot{\theta}_7 + \dot{\theta}_8 \quad (3.36)$$

where

$$\dot{D}_l = \frac{2(x_{08} - x_{06})(\dot{x}_{08} - \dot{x}_{06}) + 2(z_{08} - z_{06})(\dot{z}_{08} - \dot{z}_{06})}{2l_4l_5}$$

$$\beta_4 = (z_{08} - z_{06})l_4 \sin \theta_6 + (x_{08} - x_{06})(l_4 \cos \theta_6 + l_5)$$

$$\beta_3 = (z_{06} - z_{08})(l_4 \cos \theta_6 + l_5) + (x_{08} - x_{06})l_4 \sin \theta_6$$

$$\beta' = l_4^2 + 2l_4l_5 \cos \theta_6 + l_5^2, \beta' \neq 0$$

Lakehead University

$$\begin{aligned}\dot{\beta}_3 &= (\dot{x}_{08} - \dot{x}_{06})l_4 \sin \theta_6 + (x_{08} - z_{06})l_4 \cos \theta_6 \dot{\theta}_6 \\ &\quad + (\dot{z}_{06} - \dot{z}_{08})(l_4 \cos \theta_6 + l_5) - (z_{06} - z_{08})l_4 \sin \theta_6 \dot{\theta}_6 \\ \dot{\beta}' &= -2l_4 l_5 \sin \theta_6 \dot{\theta}_6\end{aligned}$$

Simulation is carried out to check the singular points for (3.31) and (3.35). Simulation results are shown in Figures 4.19-22. It is easily checked that $\beta_2 = 0$ as $\theta_3 = -37.8861^\circ$ and $\beta_4 = 0$ as $\theta_6 = -37.8861^\circ$. In order to guarantee the smoothness of the walking pattern and limit the speed of the desired joint angular velocities, a digital filter is used to remove the big jumps on $\theta_2', \theta_4, \theta_5, \theta_7$, see Figures 4.16 and 4.18, which are caused by the singularities.

Chapter 4

Design of Walking Trajectories

Walking trajectory planning is crucial for two-legged robots. For a stable motion of biped robots, basic constraints, such as the existence of solutions to inverse kinematics of robot legs, joint angle range and so on, have to be satisfied throughout the entire walking cycle. A basic requirement for walking trajectories is to achieve a smooth walking pattern. If both foot trajectories and the hip trajectory are known, all joint trajectories of the biped robot can be determined by inverse kinematics. Therefore the walking pattern is defined by two foot trajectories and the hip trajectory. A smooth walking pattern can be achieved by both foot trajectories and a hip trajectory with continuous first and second derivatives. The third-order spline interpolation can be used to generate a function with both first and second derivatives continuous from the original data.

4.1 Third-Order Spline Interpolation

Interpolation is a method used to generate intermediate values between *two* or more given values. These intermediate values can be generated by an appropriate interpolating function. Cubic spline interpolation is one of interpolation methods, which generates a continuous function with a continuous derivative from the original data by piecing together cubic polynomials.

Consider points $(x_1, y_1), (x_2, y_2), \dots, (x_n, y_n)$ with $x_1 < x_2 < \dots < x_n$. A cubic spline is a function $f : R \rightarrow R$ defined by

$$f(x) = \begin{cases} p_1(x) & x_1 \leq x \leq x_2 \\ p_2(x) & x_2 \leq x \leq x_3 \\ \vdots & \vdots \\ p_{n-1}(x) & x_{n-1} \leq x \leq x_n \end{cases} \quad (4.1)$$

with cubic polynomials

$$p_k(x) = y_k + c_{k1}(x - x_k) + c_{k2}(x - x_k)^2 + c_{k3}(x - x_k)^3, \quad 1 \leq k \leq n-1 \quad (4.2)$$

The first and second derivatives of $p_k(x)$ are given as follows:

$$\begin{cases} \frac{\partial}{\partial x} p_k(x) = c_{k1} + 2c_{k2}(x - x_k) + 3c_{k3}(x - x_k)^2 \\ \frac{\partial^2}{\partial x^2} p_k(x) = 2c_{k2} + 6c_{k3}(x - x_k) \end{cases} \quad 1 \leq k \leq n-1 \quad (4.3)$$

A cubic spline can be constructed by interpolating a cubic polynomial p_k between each pair of consecutive points (x_k, y_k) and (x_{k+1}, y_{k+1}) with the following constraints:

1. Each polynomial passes through the point (x_{k+1}, y_{k+1}) , i.e.

$$p_k(x_{k+1}) = y_{k+1}, \quad 1 \leq k \leq n-1$$

2. First derivatives match at interior points:

$$\frac{\partial}{\partial x} p_k(x_{k+1}) = \frac{\partial}{\partial x} p_{k+1}(x_{k+1}), \quad 1 \leq k \leq n-2$$

3. Second derivatives match at interior points

$$\frac{\partial^2}{\partial x^2} p_k(x_{k+1}) = \frac{\partial^2}{\partial x^2} p_{k+1}(x_{k+1}), \quad 1 \leq k \leq n-2$$

4. First derivatives vanish at the end points:

Lakehead University

$$\frac{\partial}{\partial x} p_1(x_1) = 0, \quad \frac{\partial}{\partial x} p_{n-1}(x_n) = 0$$

The above constraints can be used to determine the coefficients c_{k1}, c_{k2} , and c_{k3} . For convenience, let $h_k = x_{k+1} - x_k, f_k = y_{k+1} - y_k, k = 1, 2, \dots, n-1$.

It follows from the first constraint that

$$y_{k+1} = y_k + c_{k1}(x_{k+1} - x_k) + c_{k2}(x_{k+1} - x_k)^2 + c_{k3}(x_{k+1} - x_k)^3, \quad 1 \leq k \leq n-1 \quad (4.4)$$

Equation (4.4) can be rewritten as the following:

$$f_k = c_{k1}h_k + c_{k2}h_k^2 + c_{k3}h_k^3, \quad 1 \leq k \leq n-1 \quad (4.5)$$

The second constraint can be expressed as

$$c_{k1} + 2c_{k2}(x_{k+1} - x_k) + 3c_{k3}(x_{k+1} - x_k)^2 = c_{k+1,1}, \quad 1 \leq k \leq n-2 \quad (4.6)$$

Equation (4.6) can be rewritten as the following:

$$c_{k1} + 2c_{k2}h_k + 3c_{k3}h_k^2 - c_{k+1,1} = 0, \quad 1 \leq k \leq n-2 \quad (4.7)$$

Similarly, from the third constraint, we get

$$2c_{k2} + 6c_{k3}(x_{k+1} - x_k) = 2c_{k+1,2}, \quad 1 \leq k \leq n-2 \quad (4.8)$$

Equation (4.8) can be rewritten as the following:

$$2c_{k2} + 6c_{k3}h_k - 2c_{k+1,2} = 0, \quad 1 \leq k \leq n-2 \quad (4.9)$$

It follows from the fourth constraint that

$$\begin{aligned} c_{k1} &= 0 \\ c_{n-1,1} + 2c_{n-1,2}h_{n-1} + 3c_{n-1,3}h_{n-1}^2 &= 0 \end{aligned} \quad (4.10)$$

Combining Equations (4.5), (4.7), (4.9), and (4.10), the following equation can be obtained.

$$A \begin{bmatrix} c_{11} \\ c_{12} \\ c_{13} \\ c_{21} \\ c_{22} \\ c_{23} \\ \vdots \\ \vdots \\ \vdots \\ c_{(n-1)1} \\ c_{(n-1)2} \\ c_{(n-1)3} \end{bmatrix} = \begin{bmatrix} 0 \\ 0 \\ 0 \\ f_1 \\ 0 \\ 0 \\ \vdots \\ \vdots \\ \vdots \\ 0 \\ f_{n-1} \end{bmatrix}$$

where

$$A = \begin{bmatrix} 1 & 0 & 0 & 0 & 0 & 0 & 0 & 0 & \dots & 0 & 0 & 0 \\ 1 & 2h_1 & 3h_1^2 & -1 & 0 & 0 & 0 & 0 & \dots & 0 & 0 & 0 \\ 0 & 2 & 6h_1 & 0 & -2 & 0 & 0 & 0 & \dots & 0 & 0 & 0 \\ h_1 & h_1^2 & h_1^3 & 0 & 0 & 0 & 0 & 0 & \dots & 0 & 0 & 0 \\ 0 & 0 & 0 & 1 & 2h_2 & 3h_2^2 & -1 & 0 & \dots & 0 & 0 & 0 \\ 0 & 0 & 0 & 0 & 2 & 6h_2 & 0 & -2 & \dots & 0 & 0 & 0 \\ 0 & 0 & 0 & h_2 & h_2^2 & h_2^3 & 0 & 0 & \dots & 0 & 0 & 0 \\ \vdots & \ddots & \vdots & \vdots & \vdots \\ 0 & 0 & 0 & 0 & 0 & 0 & 0 & 0 & \dots & 1 & 2h_{n-1} & 3h_{n-1}^2 \\ 0 & 0 & 0 & 0 & 0 & 0 & 0 & 0 & \dots & h_{n-1} & h_{n-1}^2 & h_{n-1}^3 \end{bmatrix}$$

As a result, the coefficients c_{ij} can be uniquely determined as the following:

$$\begin{bmatrix} c_{11} \\ c_{12} \\ c_{13} \\ c_{21} \\ c_{22} \\ c_{23} \\ \vdots \\ \vdots \\ \vdots \\ c_{(n-1)1} \\ c_{(n-1)2} \\ c_{(n-1)3} \end{bmatrix} = A^{-1} \begin{bmatrix} 0 \\ 0 \\ 0 \\ f_1 \\ 0 \\ 0 \\ f_2 \\ \vdots \\ \vdots \\ 0 \\ 0 \\ f_{n-1} \end{bmatrix} \quad (4.11)$$

The coefficients $(c_{11}, c_{12}, c_{13}, \dots, c_{n-1,1}, c_{n-1,2}, c_{n-1,3})$ determined from Equation (4.11) will be used to calculate foot trajectories.

For the hip trajectory planning, there are only three points (x_1, y_1) , (x_2, y_2) , and (x_3, y_3) , so the following constraints should be used to determine the cubic spline interpolation.

1. Each polynomial passes through the point (x_{k+1}, y_{k+1}) with $K=1$ and 2 , i.e.

$$p_1(x_2) = y_2, \quad p_2(x_3) = y_3$$

2. First derivatives match at the middle point:

$$\frac{\partial}{\partial x} p_1(x_2) = \frac{\partial}{\partial x} p_2(x_2)$$

3. Second derivatives match at the middle point:

$$\frac{\partial^2}{\partial x^2} p_1(x_2) = \frac{\partial^2}{\partial x^2} p_2(x_2)$$

4. First derivative at the starting point is the same as that at the end point:

$$\frac{\partial}{\partial x} p_1(x_1) = \frac{\partial}{\partial x} p_2(x_3)$$

5. Second derivative at the starting point is the same as that at the end point:

$$\frac{\partial^2}{\partial x^2} p_1(x_1) = \frac{\partial^2}{\partial x^2} p_2(x_3)$$

According to the constraints stated above, it is not difficult to prove that the coefficients can be calculated by the following equation.

$$\begin{bmatrix} h_1 & h_1^2 & h_1^3 & 0 & 0 & 0 \\ 1 & 2h_1 & 3h_1^2 & -1 & 0 & 0 \\ 0 & 2 & 6h_1 & 0 & -2 & 0 \\ 0 & 0 & 0 & h_2 & h_2^2 & h_2^3 \\ -1 & 0 & 0 & 1 & 2h_2 & 3h_2^2 \\ 0 & -2 & 0 & 0 & 2 & 6h_2 \end{bmatrix} \begin{bmatrix} c_{11} \\ c_{12} \\ c_{13} \\ c_{21} \\ c_{22} \\ c_{23} \end{bmatrix} = \begin{bmatrix} f_1 \\ 0 \\ 0 \\ f_2 \\ 0 \\ 0 \end{bmatrix}$$

As a result, the coefficients are given by

$$\begin{bmatrix} c_{11} \\ c_{12} \\ c_{13} \\ c_{21} \\ c_{22} \\ c_{23} \end{bmatrix} = \begin{bmatrix} h_1 & h_1^2 & h_1^3 & 0 & 0 & 0 \\ 1 & 2h_1 & 3h_1^2 & -1 & 0 & 0 \\ 0 & 2 & 6h_1 & 0 & -2 & 0 \\ 0 & 0 & 0 & h_2 & h_2^2 & h_2^3 \\ -1 & 0 & 0 & 1 & 2h_2 & 3h_2^2 \\ 0 & -2 & 0 & 0 & 2 & 6h_2 \end{bmatrix}^{-1} \begin{bmatrix} f_1 \\ 0 \\ 0 \\ f_2 \\ 0 \\ 0 \end{bmatrix} \quad (4.12)$$

In summary, the cubic spline interpolation (4.11) with $n=4$ will be used for calculating foot angle trajectories while (4.11) with $n=5$ for foot position trajectories. The hip trajectory will be determined by using the cubic interpolation (4.12)

4.2 Walking Patterns of Biped Robot

Biped walking is a periodic phenomenon [3]. A complete walking cycle can be divided into two phases: a single support phase and a double support phase. During the single support phase, while one foot is stationary on the ground, the other swings in the air from the rear to the front. During the double support phase, two feet are in contact with the ground.

Assume that odd steps start with the heel of the right foot leaving the ground and end with the heel of the right foot making first contact with the ground, while even steps begin when the heel of the left foot leaves the ground and terminates when the heel of the left foot touches the ground. Let T_c denote the period of the walking cycle and D_s the step size. Then the K -th step with K an odd number starts with the double support phase at $t = KT_c$ and ends with the single support phase at $t = (K + 1)T_c$. During this double support phase, the right foot starts to turn about the toe away from the ground until it reaches a certain angle θ_b with the ground. At the same time, the left foot begins to turn about the heel from the angle θ_f with the ground until it is fully on the ground. Let T_d be the time interval of the double support phase. Then, at $t = KT_c + T_d$, the double support phase ends and the single support phase starts. In this

single support phase, the left foot is stationary on the ground, whereas the right foot leaves the ground and swings from the rear to the front until its heel touches the ground with the right foot having the angle θ_f with the ground. Assume that the swing foot reaches its highest position at $t = KT_c + T_m$.

The $(K + 1)^{th}$ step is an even step. At this step, the first phase is also the double support phase. Unlike the previous step, the left foot turns about the toe away from the ground and the right foot turns from the angle θ_f toward the ground until the left foot reaches the angle θ_b with the ground and the right foot is on the ground. The double support phase ends and the single support phase begins at $t = (K + 1)T_c + T_d$. As soon as the double support phase terminates, the left foot starts leaving the ground and swings until the heel of the left foot gets in contact with the ground at the angle θ_f while the right foot stays on the ground. A consecutive walking simulation is shown in Figure 4.1.

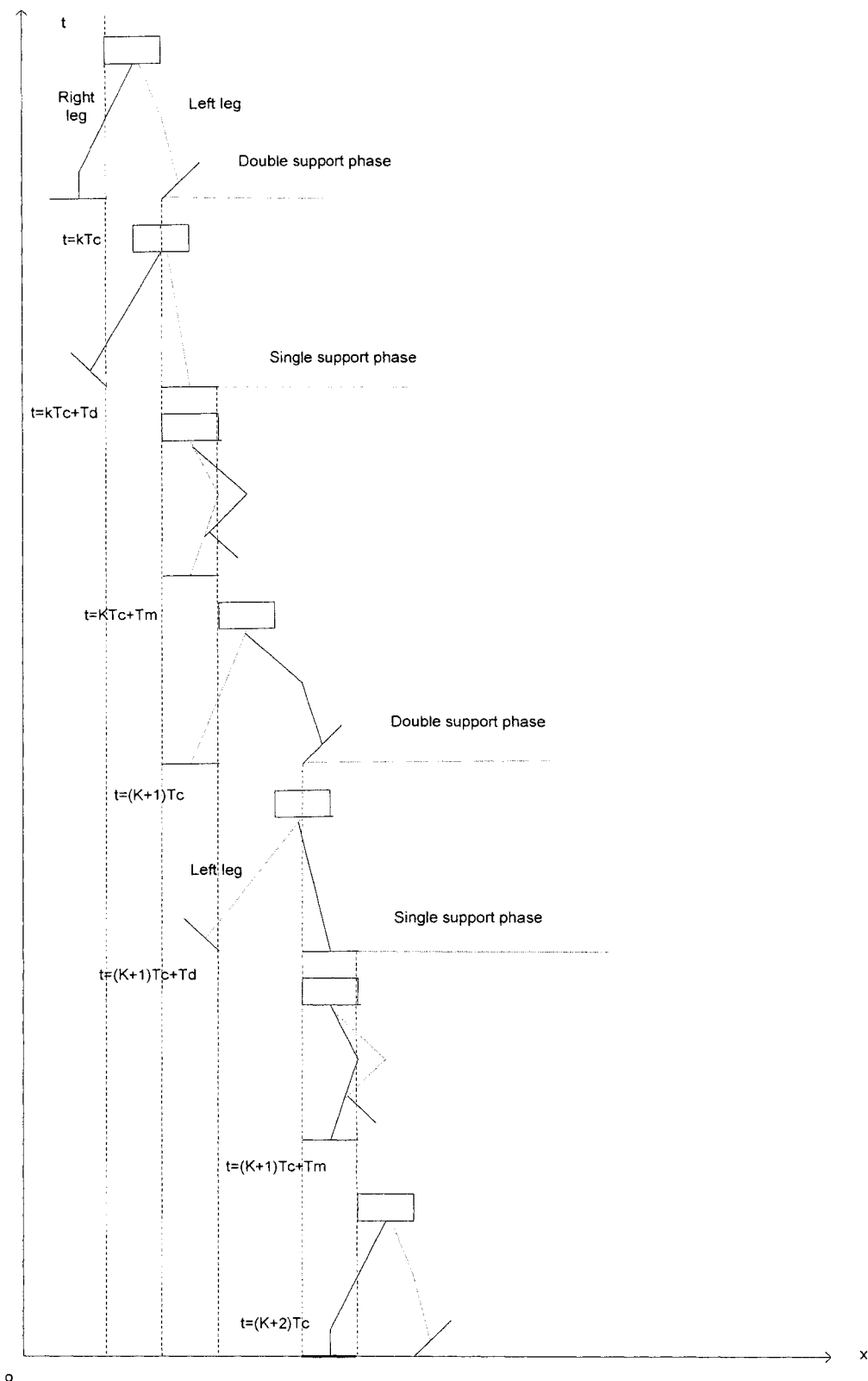
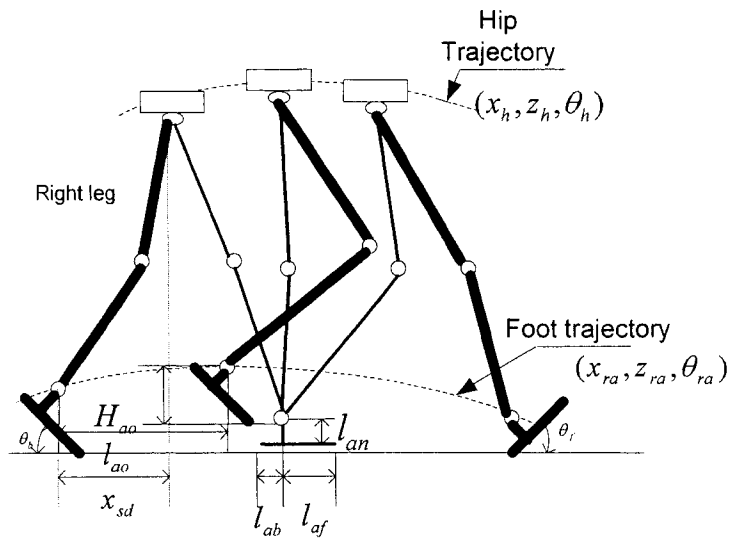
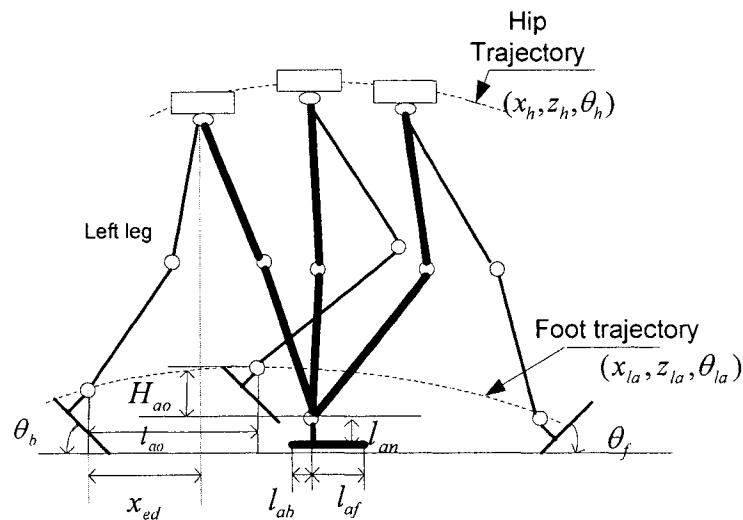


Figure 4.1 Walking cycle: single and double support phases

Assume that the biped robot walks straight forward, so that the lateral position of both feet is constant, that is, the y coordinates of both feet do not change with time. With this assumption, the right foot trajectory can be denoted by $(x_{ra}(t), z_{ra}(t), \theta_{ra}(t))$ and the left foot trajectory by $(x_{la}(t), z_{la}(t), \theta_{la}(t))$ where $(x_{ra}(t), z_{ra}(t))$ and $(x_{la}(t), z_{la}(t))$ denote the coordinates of the right and left ankle position, respectively, $\theta_{ra}(t)$ and $\theta_{la}(t)$ represent the angles of the right and left foot with the ground, respectively. (see Figure 4.2)



(a) Walking parameters of the right leg



(b) Walking parameters of the left leg

Figure 4.2 Trajectories of the biped robot

The hip trajectory can be denoted by $(x_h(t), z_h(t), \theta_h(t))$ where $(x_h(t), z_h(t))$ is the coordinate of the hip position and $\theta_h(t)$ denotes the angle of the hip with respect to the vertical direction. Figure 4.2a and 4.2b show the right and left foot trajectories, respectively, together with the hip trajectory.

4.3 Foot Trajectories

Foot trajectories are determined according to the physical constraints on the feet. For example, the foot angles and positions are subject to certain geometric conditions and the derivatives of the foot trajectories are zero at the transition moment between the single support phase and double support phase. For simplicity, we start our analysis from the K -th step with K an odd number. It can be seen from Figure 4.2a that the right foot is subject to the following constraints[1]:

$$\theta_{ra}(t) = \begin{cases} \theta_{gs} & t = KT_c \\ \theta_b & t = KT_c + T_d \\ \theta_f & t = (K+1)T_c \\ \theta_{ge} & t = (K+1)T_c + T_d \\ \theta_{ge} & (K+1)T_c + T_d \leq t \leq (K+2)T_c \end{cases} \quad (4.13)$$

$$x_{ra}(t) = \begin{cases} KD_s & t = KT_c \\ KD_s + l_{an} \sin \theta_b + l_{af}(1 - \cos \theta_b) & t = KT_c + T_d \\ KD_s + l_{ao} & t = KT_c + T_m \\ (K+2)D_s - l_{an} \sin \theta_f - l_{ab}(1 - \cos \theta_b) & t = (K+1)T_c \\ (K+2)D_s & t = (K+1)T_c + T_d \\ (K+2)D_s & (K+1)T_c + T_d \leq t \leq (K+2)T_c \end{cases} \quad (4.14)$$

$$z_{ra}(t) = \begin{cases} l_{an} & t = KT_c \\ l_{af} \sin \theta_b + l_{an} \cos \theta_b & t = KT_c + T_d \\ H_{ao} & t = KT_c + T_m \\ l_{ab} \sin \theta_f + l_{an} \cos \theta_f & t = (K+1)T_c \\ l_{an} & t = (K+1)T_c + T_d \\ l_{an} & (K+1)T_c + T_d \leq t \leq (K+2)T_c \end{cases} \quad (4.15)$$

where θ_{gs} and θ_{ge} are the angles of the ground surface under the support foot, particularly θ_{gs} and θ_{ge} equal 0 on level ground. θ_b and θ_f are the angles of the right foot and the left foot as it leaves and lands on the ground, respectively. l_{ao} and H_{ao} denote the position of the highest point of the swing foot, $KT_c + T_m$ is the time when the swing foot reaches its highest point. l_{an} is the height of the foot, l_{af} is the length from the ankle joint to the toe, and l_{ab} is the length from the ankle joint to the heel.

Equations (4.13)-(4.15) are determined as follows: At the beginning of the double support phase, $t=KT_c$, the right foot is on the ground, which means that $\theta_{ra}(t) = \theta_b, x_{ra}(t) = KD_s, z_{ra}(t) = l_{an}$ when $t=KT_c$. At the end of double support phase, $t=KT_c+T_d$, the right foot has an angle of θ_b with the surface of the ground, which, according to the trigonometrical relations,

$$\theta_{ra}(t) = \theta_b, x_{ra}(t) = KD_s + l_{af} \sin \theta_b + l_{af} (1 - \cos \theta_b), z_{ra}(t) = l_{af} \sin \theta_b + l_{an} \cos \theta_b$$

as $t=KT_c+T_d$. When the swing leg reaches its highest point at $t=KT_c+T_m$, the foot angle is not specified and $x_{ra}(t) = KD_s + l_{ao}, z_{ra}(t) = H_{ao}$. At the end of single support phase, $t=(K+1)T_c$, the right foot has an angle of θ_f with the surface of the ground, which, according to the trigonometric relations,

$$\theta_{ra}(t) = \theta_f, x_{ra}(t) = (K+2)D_s - l_{an} \sin \theta_f - l_{ab} (1 - \cos \theta_f), z_{ra}(t) = l_{ab} \sin \theta_f + l_{an} \cos \theta_f$$

as $t=(K+1)T_c$. The right foot stay on the ground during $(K+1)T_c + T_d \leq t \leq (K+2)T_c$, which implies that $\theta_{ra}(t) = \theta_{ge}, x_{ra}(t) = (K+2)D_s, z_{ra}(t) = l_{an}$.

Since the entire sole surface of the right foot is stationary on the ground at $t = KT_c$ and during the period of time $(K+1)T_c + T_d \leq t \leq (K+2)T_c$, the following derivative constraints must be satisfied:

$$\dot{\theta}_{ra}(t) = \begin{cases} 0 & t = KT_c \\ 0 & (K+1)T_c + T_d \leq t \leq (K+2)T_c \end{cases} \quad (4.16)$$

$$\dot{x}_{ra}(t) = \begin{cases} 0 & t = KT_c \\ 0 & (K+1)T_c + T_d \leq t \leq (K+2)T_c \end{cases} \quad (4.17)$$

$$\dot{z}_{ra}(t) = \begin{cases} 0 & t = KT_c \\ 0 & (K+1)T_c + T_d \leq t \leq (K+2)T_c \end{cases} \quad (4.18)$$

Similarly, the left foot is subject to the following constraints:

$$\theta_{la}(t) = \begin{cases} \theta_{gs} & t = KT_c \\ \theta_b & t = KT_c + T_d \\ \theta_f & t = (K+1)T_c \\ \theta_{ge} & t = (K+1)T_c + T_d \\ \theta_{ge} & (K+1)T_c + T_d \leq t \leq (K+2)T_c \end{cases} \quad (4.19)$$

$$x_{la}(t) = \begin{cases} KD_s & t = KT_c \\ KD_s + l_{an} \sin \theta_b + l_{af}(1 - \cos \theta_b) & t = KT_c + T_d \\ KD_s + l_{ao} & t = KT_c + T_m \\ (K+2)D_s - l_{an} \sin \theta_f - l_{ab}(1 - \cos \theta_b) & t = (K+1)T_c \\ (K+2)D_s & t = (K+1)T_c + T_d \\ (K+2)D_s & (K+1)T_c + T_d \leq t \leq (K+2)T_c \end{cases} \quad (4.20)$$

$$z_{la}(t) = \begin{cases} l_{an} & t = KT_c \\ l_{af} \sin \theta_b + l_{an} \cos \theta_b & t = KT_c + T_d \\ H_{ao} & t = KT_c + T_m \\ l_{ab} \sin \theta_f + l_{an} \cos \theta_f & t = (K+1)T_c \\ l_{an} & t = (K+1)T_c + T_d \\ l_{an} & (K+1)T_c + T_d \leq t \leq (K+2)T_c \end{cases} \quad (4.21)$$

$$\dot{\theta}_{la}(t) = \begin{cases} 0 & t = KT_c \\ 0 & (K+1)T_c + T_d \leq t \leq (K+2)T_c \end{cases} \quad (4.22)$$

$$\dot{x}_{la}(t) = \begin{cases} 0 & t = KT_c \\ 0 & (K+1)T_c + T_d \leq t \leq (K+2)T_c \end{cases} \quad (4.23)$$

$$\dot{z}_{la}(t) = \begin{cases} 0 & t = KT_c \\ 0 & (K+1)T_c + T_d \leq t \leq (K+2)T_c \end{cases} \quad (4.24)$$

To generate a smooth trajectory, it is necessary that the first derivative be differentiable and the second derivative be continuous at all time t . So the third order spline interpolation method introduced in Section 4.1 can be used to generate the right foot trajectory based on the constraints defined by Equations (4.13)-(4.18), which guarantees the continuation of the second derivative. Similarly, the left foot trajectory can be calculated from the constraints defined by Equations (4.19)-(4.24) by the third order spline interpolation method. Note that there are four points for the foot angle constraints, $\theta_{ra}(t), \theta_{la}(t)$, so the third order spline interpolation (4.11) with $n=4$ must be used while the foot position constraints, $x_{ra}(t), z_{ra}(t), x_{la}(t), z_{la}(t)$, have five points, hence (4.11) with $n=5$ is

needed. By varying the values of constraint parameters $\theta_b, \theta_f, H_{ao}$ and l_{ao} , we can produce different foot trajectories.

4.4 Hip Trajectory

The hip trajectory is subject to only geometrical constraints imposed by the structure of the biped. Assume that the biped walks on the level ground. Then it is desirable to keep the trunk angle $\theta_h(t)$ at 90° with the ground. $z_h(t)$ is set to the constant H_z .

Let x_{sd} and x_{ed} denote distances along the x -axis from the hip to the ankle of the support foot at the start and the end of the single support phase, respectively (see Figure 4.2). Then $x_h(t)$ has the following constraint:

$$x_h(t) = \begin{cases} KD_s + x_{ed} & t = KT_c \\ (K+1)D_s - x_{sd} & t = KT_c + T_d \\ (K+1)D_s + x_{ed} & t = (K+1)T_c \end{cases} \quad (4.25)$$

To generate a smooth trajectory $x_h(t)$, the following derivative constraints must be satisfied:

$$\begin{aligned} \dot{x}_h(KT_c) &= \dot{x}_h((K+1)T_c) \\ \ddot{x}_h(KT_c) &= \ddot{x}_h((K+1)T_c) \end{aligned} \quad (4.26)$$

Equation (4.12), which is the third-order interpolation introduced in Section 4.1, can be used to determine the hip trajectory for $x_h(t)$ with the constraints (4.25)-(4.26).

Note that the values of x_{sd} and x_{ed} have big effects on the stability of a biped robot walking. [1] has proposed a method to design x_{sd} and x_{ed} so that the

biped robot has a largest stability margin. This thesis focuses on testing the tracking performance of the biped robot hanging from the track. So there is no stability problem in the test. Therefore, x_{sd} and x_{ed} are chosen as $0.45D_s$ to get a smooth hip trajectories.

4.5 Joint Trajectories

Desired joint trajectories $\theta'_2, \theta_3, \theta_4, \theta_5, \theta_6, \theta_7$ can be determined from the foot trajectories and the hip trajectory generated in Sections 4.4 and 4.5 by using inverse kinematics introduced in Section 3.3. In particular, for the foot trajectories $((x_{ra}(t), z_{ra}(t), \theta_{ra}(t)), (x_{la}(t), z_{la}(t), \theta_{la}(t)))$ and the hip trajectory $(x_h(t), z_h(t), \theta_h(t))$, the desired trajectories $\theta'_2, \theta_3, \theta_4, \theta_5, \theta_6, \theta_7$ can be calculated by using the following

Equations:

$$\theta_3 = \tan^{-1}(-\sqrt{1 - D_r^2}, D_r)$$

$$\theta'_2 = 90 - \tan^{-1} \frac{(z_{03} - z_{01})(l_2 \cos \theta_3 + l_1) - (x_{03} - x_{01})l_2 \sin \theta_3}{(z_{01} - z_{03})l_2 \sin \theta_3 - (x_{03} - x_{01})(l_2 \cos \theta_3 + l_1)} + \theta_1$$

$$\theta_4 = \theta_1 - \theta'_2 - \theta_3$$

$$\theta_6 = \tan^{-1}(-\sqrt{1 - D_l^2}, D_l), D_l \neq 0$$

$$\theta_7 = \tan^{-1} \frac{(z_{08} - z_{06})l_4 \sin \theta_6 + (x_{08} - x_{06})(l_4 \cos \theta_6 + l_5)}{(z_{06} - z_{08})(l_4 \cos \theta_6 + l_5) + (x_{08} - x_{06})l_4 \sin \theta_6} + \theta_8$$

$$\theta_5 = \theta_6 - \theta_7 + \theta_8$$

$$\dot{\theta}_3 = \frac{1}{\sqrt{1 - D_r^2}} \dot{D}_r, D_r \neq 1$$

Lakehead University

$$\dot{\theta}_2 = \frac{\dot{\beta}_1\beta - \beta_1\dot{\beta}}{\beta_2\beta} - \dot{\theta}_1 - \dot{\alpha}_r, \beta_2\beta \neq 0$$

$$\dot{\theta}_4 = \dot{\theta}_1 + \dot{\theta}_2 - \dot{\theta}_3 + \dot{\alpha}_r$$

$$\dot{\theta}_6 = \frac{1}{\sqrt{1-D_l^2}} \dot{D}_l, D_l \neq 1$$

$$\dot{\theta}_7 = \frac{\dot{\beta}_3\beta' - \beta_3\dot{\beta}'}{\beta_4\beta'} + \dot{\theta}_8, \beta_4\beta' \neq 0$$

$$\dot{\theta}_5 = \dot{\theta}_6 - \dot{\theta}_7 + \dot{\theta}_8$$

(4.27)

where

$$x_{01} = x_{ra}(t), z_{01} = z_{ra}(t), \theta_1 = \theta_{ra}(t)$$

$$x_{08} = x_{la}(t), z_{08} = z_{la}(t), \theta_8 = \theta_{la}(t)$$

$$x_{03} = x_h(t), z_{03} = z_h(t)$$

$$x_{06} = x_h(t), z_{06} = z_h(t)$$

4.6 Simulation Results

The biped robot's trajectories are comprised of two parts: foot trajectories and hip trajectory (see Figure 4.2). If we know both foot trajectories and the hip trajectory of the biped robot, all its joint trajectories can be determined by inverse kinematics. Therefore, the walking pattern can be determined by both foot trajectories and the hip trajectory. By using the third-order spline interpolation, the foot and hip trajectories can be generated.

The parameters of the biped robot are listed in Table 4.1. Simulations are carried out based on the parameters shown in Table 4.1. Simulation results for

the left foot, right foot, hip, and joint trajectories are shown in Figures 4.3-4.18. Figure 4.3 shows both left and right foot trajectories in x-axis. Figure 4.5 shows both left and right foot trajectories in z-axis. Figure 4.6 shows both left and right foot trajectories of the angles between the feet and floor. Figure 4.9 shows the hip trajectory in z-axis. Figures 4.11-4.18 show the ankle, knee, hip joint trajectories and their speed.

Table 4.1 Parameters of the biped robot

| | | | | | |
|--------------------|------------|------------|------------------------------|------------------------------|----------|
| Parameters(m) | l_{ao} | D_s | H_{ao} | l_1 | l_2 |
| Values | 0.95Ds | 0.4 | 0.14 | 0.3 | 0.3 |
| Parameters(m) | l_3 | l_4 | l_5 | l_0 | l_{ab} |
| Values | 0.3 | 0.3 | $\sqrt{l_{an}^2 + l_{af}^2}$ | $\sqrt{l_{an}^2 + l_{af}^2}$ | 0.1 |
| Parameters(m) | l_{af} | l_{an} | H_{hman} | H_{hmin} | |
| Values | 0.13 | 0.1 | 0.64 | 0.64 | |
| Parameters(s) | T_d | T_m | T_c | | |
| Values | $0.2T_c$ | $0.55T_c$ | 1.0 | | |
| Parameters(degree) | θ_e | θ_s | | | |
| Values | 0 | 0 | | | |
| Parameters(m) | X_{sd} | X_{ed} | | | |
| Values | $0.45 D_s$ | $0.45 D_s$ | | | |

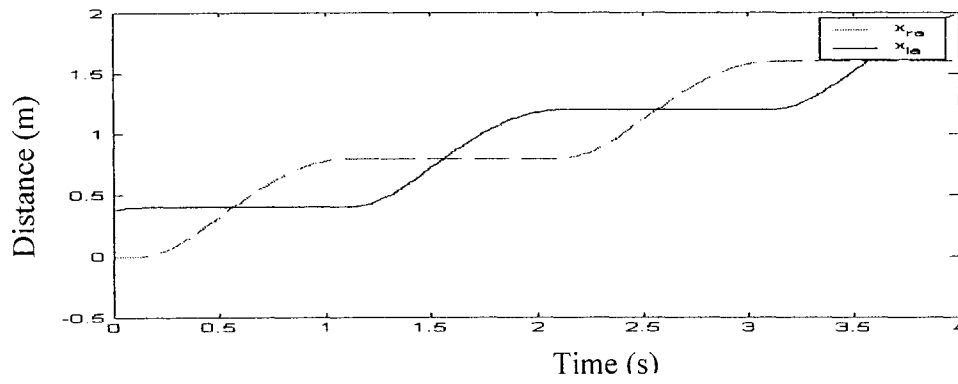


Figure 4.3 Right and left ankle trajectories in x axis

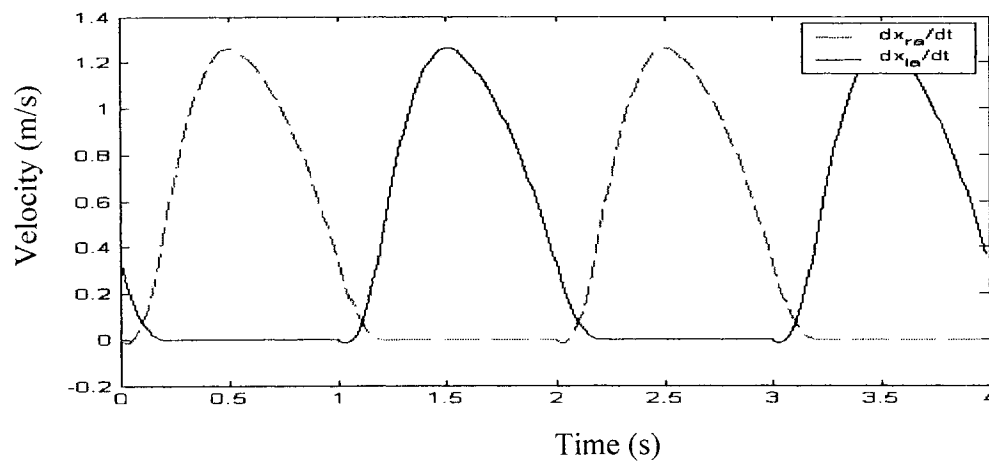


Figure 4.4 Right and left ankle velocities in x axis

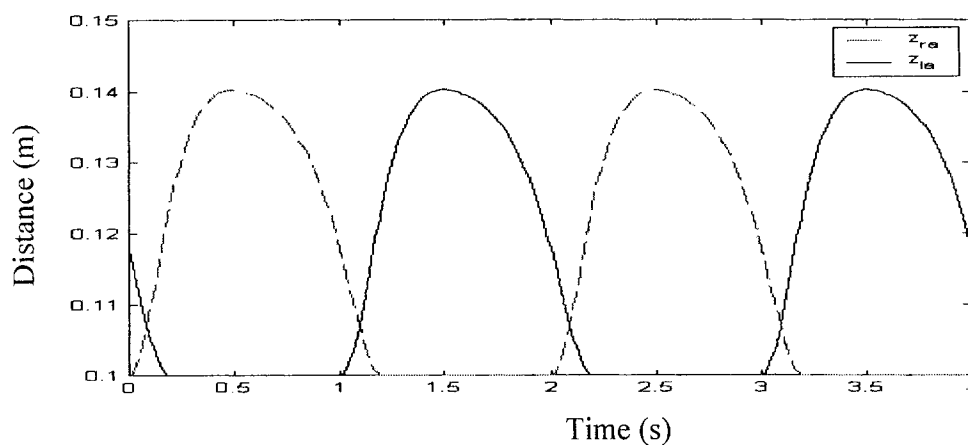


Figure 4.5 Right and left ankle trajectories in z axis

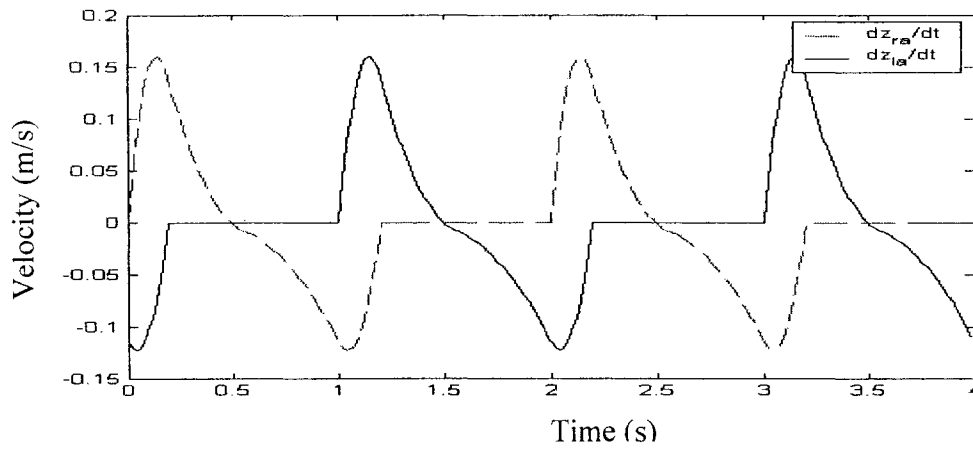


Figure 4.6 Right and left ankle velocities in z axis

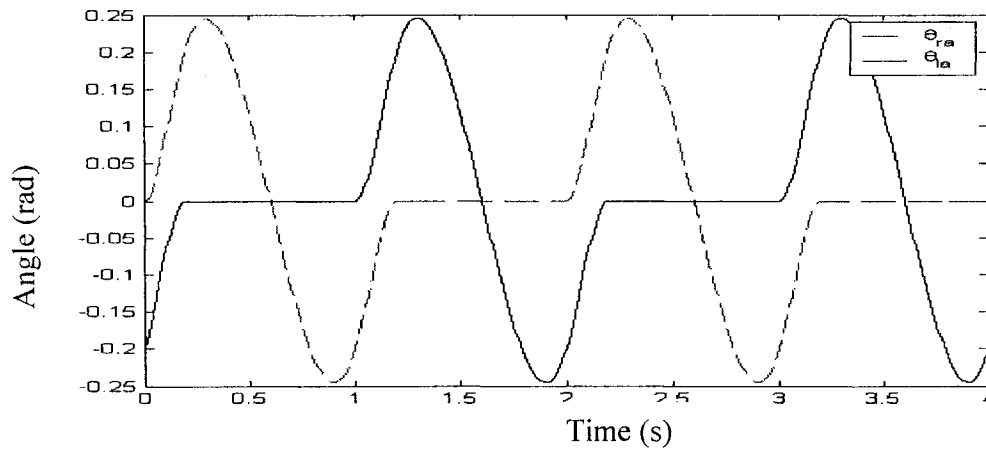


Figure 4.7 Right and left foot angles

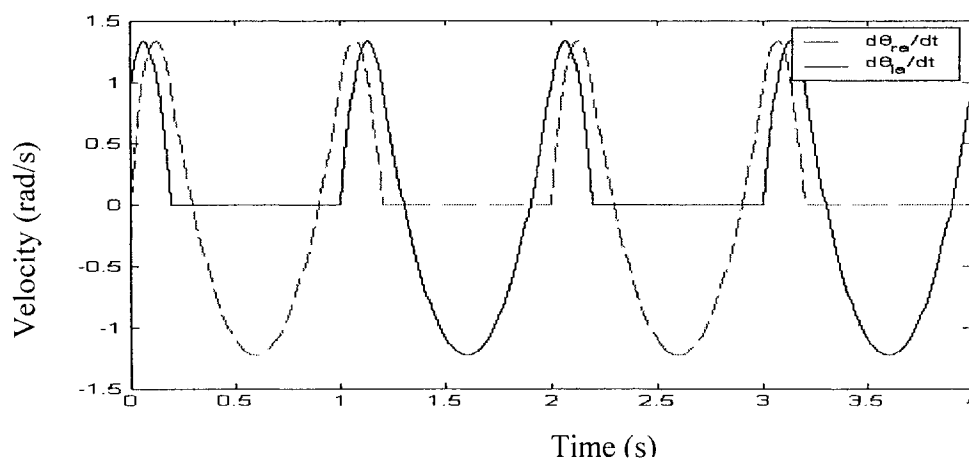


Figure 4.8 Right and left foot angular velocities

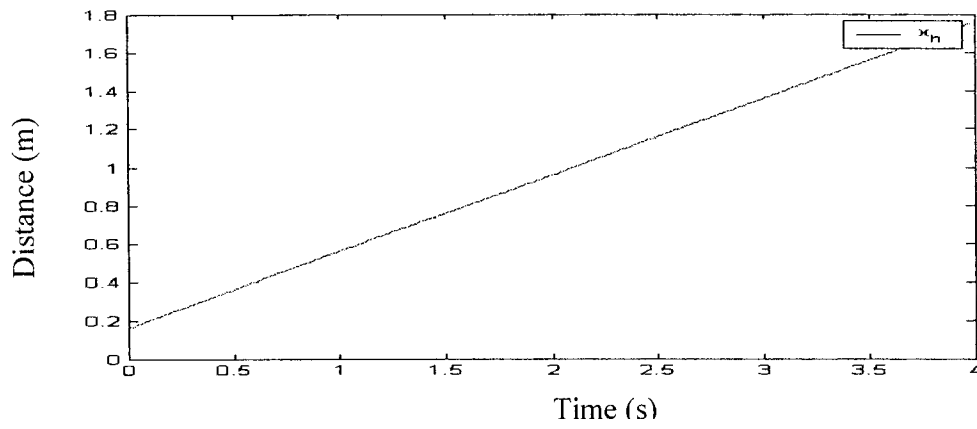


Figure 4.9 Hip trajectory in x axis

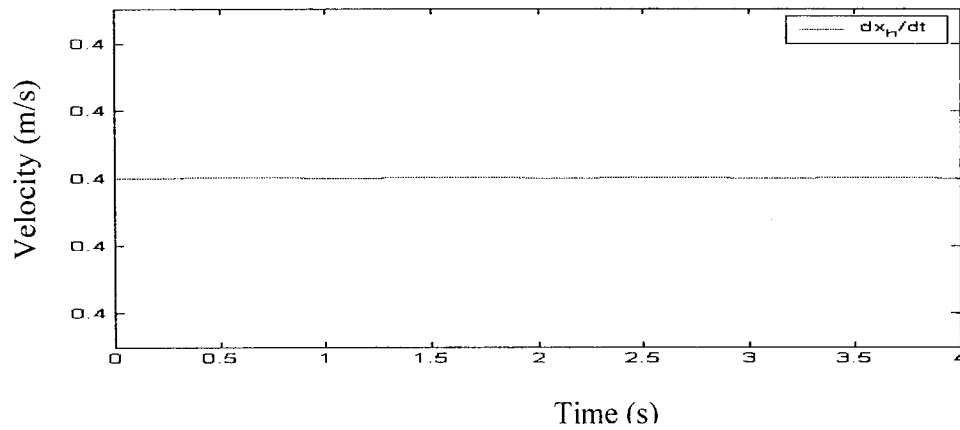


Figure 4.10 Hip velocity in x axis

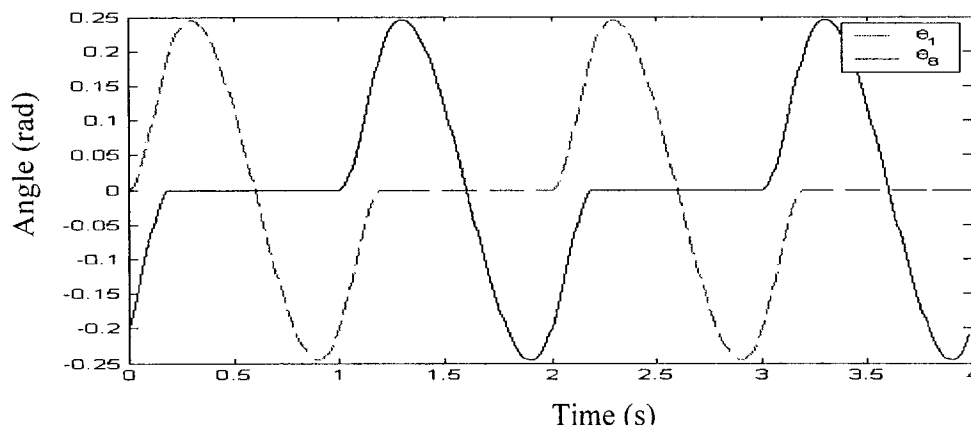


Figure 4.11 Foot angle trajectories

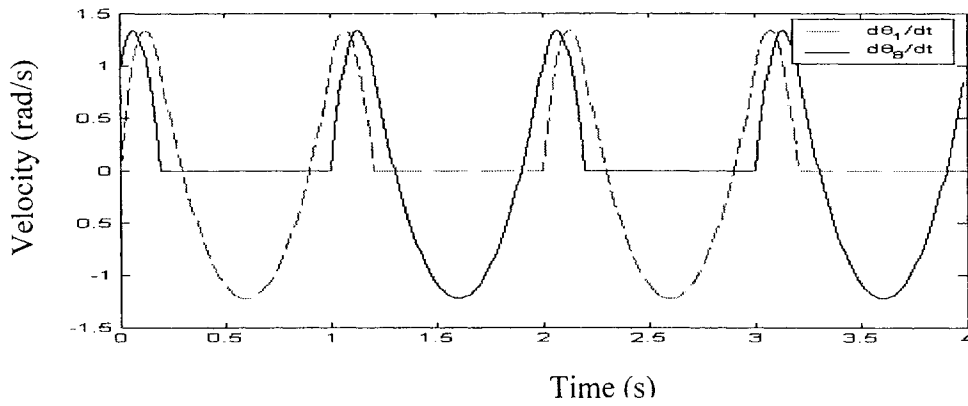


Figure 4.12 Foot angular velocities

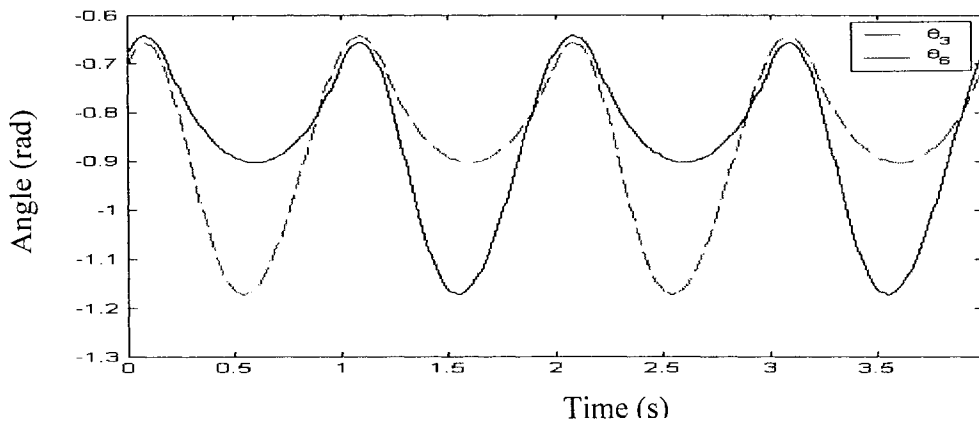


Figure 4.13 Knee joint trajectories

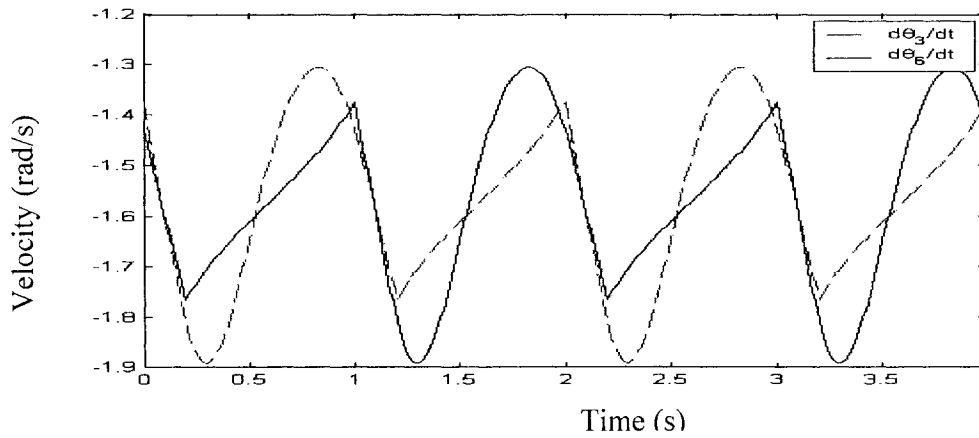


Figure 4.14 Knee joint velocities

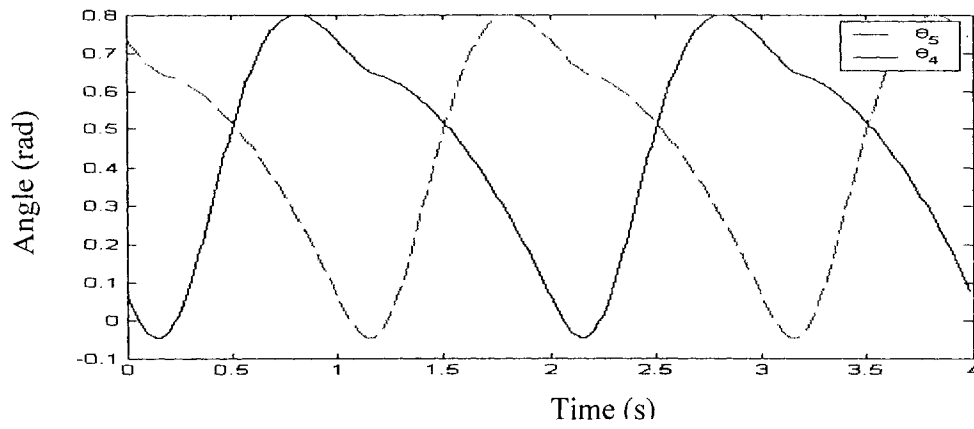


Figure 4.15 Hip joint trajectories

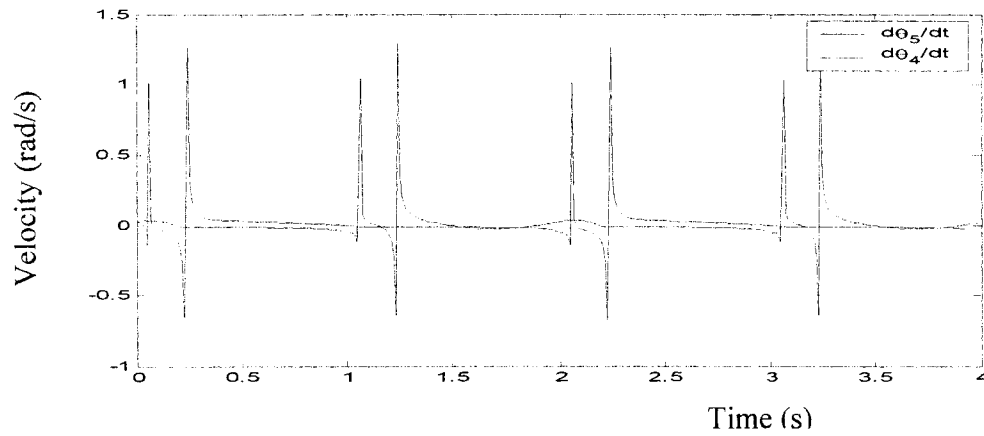


Figure 4.16 Hip joint velocities

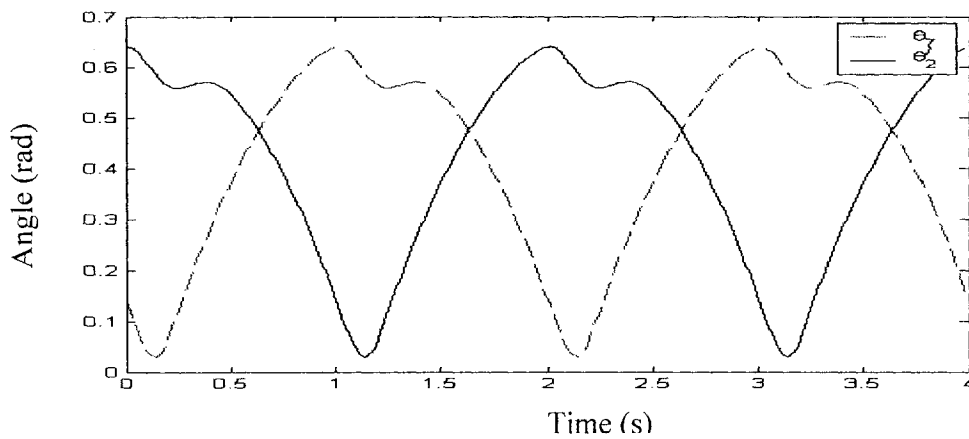


Figure 4.17 Ankle joint trajectories

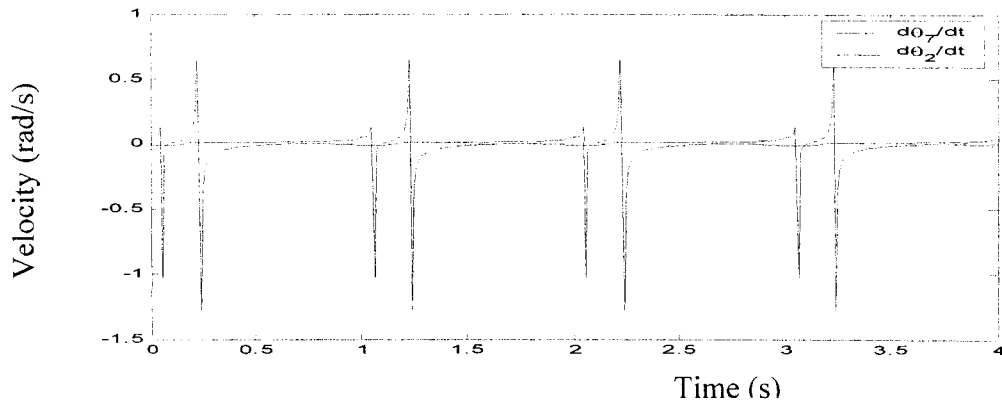


Figure 4.18 Ankle joint velocities

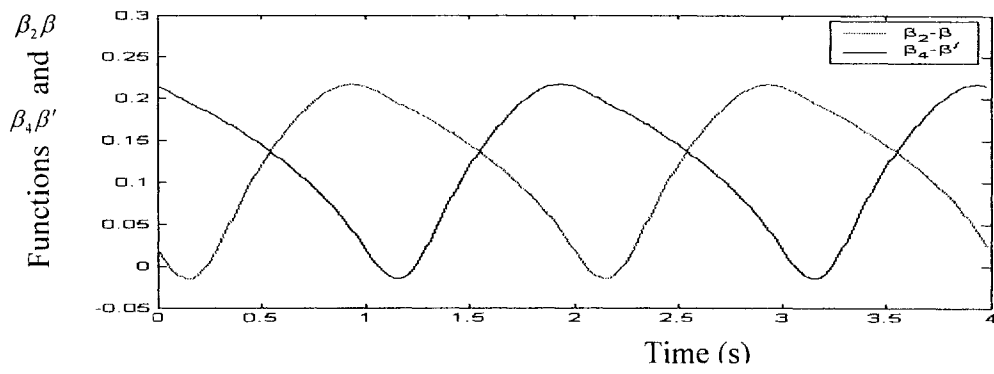


Figure 4.19 $\beta_4\beta'$ and $\beta_2\beta$ trajectories

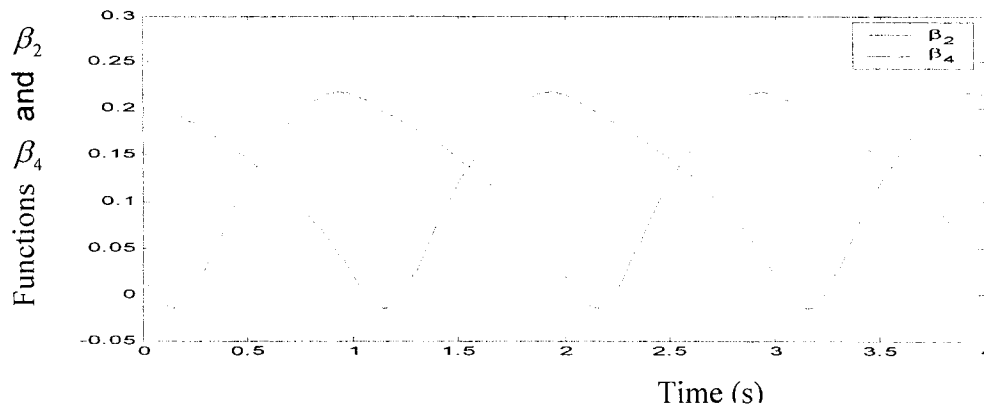


Figure 4.20 β_4 and β_2 trajectories

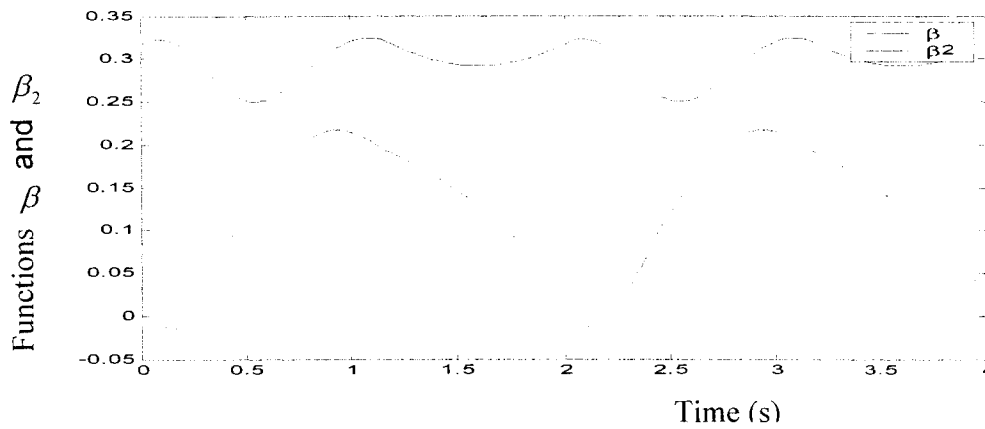


Figure 4.21 β and β_2 trajectories

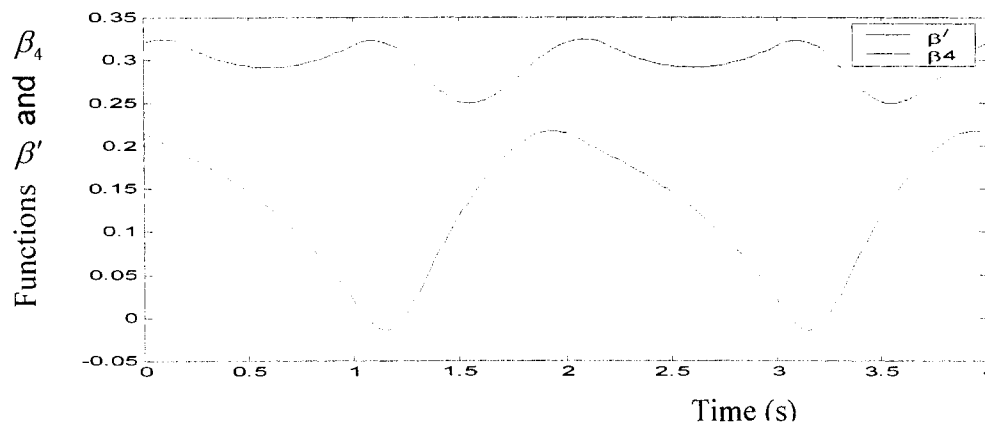


Figure 4.22 β' and β_4 trajectories

The simulation results show that the foot and hip trajectories can be determined based on the third order spline interpolation. On the other hand, the ankle, knee and hip joint trajectories can be determined based on inverse kinematics. Finally, the walking pattern is simulated by using both Matlab and OpenGL.

Chapter 5

PID Controller Design

5.1 PID Control Theory

PID controllers can be applied to most of industrial robots. A PID controller consists of three parts: the proportional, integral and derivative components.

Proportional control is a primary alternative to on-off control. If the error between the actual output signal and its desired value is large, then a large input signal is applied. If the error is small, then a small input signal is used. Mathematically, the control signal in a proportional controller is given as follows:

$$u = K_p e \quad (5.1)$$

where e is the error signal, K_p is the proportional gain of the controller and indicates the change in the control signal per unit change in the error signal.

Proportional control is satisfactory if requirements on a control system are not strict. However, in most cases, it is required to design a controller to meet some strict requirements on the response time, overshoot, and steady-state error. It has been proven that a large proportional gain can reduce the steady-state error with a large overshoot and sometime it gives rise to an oscillatory response. Therefore, it is hard, even impossible for many practical systems, to find a proportional controller to achieve certain control objectives.

Proportional-Derivative (PD) controllers of the form

$$u = K_p e + K_d \frac{de}{dt} \quad (5.2)$$

are widely used in industries where K_d is the derivative gain.

The controller output of the PD controller is calculated based on both the error and the rate of change of the error with respect to time. The net effect is a slower response with a far less overshoot than a proportional controller alone. The derivative action may also result in difficulties if high frequency measurement noises are present. These difficulties are normally resolved using additional filtering techniques.

Generally speaking, steady-state errors can be reduced by integral control.

The PID controller is defined by

$$u = K_p e + K_i \int e dt + K_d \frac{de}{dt} \quad (5.3)$$

where K_i is the integral gain.

Each of the three components of the PID controller has its own distinctive function to fulfill certain control objectives. In real applications, different combinations of the P, I and D components may be used depending mainly on the process and the control requirements.

For the biped robot built for experiments, both PID and PD controllers are used to control robot walking.

5.2 Control Design

In this section, PD and PID controllers will be designed for the biped robot based on the desired joint trajectories derived in Chapter 4. To this end, we still use θ'_2, θ'_3 and θ'_4 to denote the desired angles of the right ankle, knee, and hip joints, respectively, while α_2, α_3 and α_4 represent their actual angles. $\dot{\theta}'_2, \dot{\theta}'_3, \dot{\theta}'_4, \dot{\alpha}_2, \dot{\alpha}_3$ and $\dot{\alpha}_4$ are the desired angular velocities and the actual angular velocities of the right ankle, knee, and hip joints, respectively. On the other hand, θ_5, θ_6 and θ_7 represent the desired angles of the left hip, knee, and ankle joints, respectively, whereas α_5, α_6 and α_7 represent their actual angles. $\dot{\theta}_5, \dot{\theta}_6, \dot{\theta}_7, \dot{\alpha}_5, \dot{\alpha}_6$ and $\dot{\alpha}_7$ are the desired angular velocities and the actual angular velocities of the left hip, knee and ankle, respectively. Then, a PID controller can be used for each joint motor to achieve walking pattern control. PID controllers are given as follows:

$$\begin{aligned}
 u_1 &= u_{01} + K_{p1}(\theta'_2 - \alpha_2) + K_{d1}(\dot{\theta}'_2 - \dot{\alpha}_2) + K_{i1} \int (\theta'_2 - \alpha_2) dt \\
 u_2 &= u_{02} + K_{p2}(\theta'_3 - \alpha_3) + K_{d2}(\dot{\theta}'_3 - \dot{\alpha}_3) + K_{i2} \int (\theta'_3 - \alpha_3) dt \\
 u_3 &= u_{03} + K_{p3}(\theta'_4 - \alpha_4) + K_{d3}(\dot{\theta}'_4 - \dot{\alpha}_4) + K_{i3} \int (\theta'_4 - \alpha_4) dt \\
 u_4 &= u_{04} + K_{p4}(\theta_5 - \alpha_5) + K_{d4}(\dot{\theta}_5 - \dot{\alpha}_5) + K_{i4} \int (\theta_5 - \alpha_5) dt \\
 u_5 &= u_{05} + K_{p5}(\theta_6 - \alpha_6) + K_{d5}(\dot{\theta}_6 - \dot{\alpha}_6) + K_{i5} \int (\theta_6 - \alpha_6) dt \\
 u_6 &= u_{06} + K_{p6}(\theta_7 - \alpha_7) + K_{d6}(\dot{\theta}_7 - \dot{\alpha}_7) + K_{i6} \int (\theta_7 - \alpha_7) dt
 \end{aligned} \tag{5.4}$$

where u_i is the voltage of the motor i or the duty-cycle to the motor driver for the motor i , u_{0i} is the desired voltage of the motor i or the desired duty-cycle to the

Lakehead University

motor driver for the motor i , which corresponds to the value that makes the link stop, K_{pi}, K_{di}, K_{ii} are the proportional gain, derivative gain, integral gain, respectively.

For the biped robot used in our experiments, u_i represents the duty-cycle because each motor is controlled through a motor driver, which accepts a PWM signal.

Note that theoretically u_{0i} are the desired duty ratios corresponding to the designed trajectories, which can be calculated based on the dynamical model of the biped robot. However, the dynamic model is very complicated for the biped robot, it might take too much time for the computer to calculate the u_{0i} . Therefore, $u_{0i} = 50\%$ will be used to achieve the tracking control for the biped robot in the lab, which might give big errors.

Chapter 6

Experimental Results

The PID controllers designed in Chapter 5 are implemented on the biped robot hung on the track. The desired trajectories used in the experiments are determined by using the inverse kinematics based on the foot and hip trajectories, which were calculated by the third order spline interpolation method discussed in Chapter 4.

Two sets of experiments were carried out. The first set of experiments was done for the PD controllers while the second set of experiments was performed for the PID controllers (see Figure 6.1).

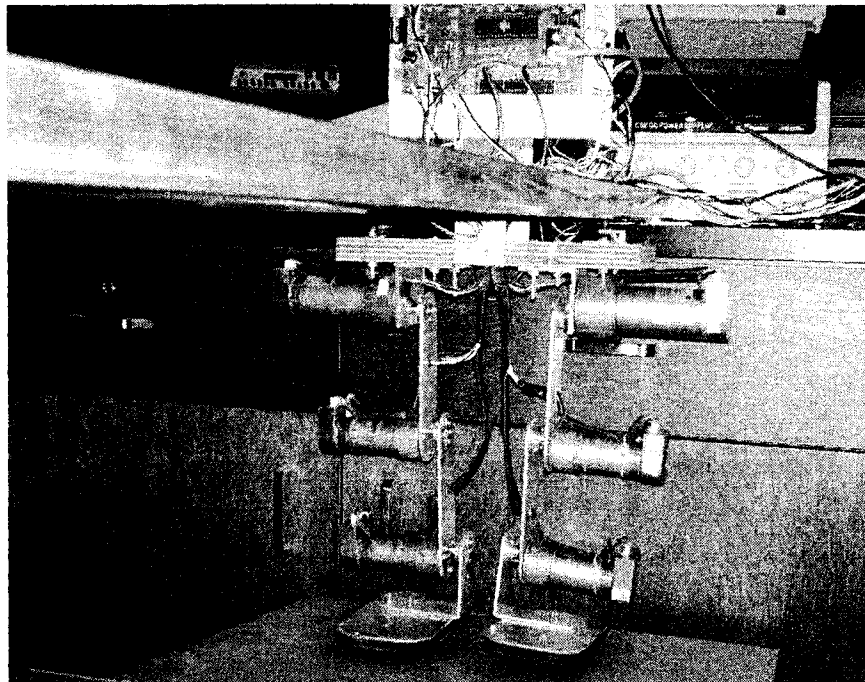


Figure 6.1 The biped robot experimental setup

6.1 Experiment with PD Controllers

In the first step, the controller gains are chosen as

kp1=50.0; kp2=50.0; kp3=50.0; kd1=0.01; kd2=0.01; kd3=0.01;

kp4=50.0; kp5=50.0; kp6=50.0; kd4=0.01; kd5=0.01; kd6=0.01;

in order to speed up the biped robot at the beginning of walk. From the second step, lots of parameters are tried to use in the experiment. The following suitable controller gains are used.

- **Control parameters I**

kp1=110.0; kp2=200.0; kp3=140.0; kd1=0.01; kd2=0.01; kd3=0.01;

kp4=110.0; kp5=200.0; kp6=150.0; kd4=0.01; kd5=0.01; kd6=0.01;

Control parameters II

kp1=100.0; kp2=180.0; kp3=150.0; kd1=0.1; kd2=0.01; kd3=0.1;

kp4=100.0; kp5=180.0; kp6=150.0; kd4=0.1; kd5=0.01; kd6=0.1;

The experimental results with the control parameters I and II are shown in Figures 6.2-6.25.

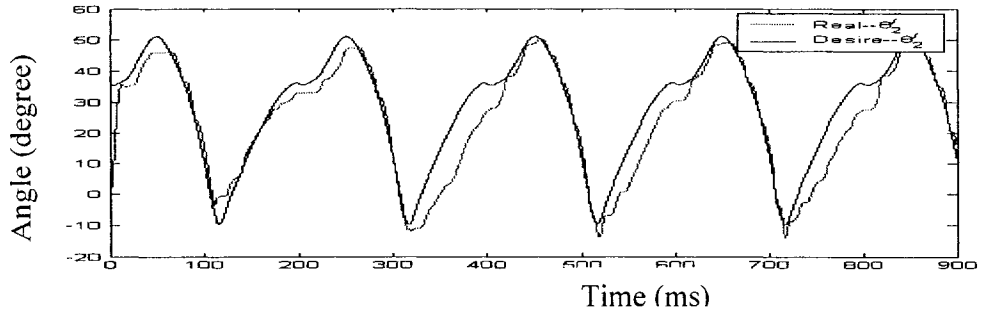


Figure 6.2 Tracking performance for the right ankle (Parameter I)

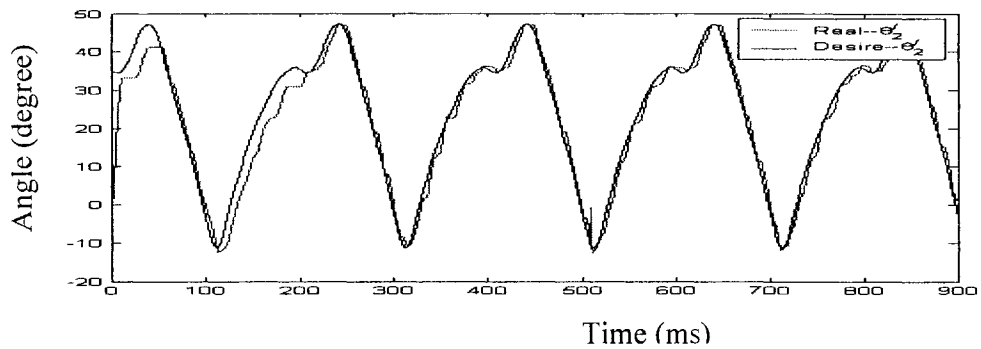


Figure 6.3 Tracking performance for the right ankle (Parameter II)

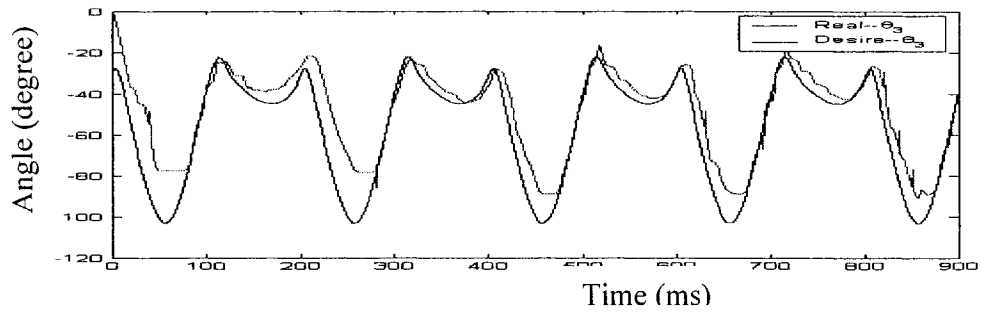


Figure 6.4 Tracking performance for the right knee (Parameter I)

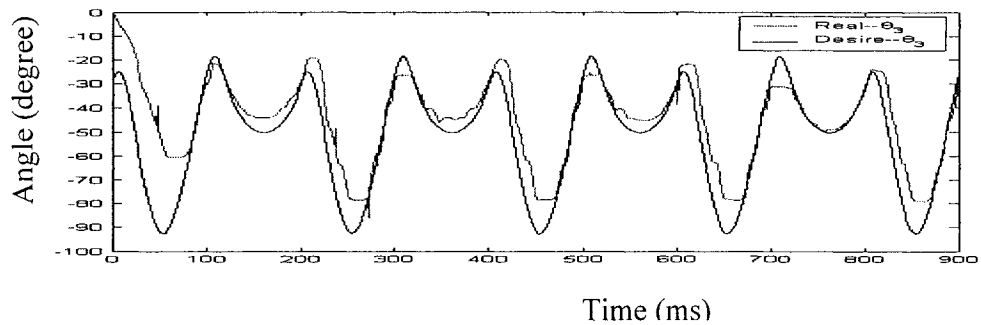


Figure 6.5 Tracking performance for the right knee (Parameter II)

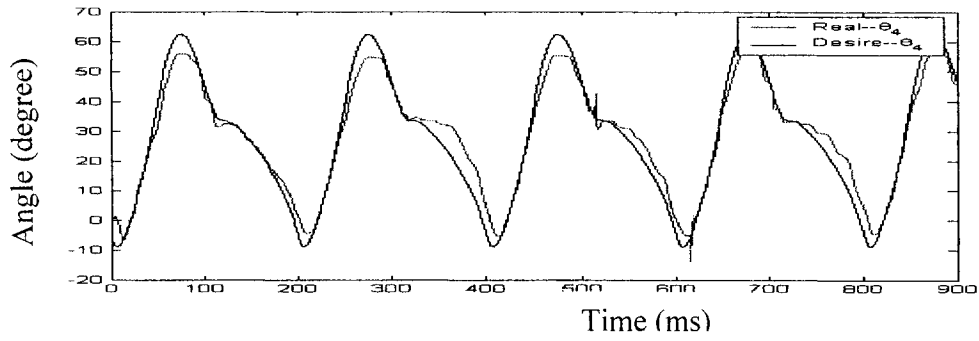


Figure 6.6 Tracking performance for the right hip (Parameter I)

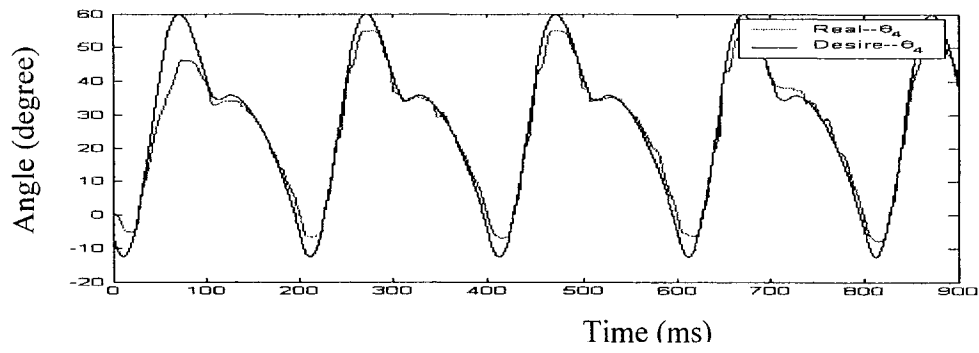


Figure 6.7 Tracking performance for the right hip (Parameter II)

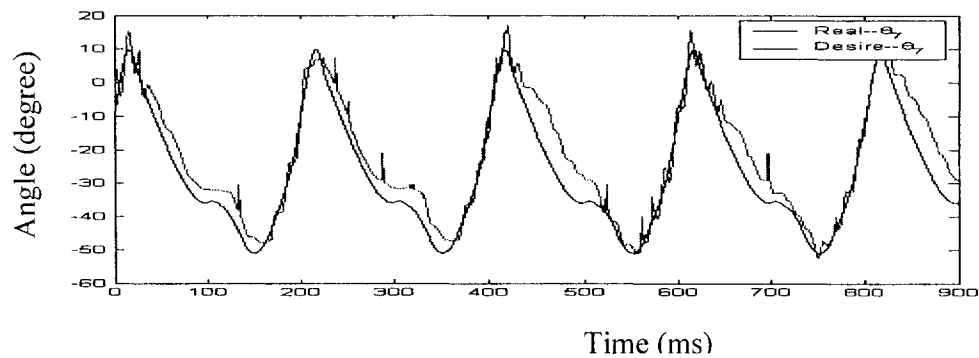


Figure 6.8 Tracking performance for the left ankle (Parameter I)

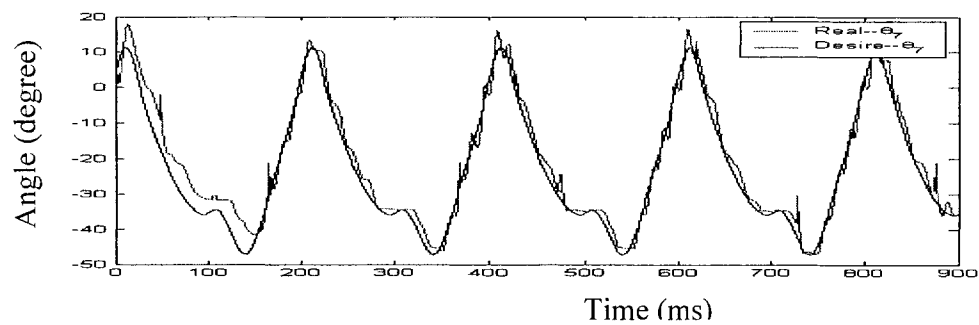


Figure 6.9 Tracking performance for the left ankle (Parameter II)

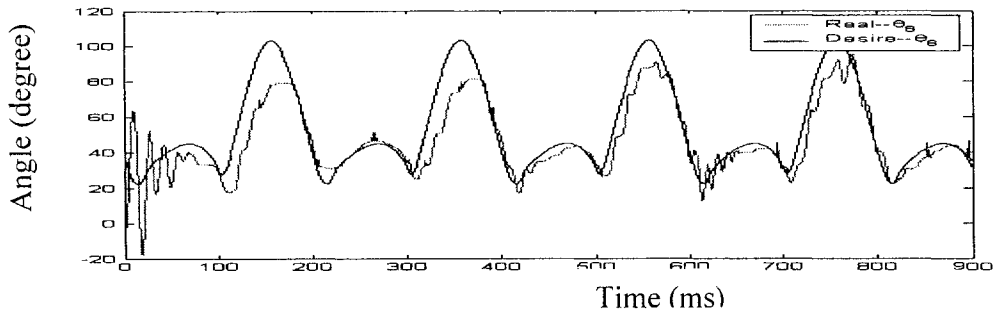


Figure 6.10 Tracking performance for the left knee (Parameter I)

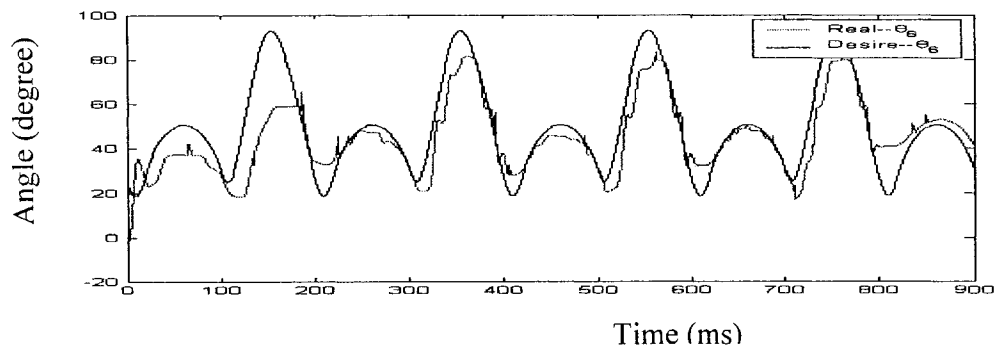


Figure 6.11 Tracking performance for the left knee (Parameter II)

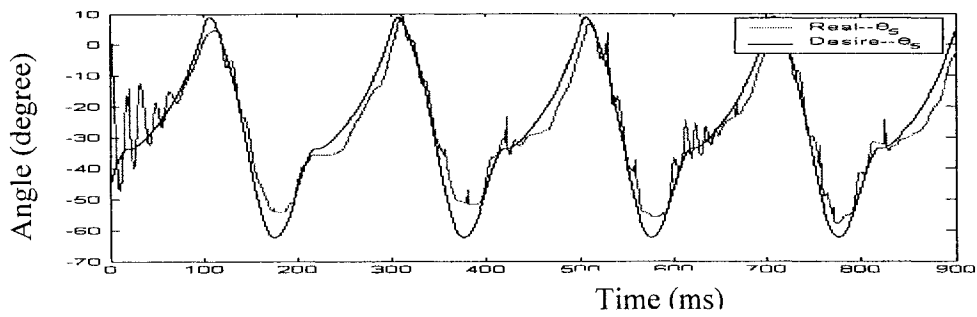


Figure 6.12 Tracking performance for the left hip (Parameter I)

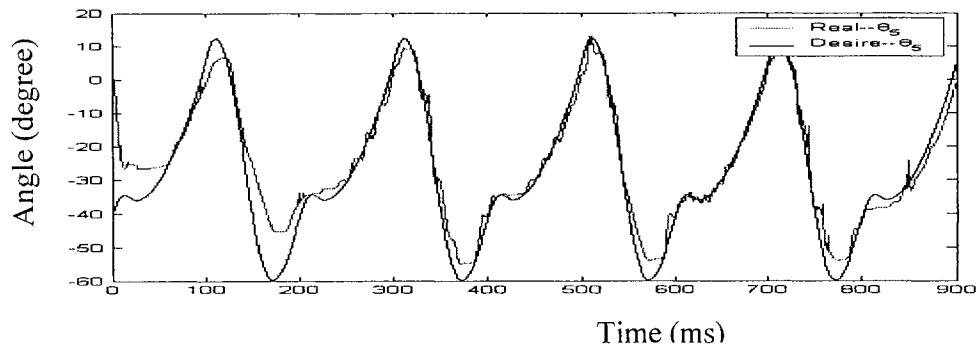


Figure 6.13 Tracking performance for the left hip (Parameter II)

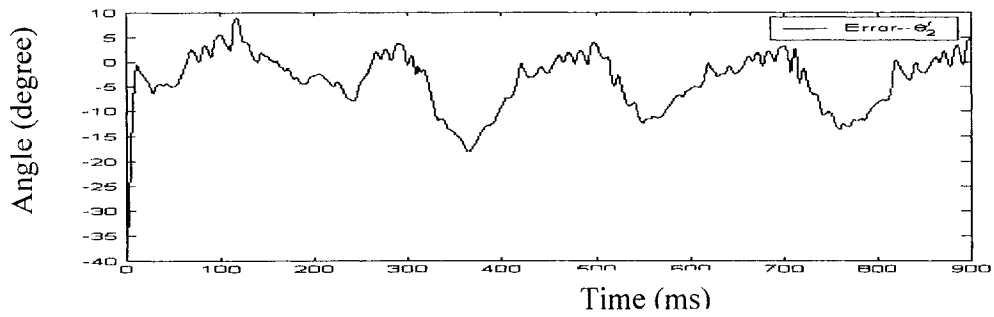


Figure 6.14 Tracking error for the right ankle (Parameter I)

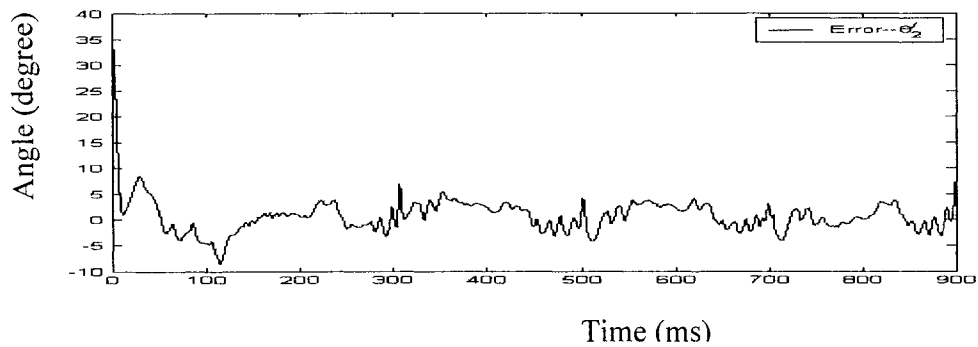


Figure 6.15 Tracking error for the right ankle (Parameter II)

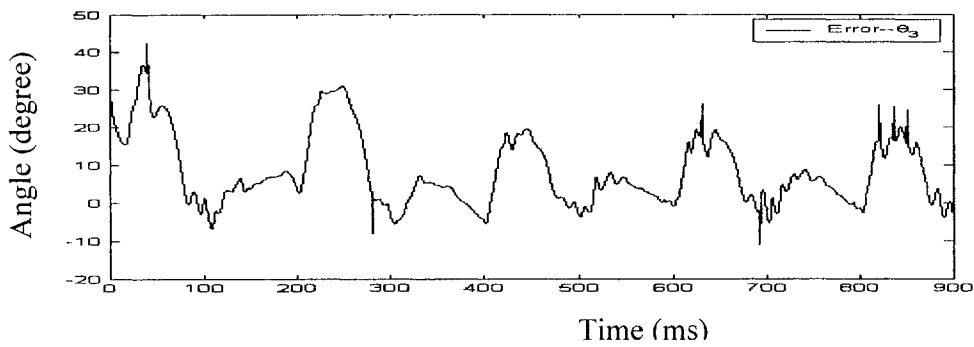


Figure 6.16 Tracking error for the right knee (Parameter I)

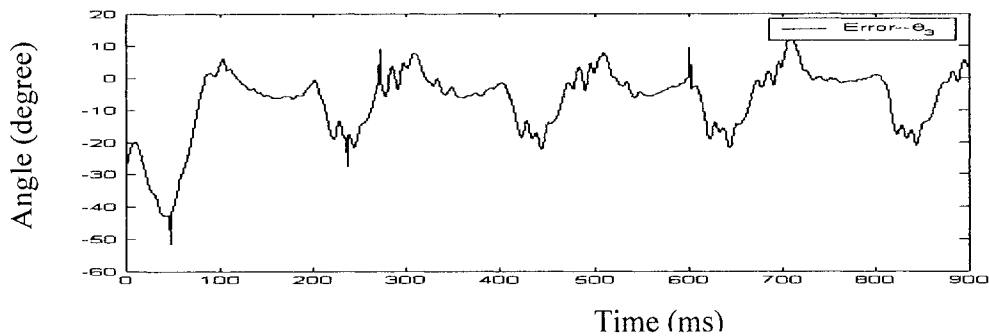


Figure 6.17 Tracking error for the right knee (Parameter II)

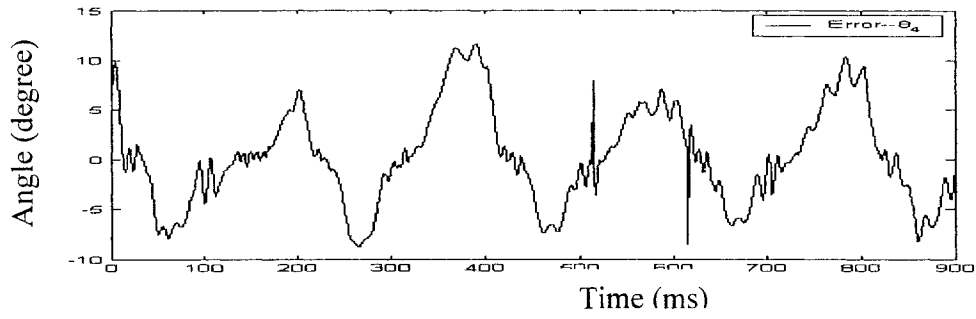


Figure 6.18 Tracking error for the right hip (Parameter I)

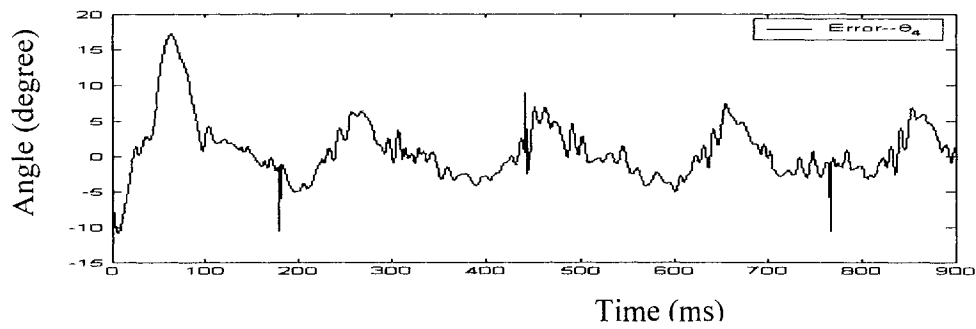


Figure 6.19 Tracking error for the right hip (Parameter II)

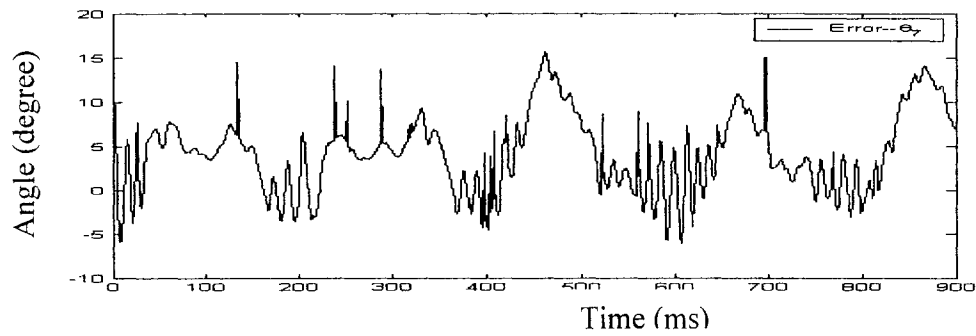


Figure 6.20 Tracking error for the left ankle (Parameter I)

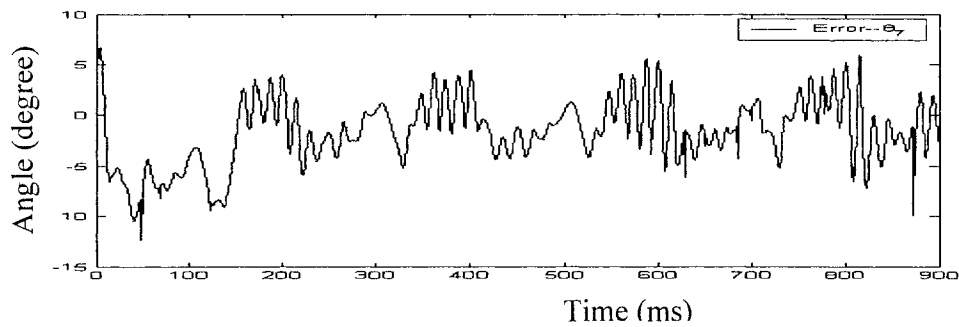


Figure 6.21 Tracking error for the left ankle (Parameter II)

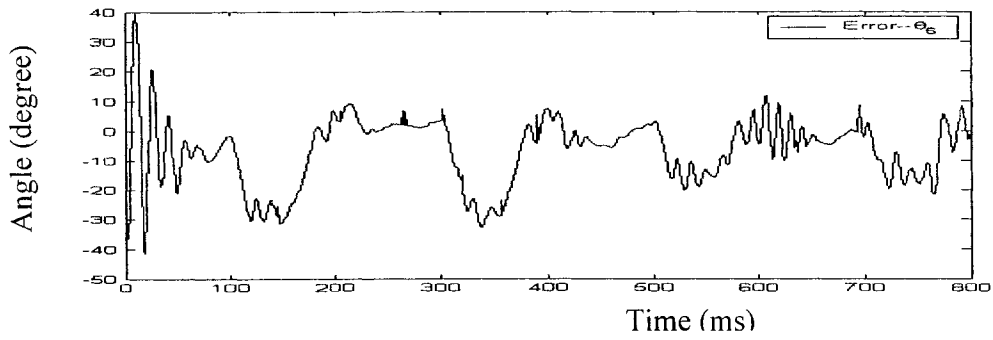


Figure 6.22 Tracking error for the left knee (Parameter I)

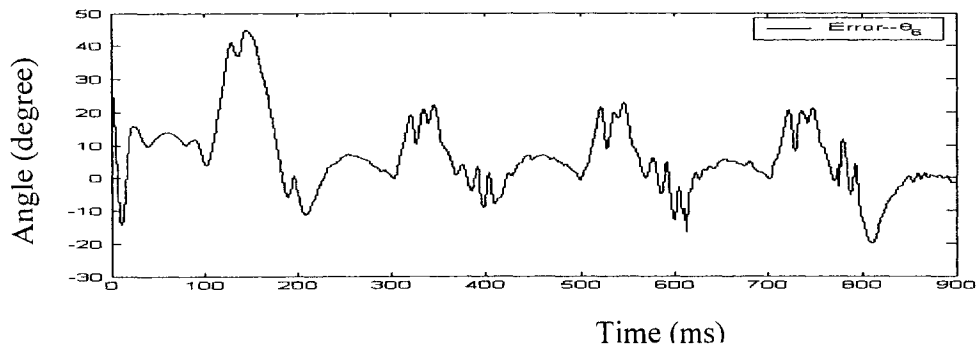


Figure 6.23 Tracking error for the left knee (Parameter II)

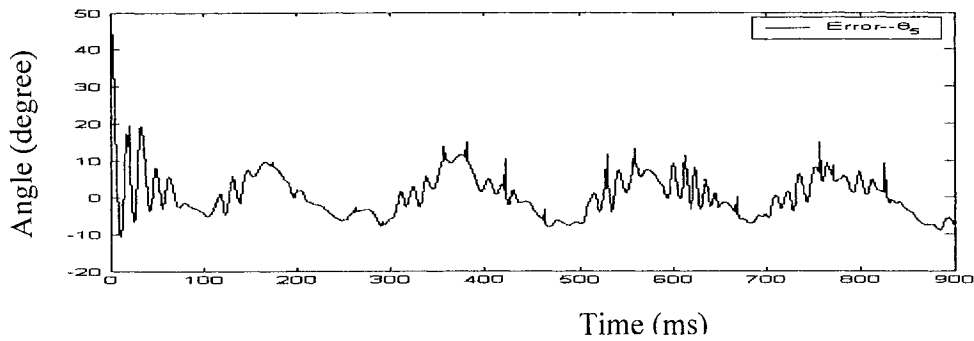


Figure 6.24 Tracking error for the left hip (Parameter I)

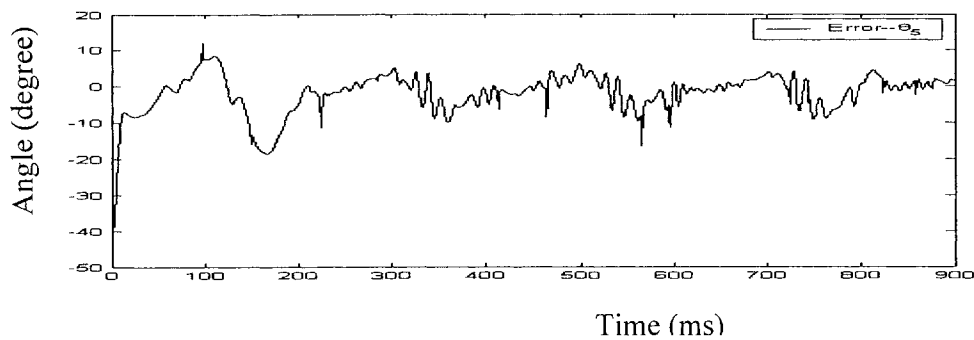


Figure 6.25 Tracking error for the left hip (Parameter II)

Lakehead University

Figures 6.2 to 6.13 show the real and desired angle trajectories of both legs of the biped robot with the control parameters I and II, respectively. Figures 6.14 to 6.25 show the tracking errors between the real and desired angles for the biped robot with the control parameters I and II, respectively.

6.2 Experiment with PID Controllers

In the first step, the controller gains are chosen as

$kp1=50.0$; $kp2=50.0$; $kp3=50.0$; $kd1=0.01$; $kd2=0.01$; $kd3=0.01$;

$ki1=0.01$; $ki2=0.01$; $ki3=0.01$;

$kp4=50.0$; $kp5=50.0$; $kp6=50.0$; $kd4=0.01$; $kd5=0.01$; $kd6=0.01$;

$ki4=0.01$; $ki5=0.01$; $ki6=0.01$;

in order to speed up the biped robot at rest. From the second step, we tried to use lots of controller gains in the experiment. The following suitable controller gains are used.

- **Control parameters I**

$kp1=90.0$; $kp2=100.0$; $kp3=90.0$; $kd1=0.05$; $kd2=1$; $kd3=0.05$;

$kp4=90.0$; $kp5=100.0$; $kp6=90.0$; $kd4=0.05$; $kd5=1$; $kd6=0.05$;

$ki1=0.1$; $ki2=0.1$; $ki3=0.1$; $ki4=0.1$; $ki5=0.1$; $ki6=0.1$

- **Control parameters II**

$kp1=100.0$; $kp2=180.0$; $kp3=150.0$; $kd1=5$; $kd2=5$; $kd3=5$;

$kp4=100.0$; $kp5=180.0$; $kp6=150.0$; $kd4=5$; $kd5=5$; $kd6=5$;

$ki1=30$; $ki2=30$; $ki3=30$; $ki4=30$; $ki5=30$; $ki6=30$

The experimental results with the control parameters I and II are shown in Figures 6.26-6.49.

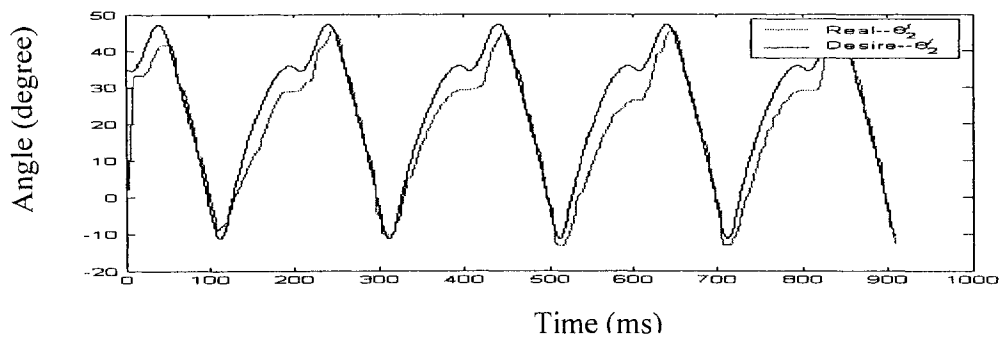


Figure 6.26 Tracking performance for the right ankle (Parameter I)

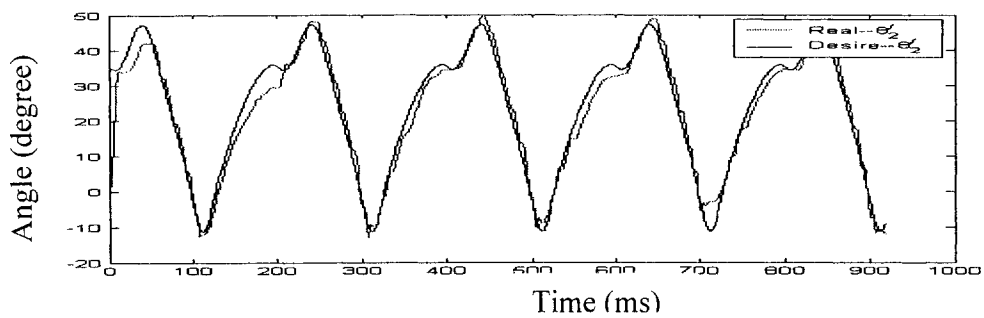


Figure 6.27 Tracking performance for the right ankle (Parameter II)

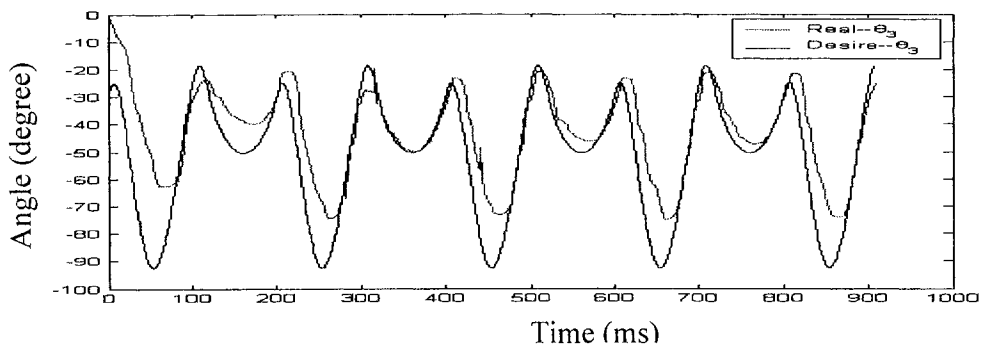


Figure 6.28 Tracking performance for the right knee (Parameter I)

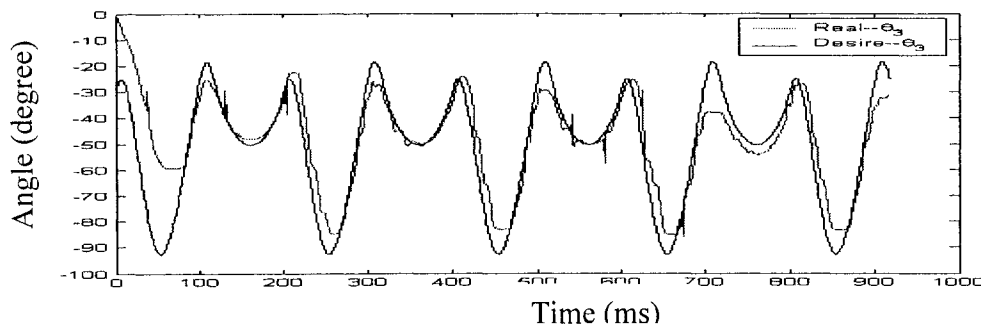


Figure 6.29 Tracking performance for the right knee (Parameter II)

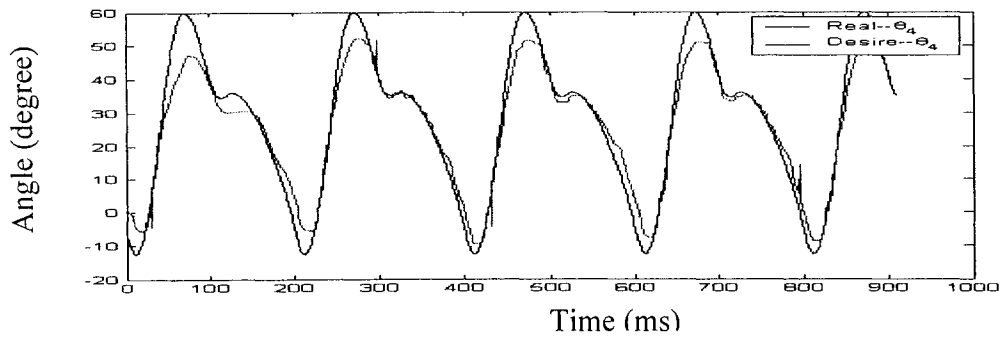


Figure 6.30 Tracking performance for the right hip (Parameter I)

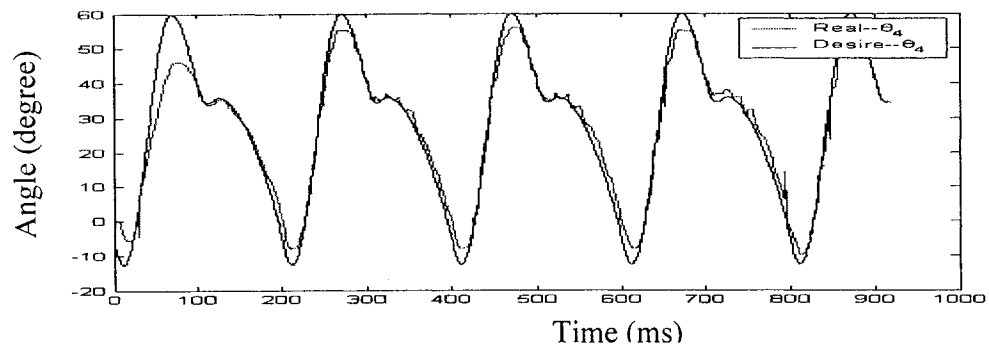


Figure 6.31 Tracking performance for the right hip (Parameter II)

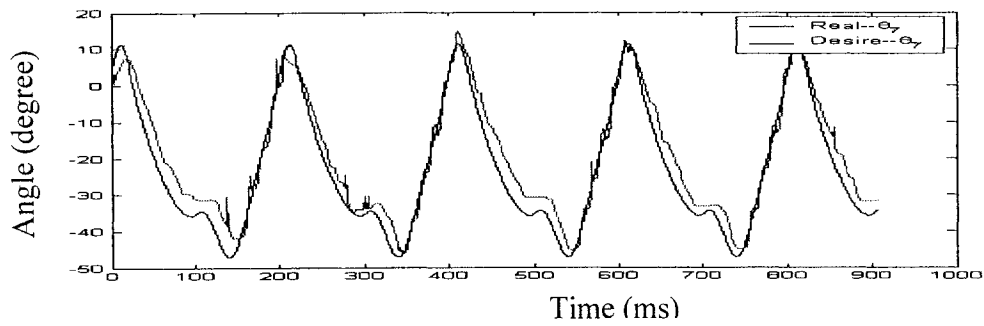


Figure 6.32 Tracking performance for the left ankle (Parameter I)

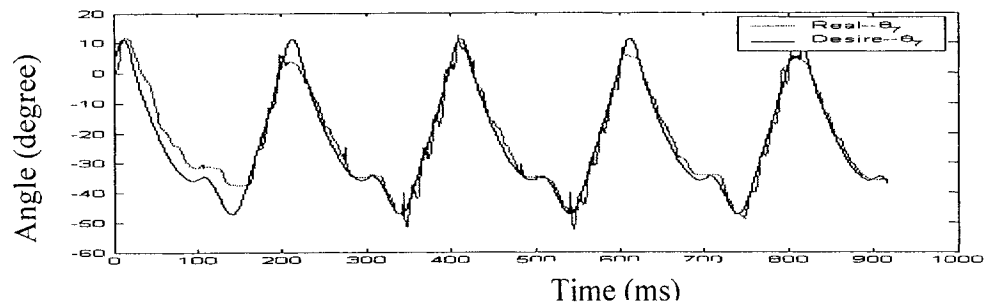


Figure 6.33 Tracking performance for the left ankle (Parameter II)

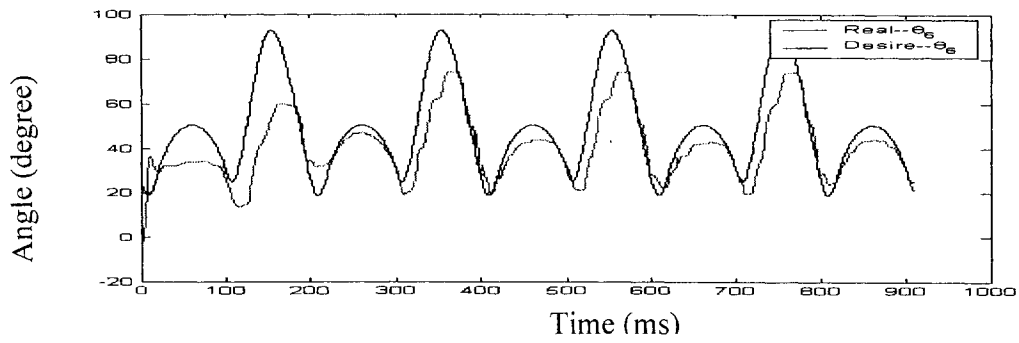


Figure 6.34 Tracking performance for the left knee (Parameter I)

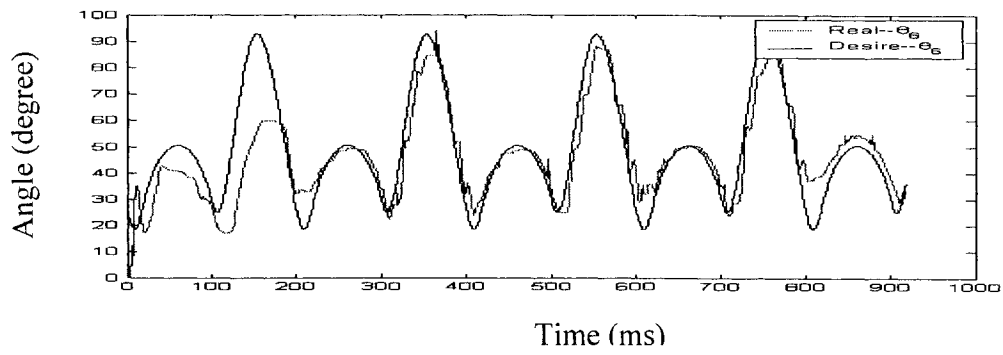


Figure 6.35 Tracking performance for the left knee (Parameter II)

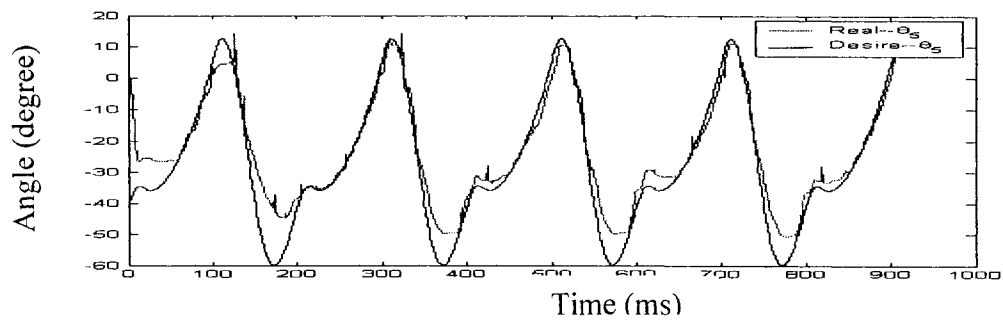


Figure 6.36 Tracking performance for the left hip (Parameter I)

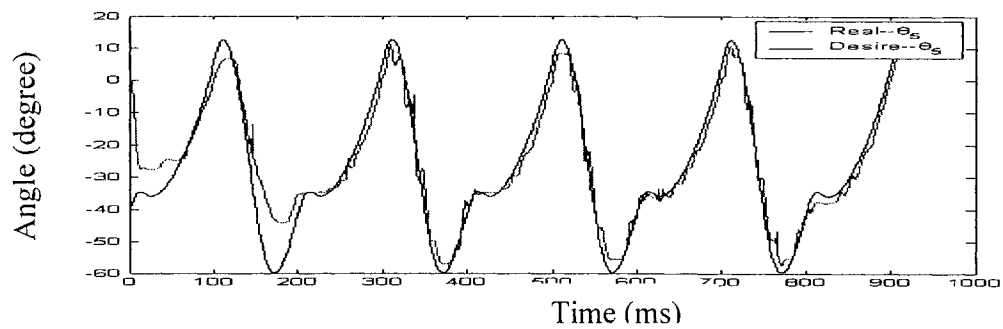


Figure 6.37 Tracking performance for the left hip (Parameter II)

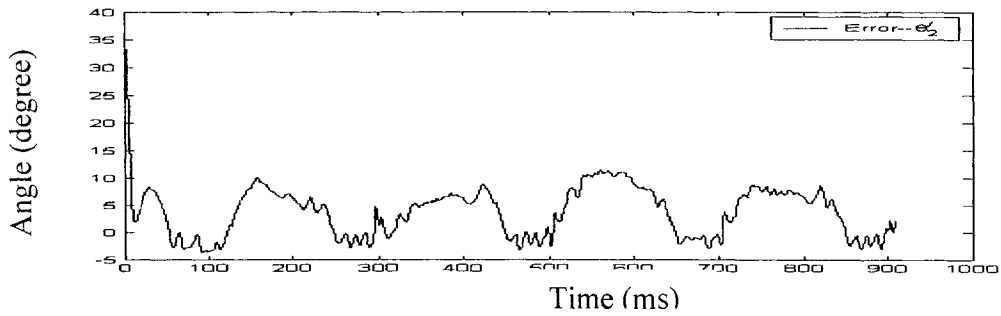


Figure 6.38 Tracking error for the right ankle (Parameter I)

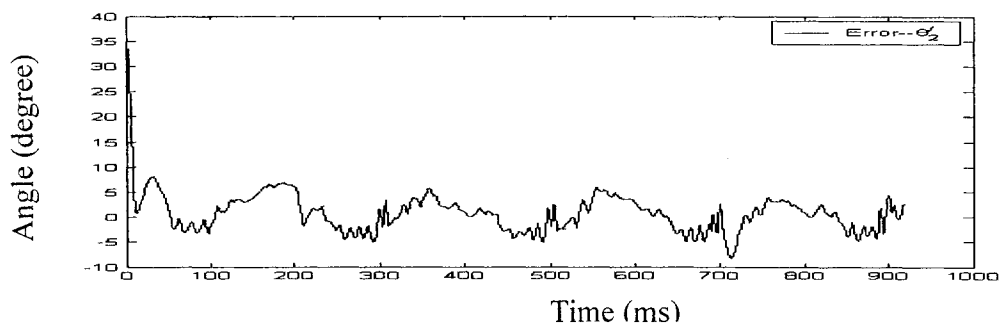


Figure 6.39 Tracking error for the right ankle (Parameter II)

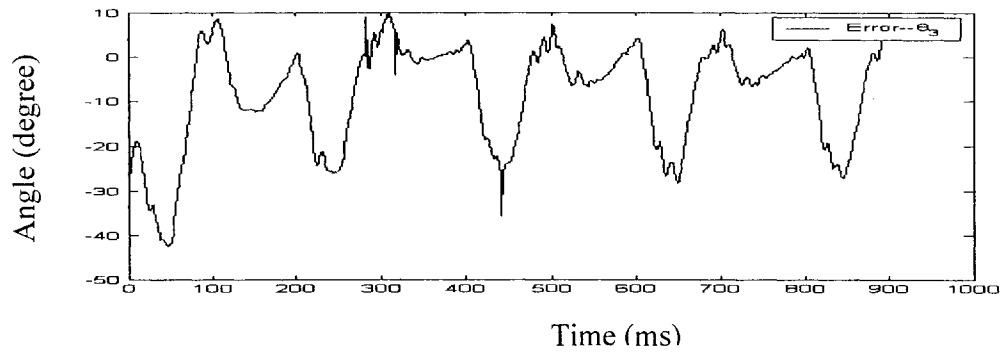


Figure 6.40 Tracking error for the right knee (Parameter I)

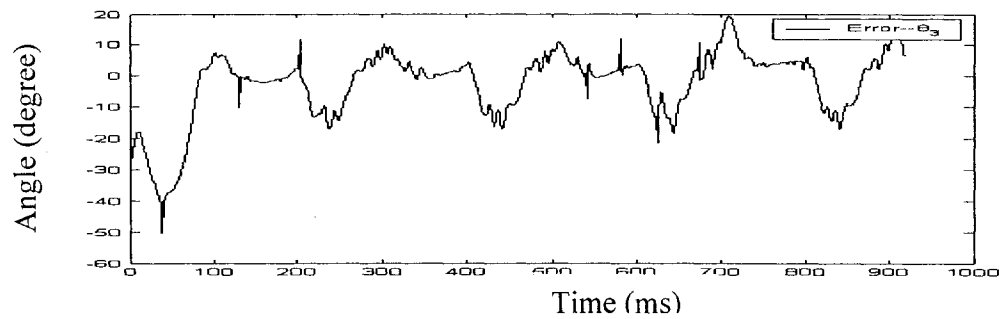


Figure 6.41 Tracking error for the right knee (Parameter II)

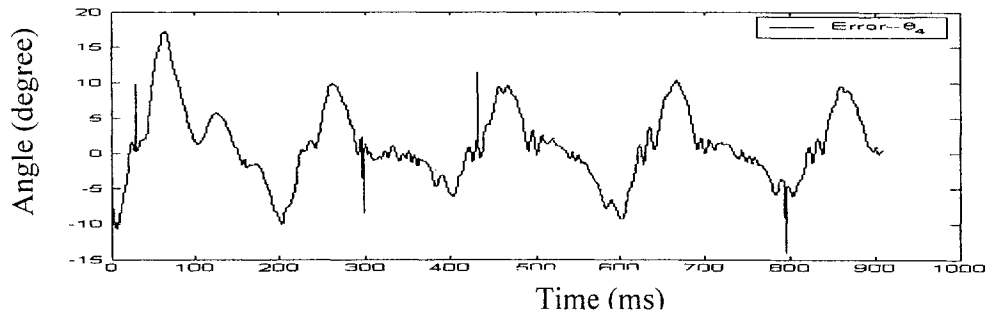


Figure 6.42 Tracking error for the right hip (Parameter I)

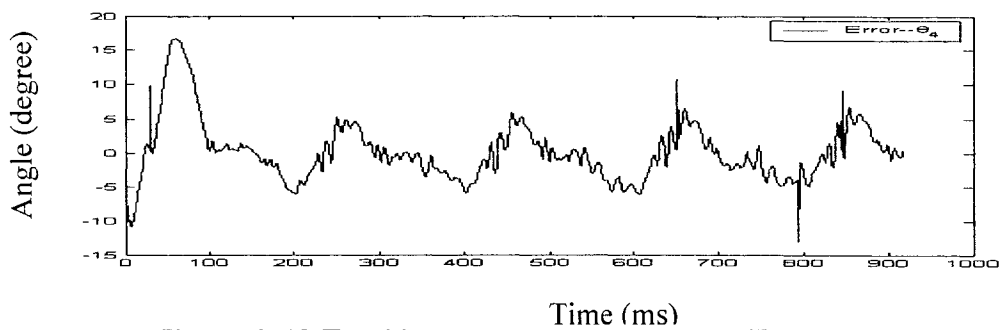


Figure 6.43 Tracking error for the right hip (Parameter II)

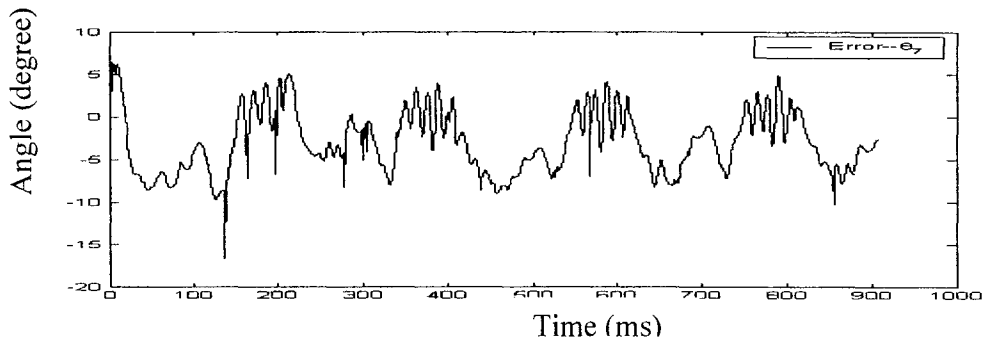


Figure 6.44 Tracking error for the left ankle (Parameter I)

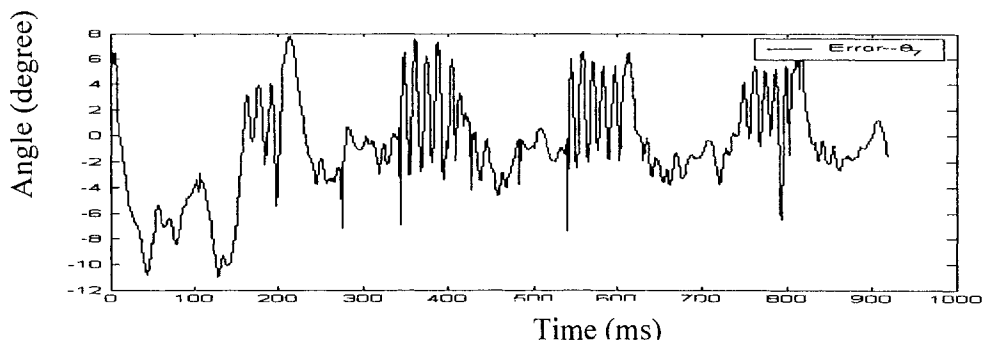


Figure 6.45 Tracking error for the left ankle (Parameter II)

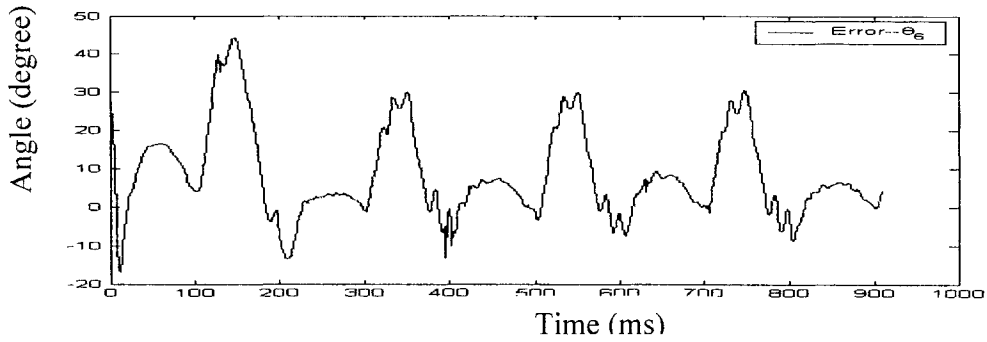


Figure 6.46 Tracking error for the left knee (Parameter I)

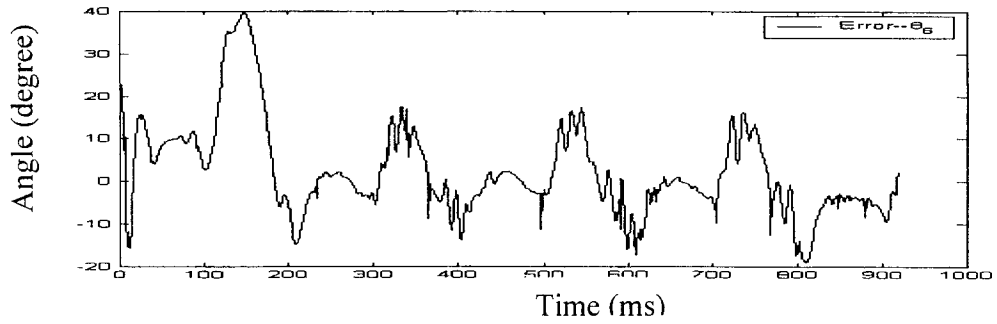


Figure 6.47 Tracking error for the left knee (Parameter II)

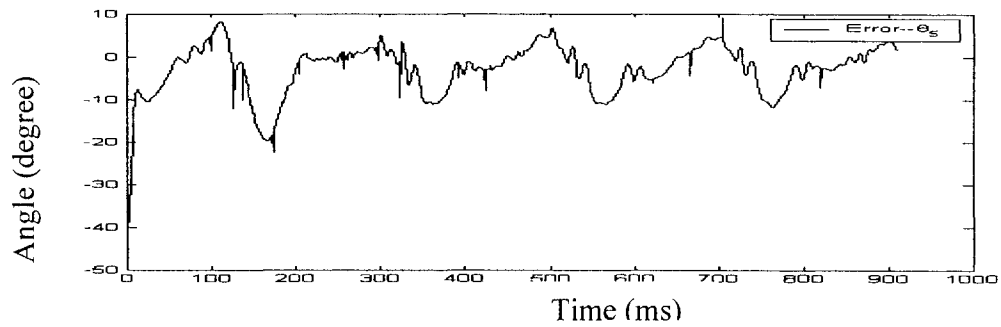


Figure 6.48 Tracking error for the left hip (Parameter I)

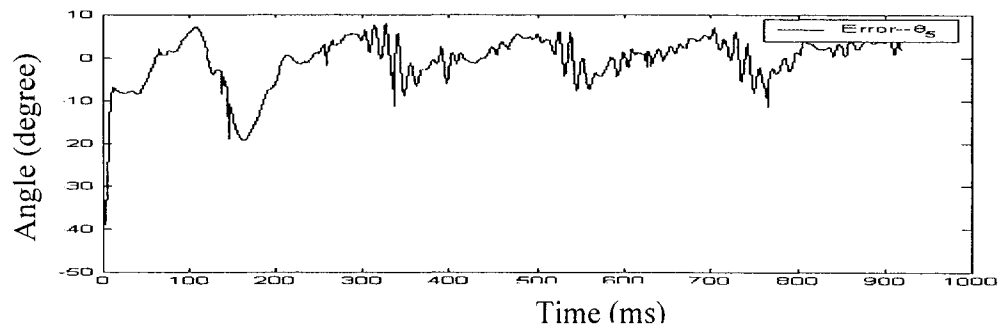


Figure 6.49 Tracking error for the left hip (Parameter II)

Figures 6.26 to 6.37 show the real and desired angle trajectories of both legs of the biped robot with the control parameters I and II, respectively. Figures 6.38 to 6.49 show the tracking errors between the real and desired angles for the biped robot with the control parameters I and II, respectively.

6.3 Analysis of Experimental Results

It can be observed from the tracking error graphs that the tracking errors in the first step are bigger than those in the intermediate steps. The reason for this is that the smaller controller gains are used in the first step in order to reduce the biped robot's shaking at the beginning of walk.

After the biped robot reaches the steady state condition, the tracking errors become smaller. For comparison, the maximum steady state tracking errors in degrees for the PD and PID controllers are summarized in Tables 6.1 and 6.2, respectively.

Table 6.1 The maximum steady-state tracking errors with the PD controllers

| | Control Parameters I | | Control Parameters II | |
|---------------|----------------------|----------|-----------------------|----------|
| | Right Leg | Left Leg | Right Leg | Left Leg |
| Ankle(degree) | 12.48 | 14.05 | 5.825 | 6.972 |
| Knee(degree) | 21.65 | 21.75 | 20.40 | 21.35 |
| Hip(degree) | 9.511 | 9.33 | 7.42 | 9.445 |

Table 6.2 The maximum steady-state tracking errors with the PID controllers

| | Control Parameters I | | Control Parameters II | |
|---------------|----------------------|----------|-----------------------|----------|
| | Right Leg | Left Leg | Right Leg | Left Leg |
| Ankle(degree) | 8.682 | 9.104 | 5.755 | 5.059 |
| Knee(degree) | 28.28 | 30.05 | 17.18 | 17.52 |
| Hip(degree) | 9.725 | 11.21 | 5.975 | 7.69 |

For the PD controllers, it can be observed from Table 6.1 that the tracking errors for the control parameters II are smaller than those with the control

parameters I, which implies that the errors can be reduced by appropriately choosing the proportional and derivative gains. Similarly, the tracking errors can be made smaller by properly selecting the controller gains for the PID controllers. It is obvious that the controller parameters II produce smaller tracking errors compared with the control parameters I.

Comparing the PD and PID controllers, the PID controllers with the control parameters II outperform the PD controllers with both control parameters I and II.

Even though a great effort has been made to adjust the controller gains to reduce the tracking errors, the tracking errors from the best controllers, i.e. the PID controllers with the control parameters II, are still far from the design objectives. The poor control performance of the PID controllers proposed in Chapter 5 might be contributed by the following reasons. First, the PID controllers are designed without taking into account the factors, such as the gravity, friction, dynamics of the motors and the robot links, backlash of the gear systems, and so on. Second, the PID controllers are implemented by using two serial communication channels with the baud rate of 9600bps. The serial communications create some time delay for the controllers. This might indicate that the PID controllers might not be suitable to control the biped robot. More advanced control techniques might be required and the dynamics model might be needed to achieve a better performance. For example, smaller tracking errors might be achieved by using PID control with gravity compensation, sliding mode control, computed torque control, adaptive control, and so on.

Chapter 7

Conclusions and Future work

7.1 Conclusions

A 6 DOF biped robot with two legs, two feet, and one trunk has been developed with aluminum plates, aluminum angles, and rubber materials. Six gear head DC motors with built-in encoders have been selected to actuate the biped robot joints.

A control system, including six gear head DC motors with encoders, two microcontrollers, and one PC computer, has been designed for the biped robot. Two Atmega16 microcontrollers have been used to process data from the biped robot and the PC computer and two RS232 serial communication channels have been designed to achieve data transfer between the microcontrollers and the PC computer.

Foot trajectories and hip trajectory have been calculated by using the 3rd order spline interpolation method. Walking pattern has been designed by using the inverse kinematics. Simulation has been carried out to demonstrate the walking pattern.

Both PD and PID controllers have been designed for controlling the biped robot to move according to the designed walking pattern. Experimental results on the PD and PID controllers show that the biped robot with the designed controllers is able to follow the desired walking pattern even though the tracking errors are noticeable. The reason for the noticeable tracking errors may be

caused by frictions, biped robot dynamics, motor dynamics, delay resulted from communication between the microcontrollers and PC computer, and so on.

7.2 Future work

It should be pointed out that the biped robot built for this research is the first prototype, so it is not well designed. For example, the motors used could not provide enough torque for the biped robot to stand up by itself, which is why the robot was hung from the track; faster communication method is required to speed up data transfer between the microcontrollers and PC computer. In addition, biped robot dynamics is not taken into account when the controllers are designed, which leads to the poor control performance. Therefore, a mathematical model is needed for the controller design. Both static balancing and dynamic balancing have not been discussed in this thesis. All the above discussed are important topics in the field of biped robots which will be addressed in the future prototypes.

References

- [1] Q. Huang and S. Kajita. "Planning Walking Patterns for a Biped Robot", IEEE Transactions on Robotics and Automation, Vol.17, No.3, 2001.
- [2] J. Vermeulen and D. Lefeber. "Trajectory Planning for the Walking Biped Robot "Lucy"", CLAWAR 2004, 7th International Conference on Climbing and Walking Robots and the Support Technologies for Mobile Machines, Madrid, Spain, September 2004.
- [3] Zh. Tang, Ch.J Zhou, and Z. Q Sun. "Trajectory Planning for Smooth Transition of a Biped Robot", Proceedings of the 2003 IEEE International Conference on Robotics & Automation, pp. 2455-2460, 2003.
- [4] R. X. Zhang and P. Vadakkepat. "Motion Planning of Biped Robot Climbing Stairs", Proceedings of FIRA Robot World Cup, Austria, October 2003.
- [5] R. X. Zhang, P. Vadakkepat, and Ch. M. Chew. "Development and Walking Control of a Biped Robot", submitted to IEEE Transactions on Mechatronics.
- [6] D. Ito, T. Murakami, and K. Ohnishi. "An Approach to Generation of Smooth Walking Pattern for Biped Robot", Proceeding of the 7th Workshop on Advanced Motion Control, pp. 98-103, 2002.
- [7] Q. Huang and S. Kajita. "A High Stability Smooth Walking Pattern for a Biped Robot", Proceedings of the 1999 IEEE International Conference on Robotics and Automation, Detroit, Michigan, Vol.1, pp. 65-71, 1999.

- [8] Q. Huang, S. Kajita, N. Koyachi, K. Kaneko, and K. Yokoi. "Walking Patterns and Actuator Specifications for a Biped Robot", Proceedings of the 1999 IEEE/VRSJ International Conference on Intelligent Robots and Systems, Vol. 3, pp. 1462–1468, 1999.
- [9] E. Cuevas, D. Zaldívar, and R. Rojas. "Walking Trajectory Control of a Biped Robot", Technical Report B-04-18, Free University of Berlin, Department of Computer Science.
- [10] Ch. L. Shih. "Ascending and Descending Stairs for a Biped Robot" IEEE Transactions on Systems, Man and Cybernetics, Part A: Systems and Humans, Vol. 29, No. 3, pp. 255-268, 1999.
- [11] J. M. Jeanne. "Developing Adjustable Walking Patterns for Natural Walking in Humanoid Robots", <http://ehw.jpl.nasa.gov/humanoid/>.
- [12] L. Cambrini, C. Chevallereau, C.H. Moog, and R. Stojic. "Stable Trajectory Tracking for Biped Robots", Proceeding of the 39th IEEE Conference on Decision and Control, Sydney, Australia, Vol.5, pp. 4815-4820, 2000.
- [13] J. Pratt, P. Dilworth, and G. Pratt. "Virtual Model Control of a Bipedal Walking Robot", Proceedings of the 1997 International Conference on Robotics and Automation, pp. 193-198, 1997.
- [14] R. Kurazume, Sh. Tanaka, and M. Yamashita. "Straight Legged Walking of a Biped Robot", Proceedings of 2005 IEEE/RSJ International Conference on Intelligent Robots and Systems, pp. 3095-3101, 2005.
- [15] Margaret M. Skelly, and Howard Jay Chizeck. " Simulation of Bipedal Walking", UWEE Technical Report, Number 2001-0001, October 3, 2001

- [16] K. Mitobe, N. Mori, Aida, and Y. Nasu. "Nonlinear Feedback Control of a Biped Walking Robot", Proceedings of IEEE International Conference on Robotics and Automation, pp. 2865-2870, 1995.
- [17] A. San and J. Furusho. "Realization of Natural Dynamic Walking Using the Angular Momentum Information", Proceedings of IEEE International Conference on Robotics and Automation, pp. 1476-1481, 1990.
- [18] Chi Zhu, Mikio Okamura, Atsuo Kawamura, and Yoshihito Tomizawa. "Experimental Approach for High Speed Walking of Biped Robot MARI-1", Proceedings of the 8th IEEE International Workshop on Advanced Motion Control, pp. 427-432, 2004.
- [19] K. Mitobe, N. Mori, and Y. Nasu. "Control of a Biped Walking Robot during the Double Support Phase", Autonomous Robots, 287-296, 1997.
- [20] C.L. Shih, Y.Z. Li, S. Churng, T.T. Lee, and W.A. Gruver. "Trajectory Synthesis and Physical Admissibility for a Biped Robot during the Single Support Phase", Proceedings of IEEE International Conference on Robotics and Automation, pp. 1646-1652, 1990.
- [21] Ch. L. Shih, and Y. Zhu. "Optimization of the Biped Robot Trajectory", Systems, Man and Cybernetics, 1991 Decision Aiding for Complex Systems, Vol.2, pp. 899-903, 1991.
- [22] Morton and D. Todd. "Embedded Computer System", Prentice-Hall, Inc., 2001
- [23] M. W. Spong and M. Vidyasagar. "Robot Dynamics and Control", New York, 1989.

Lakehead University

- [24] Mu, X. and Wu, Q. "Synthesis of A Complete Sagittal Gait Cycle for a Five-Link Biped Robot", *Robotics*, Vol. 21. pp. 581-587, 2003.

Appendix

Homogeneous Transformation

The matrices, ${}^i T_i$, are given as follows:

$${}^1_0 T = \begin{bmatrix} -\cos(\theta_1 + \alpha_r) & \sin(\theta_1 + \alpha_r) & 0 & -l_0 \cos(\theta_1 + \alpha_r) \\ -\sin(\theta_1 + \alpha_r) & -\cos(\theta_1 + \alpha_r) & 0 & -l_0 \sin(\theta_1 + \alpha_r) \\ 0 & 0 & 1 & 0 \\ 0 & 0 & 0 & 1 \end{bmatrix} \quad (1)$$

$${}^2_1 T = \begin{bmatrix} \cos \theta_2 & -\sin \theta_2 & 0 & l_1 \cos \theta_2 \\ \sin \theta_2 & \cos \theta_2 & 0 & l_1 \sin \theta_2 \\ 0 & 0 & 1 & 0 \\ 0 & 0 & 0 & 1 \end{bmatrix} \quad (2)$$

$${}^3_2 T = \begin{bmatrix} \cos \theta_3 & \sin \theta_3 & 0 & l_2 \cos \theta_3 \\ -\sin \theta_3 & \cos \theta_3 & 0 & -l_2 \sin \theta_3 \\ 0 & 0 & 1 & 0 \\ 0 & 0 & 0 & 1 \end{bmatrix} \quad (3)$$

$${}^4_3 T = \begin{bmatrix} \cos \theta_4 & \sin \theta_4 & 0 & l_6 \cos \theta_4 \\ -\sin \theta_4 & \cos \theta_4 & 0 & -l_6 \sin \theta_4 \\ 0 & 0 & 1 & 0 \\ 0 & 0 & 0 & 1 \end{bmatrix} \quad (4)$$

$${}^5_4 T = \begin{bmatrix} -1 & 0 & 0 & 0 \\ 0 & -1 & 0 & 0 \\ 0 & 0 & -1 & l_3 \\ 0 & 0 & 0 & 1 \end{bmatrix} \quad (5)$$

$${}^6_5T = \begin{bmatrix} 1 & 0 & 0 & l_6 \\ 0 & 1 & 0 & 0 \\ 0 & 0 & 1 & 0 \\ 0 & 0 & 0 & 1 \end{bmatrix} \quad (6)$$

$${}^7_6T = \begin{bmatrix} \cos\theta_5 & \sin\theta_5 & 0 & l_4 \cos\theta_5 \\ -\sin\theta_5 & \cos\theta_5 & 0 & -l_4 \sin\theta_5 \\ 0 & 0 & 1 & 0 \\ 0 & 0 & 0 & 1 \end{bmatrix} \quad (7)$$

$${}^8_7T = \begin{bmatrix} \cos\theta_6 & -\sin\theta_6 & 0 & l_5 \cos\theta_6 \\ \sin\theta_6 & \cos\theta_6 & 0 & l_5 \sin\theta_6 \\ 0 & 0 & 1 & 0 \\ 0 & 0 & 0 & 1 \end{bmatrix} \quad (8)$$

$${}^9_8T = \begin{bmatrix} \cos\theta_7 & \sin\theta_7 & 0 & l_{an} \cos\theta_7 \\ -\sin\theta_7 & \cos\theta_7 & 0 & -l_{an} \sin\theta_7 \\ 0 & 0 & 1 & 0 \\ 0 & 0 & 0 & 1 \end{bmatrix} \quad (9)$$

The matrices, i_0T , are calculated as follows:

$${}^1_0T = \begin{bmatrix} -\cos(\theta_1 + \alpha_r) & \sin(\theta_1 + \alpha_r) & 0 & -l_0 \cos(\theta_1 + \alpha_r) \\ -\sin(\theta_1 + \alpha_r) & -\cos(\theta_1 + \alpha_r) & 0 & -l_0 \sin(\theta_1 + \alpha_r) \\ 0 & 0 & 1 & 0 \\ 0 & 0 & 0 & 1 \end{bmatrix} \quad (10)$$

$$\begin{aligned}
 {}^2_0T = {}^1_0T {}^2_1T &= \begin{bmatrix} -\cos(\theta_1 + \alpha_r) & \sin(\theta_1 + \alpha_r) & 0 & -l_0 \cos(\theta_1 + \alpha_r) \\ -\sin(\theta_1 + \alpha_r) & -\cos(\theta_1 + \alpha_r) & 0 & -l_0 \sin(\theta_1 + \alpha_r) \\ 0 & 0 & 1 & 0 \\ 0 & 0 & 0 & 1 \end{bmatrix} \\
 &= \begin{bmatrix} \cos \theta_2 & -\sin \theta_2 & 0 & l_1 \cos \theta_2 \\ \sin \theta_2 & \cos \theta_2 & 0 & l_1 \sin \theta_2 \\ 0 & 0 & 1 & 0 \\ 0 & 0 & 0 & 1 \end{bmatrix} \\
 &= \begin{bmatrix} -\cos(\theta_1 + \theta_2 + \alpha_r) & \sin(\theta_1 + \theta_2 + \alpha_r) & 0 & -l_1 \cos(\theta_1 + \theta_2 + \alpha_r) - l_0 \cos(\theta_1 + \alpha_r) \\ -\sin(\theta_1 + \theta_2 + \alpha_r) & -\cos(\theta_1 + \theta_2 + \alpha_r) & 0 & -l_1 \sin(\theta_1 + \theta_2 + \alpha_r) - l_0 \sin(\theta_1 + \alpha_r) \\ 0 & 0 & 1 & 0 \\ 0 & 0 & 0 & 1 \end{bmatrix}
 \end{aligned} \tag{11}$$

$$\begin{aligned}
 {}^3_0T = {}^2_0T {}^3_2T &= \begin{bmatrix} -\cos(\theta_1 + \theta_2 + \alpha_r) & \sin(\theta_1 + \theta_2 + \alpha_r) & 0 & -l_1 \cos(\theta_1 + \theta_2 + \alpha_r) - l_0 \cos(\theta_1 + \alpha_r) \\ -\sin(\theta_1 + \theta_2 + \alpha_r) & -\cos(\theta_1 + \theta_2 + \alpha_r) & 0 & -l_1 \sin(\theta_1 + \theta_2 + \alpha_r) - l_0 \sin(\theta_1 + \alpha_r) \\ 0 & 0 & 1 & 0 \\ 0 & 0 & 0 & 1 \end{bmatrix} \\
 &= \begin{bmatrix} \cos \theta_3 & \sin \theta_3 & 0 & l_2 \cos \theta_3 \\ -\sin \theta_3 & \cos \theta_3 & 0 & -l_2 \sin \theta_3 \\ 0 & 0 & 1 & 0 \\ 0 & 0 & 0 & 1 \end{bmatrix} \\
 &= \begin{bmatrix} -\cos(\theta_1 + \theta_2 - \theta_3 + \alpha_r) & \sin(\theta_1 + \theta_2 - \theta_3 + \alpha_r) & 0 & DD1 \\ -\sin(\theta_1 + \theta_2 - \theta_3 + \alpha_r) & -\cos(\theta_1 + \theta_2 - \theta_3 + \alpha_r) & 0 & DD2 \\ 0 & 0 & 1 & 0 \\ 0 & 0 & 0 & 1 \end{bmatrix}
 \end{aligned} \tag{12}$$

$$\begin{aligned}
 {}^4T_0 = {}^3T_3 {}^4T_3 &= \begin{bmatrix} -\cos(\theta_1 + \theta_2 - \theta_3 + \alpha_r) & \sin(\theta_1 + \theta_2 - \theta_3 + \alpha_r) & 0 & DD1 \\ -\sin(\theta_1 + \theta_2 - \theta_3 + \alpha_r) & -\cos(\theta_1 + \theta_2 - \theta_3 + \alpha_r) & 0 & DD2 \\ 0 & 0 & 1 & 0 \\ 0 & 0 & 0 & 1 \end{bmatrix} \\
 &= \begin{bmatrix} \cos \theta_4 & \sin \theta_4 & 0 & l_6 \cos \theta_4 \\ -\sin \theta_4 & \cos \theta_4 & 0 & -l_6 \sin \theta_4 \\ 0 & 0 & 1 & 0 \\ 0 & 0 & 0 & 1 \end{bmatrix} \\
 &= \begin{bmatrix} -\cos(\theta_1 + \theta_2 - \theta_3 - \theta_4 + \alpha_r) & \sin(\theta_1 + \theta_2 - \theta_3 - \theta_4 + \alpha_r) & 0 & DD3 \\ -\sin(\theta_1 + \theta_2 - \theta_3 - \theta_4 + \alpha_r) & -\cos(\theta_1 + \theta_2 - \theta_3 - \theta_4 + \alpha_r) & 0 & DD4 \\ 0 & 0 & 1 & 0 \\ 0 & 0 & 0 & 1 \end{bmatrix}
 \end{aligned} \tag{13}$$

$$\begin{aligned}
 {}^5T_0 = {}^4T_4 {}^5T_4 &= \begin{bmatrix} -\cos(\theta_1 + \theta_2 - \theta_3 - \theta_4 + \alpha_r) & \sin(\theta_1 + \theta_2 - \theta_3 - \theta_4 + \alpha_r) & 0 & DD3 \\ -\sin(\theta_1 + \theta_2 - \theta_3 - \theta_4 + \alpha_r) & -\cos(\theta_1 + \theta_2 - \theta_3 - \theta_4 + \alpha_r) & 0 & DD4 \\ 0 & 0 & 1 & 0 \\ 0 & 0 & 0 & 1 \end{bmatrix} \\
 &= \begin{bmatrix} -1 & 0 & 0 & 0 \\ 0 & -1 & 0 & 0 \\ 0 & 0 & -1 & l_3 \\ 0 & 0 & 0 & 1 \end{bmatrix} \\
 &= \begin{bmatrix} \cos(\theta_1 + \theta_2 - \theta_3 - \theta_4 + \alpha_r) & -\sin(\theta_1 + \theta_2 - \theta_3 - \theta_4 + \alpha_r) & 0 & DD3 \\ \sin(\theta_1 + \theta_2 - \theta_3 - \theta_4 + \alpha_r) & \cos(\theta_1 + \theta_2 - \theta_3 - \theta_4 + \alpha_r) & 0 & DD4 \\ 0 & 0 & -1 & l_3 \\ 0 & 0 & 0 & 1 \end{bmatrix} \\
 &= \begin{bmatrix} \cos \theta_a & -\sin \theta_a & 0 & DD3 \\ \sin \theta_a & \cos \theta_a & 0 & DD4 \\ 0 & 0 & -1 & l_3 \\ 0 & 0 & 0 & 1 \end{bmatrix}
 \end{aligned} \tag{14}$$

$$\begin{aligned}
 {}^6_0T = {}^5_0T {}^6_5T &= \begin{bmatrix} \cos\theta_a & -\sin\theta_a & 0 & DD3 \\ \sin\theta_a & \cos\theta_a & 0 & DD4 \\ 0 & 0 & -1 & l_3 \\ 0 & 0 & 0 & 1 \end{bmatrix} \begin{bmatrix} 1 & 0 & 0 & l_6 \\ 0 & 1 & 0 & 0 \\ 0 & 0 & 1 & 0 \\ 0 & 0 & 0 & 1 \end{bmatrix} \\
 &= \begin{bmatrix} \cos\theta_a & -\sin\theta_a & 0 & DD5 \\ \sin\theta_a & \cos\theta_a & 0 & DD6 \\ 0 & 0 & -1 & l_3 \\ 0 & 0 & 0 & 1 \end{bmatrix}
 \end{aligned} \tag{15}$$

$$\begin{aligned}
 {}^7_0T = {}^6_0T {}^7_6T &= \begin{bmatrix} \cos\theta_a & -\sin\theta_a & 0 & DD5 \\ \sin\theta_a & \cos\theta_a & 0 & DD6 \\ 0 & 0 & -1 & l_3 \\ 0 & 0 & 0 & 1 \end{bmatrix} \begin{bmatrix} \cos\theta_5 & \sin\theta_5 & 0 & l_4 \cos\theta_5 \\ -\sin\theta_5 & \cos\theta_5 & 0 & -l_4 \sin\theta_5 \\ 0 & 0 & 1 & 0 \\ 0 & 0 & 0 & 1 \end{bmatrix} \\
 &= \begin{bmatrix} \cos(\theta_a - \theta_5) & -\sin(\theta_a - \theta_5) & 0 & DD7 \\ \sin(\theta_a - \theta_5) & \cos(\theta_a - \theta_5) & 0 & DD8 \\ 0 & 0 & -1 & l_3 \\ 0 & 0 & 0 & 1 \end{bmatrix}
 \end{aligned} \tag{16}$$

$$\begin{aligned}
 {}^8_0T = {}^7_0T {}^8_7T &= \begin{bmatrix} \cos(\theta_a - \theta_5) & -\sin(\theta_a - \theta_5) & 0 & DD7 \\ \sin(\theta_a - \theta_5) & \cos(\theta_a - \theta_5) & 0 & DD8 \\ 0 & 0 & -1 & l_3 \\ 0 & 0 & 0 & 1 \end{bmatrix} \begin{bmatrix} \cos\theta_6 & -\sin\theta_6 & 0 & l_5 \cos\theta_6 \\ \sin\theta_6 & \cos\theta_6 & 0 & l_5 \sin\theta_6 \\ 0 & 0 & 1 & 0 \\ 0 & 0 & 0 & 1 \end{bmatrix} \\
 &= \begin{bmatrix} \cos(\theta_a - \theta_5 + \theta_6) & -\sin(\theta_a - \theta_5 + \theta_6) & 0 & DD9 \\ \sin(\theta_a - \theta_5 + \theta_6) & \cos(\theta_a - \theta_5 + \theta_6) & 0 & DD10 \\ 0 & 0 & -1 & l_3 \\ 0 & 0 & 0 & 1 \end{bmatrix}
 \end{aligned} \tag{17}$$

$$\begin{aligned}
 {}^9_0T = {}^8_0T {}^9_8T &= \begin{bmatrix} \cos(\theta_a - \theta_5 + \theta_6) & -\sin(\theta_a - \theta_5 + \theta_6) & 0 & DD9 \\ \sin(\theta_a - \theta_5 + \theta_6) & \cos(\theta_a - \theta_5 + \theta_6) & 0 & DD10 \\ 0 & 0 & -1 & l_3 \\ 0 & 0 & 0 & 1 \end{bmatrix} \\
 &\begin{bmatrix} \cos \theta_7 & \sin \theta_7 & 0 & l_{an} \cos \theta_7 \\ -\sin \theta_7 & \cos \theta_7 & 0 & -l_{an} \sin \theta_7 \\ 0 & 0 & 1 & 0 \\ 0 & 0 & 0 & 1 \end{bmatrix} \\
 &= \begin{bmatrix} \cos(\theta_a - \theta_5 + \theta_6 - \theta_7) & -\sin(\theta_a - \theta_5 + \theta_6 - \theta_7) & 0 & DD11 \\ \sin(\theta_a - \theta_5 + \theta_6 - \theta_7) & \cos(\theta_a - \theta_5 + \theta_6 - \theta_7) & 0 & DD12 \\ 0 & 0 & -1 & l_3 \\ 0 & 0 & 0 & 1 \end{bmatrix}
 \end{aligned} \tag{18}$$

where

$$DD1 = -l_2 \cos(\theta_1 + \theta_2 - \theta_3 + \alpha_r) - l_1 \cos(\theta_1 + \theta_2 + \alpha_r) - l_0 \cos(\theta_1 + \alpha_r)$$

$$DD2 = -l_2 \sin(\theta_1 + \theta_2 - \theta_3 + \alpha_r) - l_1 \sin(\theta_1 + \theta_2 + \alpha_r) - l_0 \sin(\theta_1 + \alpha_r)$$

$$DD3 = -l_6 \cos(\theta_1 + \theta_2 - \theta_3 - \theta_4 + \alpha_r) + DD1$$

$$DD4 = -l_6 \sin(\theta_1 + \theta_2 - \theta_3 - \theta_4 + \alpha_r) + DD2$$

$$DD5 = l_6 \cos \theta_a + DD3$$

$$DD6 = l_6 \sin \theta_a + DD4$$

$$DD7 = l_4 \cos(\theta_a - \theta_5) + DD5$$

$$DD8 = l_4 \sin(\theta_a - \theta_5) + DD6$$

$$DD9 = l_5 \cos(\theta_a - \theta_5 + \theta_6) + DD7$$

$$DD10 = l_5 \sin(\theta_a - \theta_5 + \theta_6) + DD8$$

$$DD11 = l_{an} \cos(\theta_a - \theta_5 + \theta_6 - \theta_7) + DD9$$

$$DD12 = l_{an} \sin(\theta_a - \theta_5 + \theta_6 - \theta_7) + DD10$$

$$\theta_a = \theta_1 + \theta_2 - \theta_3 - \theta_4 + \alpha_r$$

The homogeneous transformation matrices, ${}^i_r T$, can be expressed as follows:

$${}^0_r T = \begin{bmatrix} 1 & 0 & 0 & x_a \\ 0 & 0 & 1 & 0 \\ 0 & -1 & 0 & 0 \\ 0 & 0 & 0 & 1 \end{bmatrix} \quad (19)$$

$$\begin{aligned} {}^1_r T &= {}^0_r T {}^1_0 T = \begin{bmatrix} 1 & 0 & 0 & x_a \\ 0 & 0 & 1 & 0 \\ 0 & -1 & 0 & 0 \\ 0 & 0 & 0 & 1 \end{bmatrix} \begin{bmatrix} -\cos(\theta_1 + \alpha_r) & \sin(\theta_1 + \alpha_r) & 0 & -l_0 \cos(\theta_1 + \alpha_r) \\ -\sin(\theta_1 + \alpha_r) & -\cos(\theta_1 + \alpha_r) & 0 & -l_0 \sin(\theta_1 + \alpha_r) \\ 0 & 0 & 1 & 0 \\ 0 & 0 & 0 & 1 \end{bmatrix} \\ &= \begin{bmatrix} -\cos(\theta_1 + \alpha_r) & \sin(\theta_1 + \alpha_r) & 0 & x_a - l_0 \cos(\theta_1 + \alpha_r) \\ 0 & 0 & 1 & 0 \\ \sin(\theta_1 + \alpha_r) & \cos(\theta_1 + \alpha_r) & 0 & l_0 \sin(\theta_1 + \alpha_r) \\ 0 & 0 & 0 & 1 \end{bmatrix} \end{aligned} \quad (20)$$

$$\begin{aligned} {}^2_r T &= {}^0_r T {}^1_0 T {}^2_1 T = \begin{bmatrix} 1 & 0 & 0 & x_a \\ 0 & 0 & 1 & 0 \\ 0 & -1 & 0 & 0 \\ 0 & 0 & 0 & 1 \end{bmatrix} \begin{bmatrix} -\cos(\theta_1 + \theta_2 + \alpha_r) & \sin(\theta_1 + \theta_2 + \alpha_r) & 0 & -l_1 \cos(\theta_1 + \theta_2 + \alpha_r) - l_0 \cos(\theta_1 + \alpha_r) \\ -\sin(\theta_1 + \theta_2 + \alpha_r) & -\cos(\theta_1 + \theta_2 + \alpha_r) & 0 & -l_1 \sin(\theta_1 + \theta_2 + \alpha_r) - l_0 \sin(\theta_1 + \alpha_r) \\ 0 & 0 & 1 & 0 \\ 0 & 0 & 0 & 1 \end{bmatrix} \\ &= \begin{bmatrix} -\cos(\theta_1 + \theta_2 + \alpha_r) & \sin(\theta_1 + \theta_2 + \alpha_r) & 0 & x_a - l_1 \cos(\theta_1 + \theta_2 + \alpha_r) - l_0 \cos(\theta_1 + \alpha_r) \\ 0 & 0 & 1 & 0 \\ \sin(\theta_1 + \theta_2 + \alpha_r) & \cos(\theta_1 + \theta_2 + \alpha_r) & 0 & l_1 \sin(\theta_1 + \theta_2 + \alpha_r) + l_0 \sin(\theta_1 + \alpha_r) \\ 0 & 0 & 0 & 1 \end{bmatrix} \end{aligned} \quad (21)$$

$$\begin{aligned}
 {}^3_rT = {}^0_rT {}^3_0T &= \begin{bmatrix} 1 & 0 & 0 & x_a \\ 0 & 0 & 1 & 0 \\ 0 & -1 & 0 & 0 \\ 0 & 0 & 0 & 1 \end{bmatrix} \\
 &= \begin{bmatrix} -\cos(\theta_1 + \theta_2 - \theta_3 + \alpha_r) & \sin(\theta_1 + \theta_2 - \theta_3 + \alpha_r) & 0 & DD\ 1 \\ -\sin(\theta_1 + \theta_2 - \theta_3 + \alpha_r) & -\cos(\theta_1 + \theta_2 - \theta_3 + \alpha_r) & 0 & DD\ 2 \\ 0 & 0 & 1 & 0 \\ 0 & 0 & 0 & 1 \end{bmatrix} \\
 &= \begin{bmatrix} -\cos(\theta_1 + \theta_2 - \theta_3 + \alpha_r) & \sin(\theta_1 + \theta_2 - \theta_3 + \alpha_r) & 0 & x_a + DD\ 1 \\ 0 & 0 & 1 & 0 \\ \sin(\theta_1 + \theta_2 - \theta_3 + \alpha_1) & \cos(\theta_1 + \theta_2 - \theta_3 + \alpha_1) & 0 & -DD\ 2 \\ 0 & 0 & 0 & 1 \end{bmatrix}
 \end{aligned} \tag{22}$$

$$\begin{aligned}
 {}^4_rT = {}^0_rT {}^4_0T &= \begin{bmatrix} 1 & 0 & 0 & x_a \\ 0 & 0 & 1 & 0 \\ 0 & -1 & 0 & 0 \\ 0 & 0 & 0 & 1 \end{bmatrix} \begin{bmatrix} -\cos(\theta_1 + \theta_2 - \theta_3 - \theta_4 + \alpha_r) & \sin(\theta_1 + \theta_2 - \theta_3 - \theta_4 + \alpha_r) & 0 & DD\ 3 \\ -\sin(\theta_1 + \theta_2 - \theta_3 - \theta_4 + \alpha_r) & -\cos(\theta_1 + \theta_2 - \theta_3 - \theta_4 + \alpha_r) & 0 & DD\ 4 \\ 0 & 0 & 1 & 0 \\ 0 & 0 & 0 & 1 \end{bmatrix} \\
 &= \begin{bmatrix} -\cos(\theta_1 + \theta_2 - \theta_3 - \theta_4 + \alpha_r) & \sin(\theta_1 + \theta_2 - \theta_3 - \theta_4 + \alpha_r) & 0 & x_a + DD\ 3 \\ 0 & 0 & 1 & 0 \\ \sin(\theta_1 + \theta_2 - \theta_3 - \theta_4 + \alpha_r) & \cos(\theta_1 + \theta_2 - \theta_3 - \theta_4 + \alpha_r) & 0 & -DD\ 4 \\ 0 & 0 & 0 & 1 \end{bmatrix}
 \end{aligned} \tag{23}$$

$$\begin{aligned}
 {}^5_rT = {}^0_rT {}^5_0T &= \begin{bmatrix} 1 & 0 & 0 & x_a \\ 0 & 0 & 1 & 0 \\ 0 & -1 & 0 & 0 \\ 0 & 0 & 0 & 1 \end{bmatrix} \begin{bmatrix} \cos\theta_a & -\sin\theta_a & 0 & DD\ 3 \\ \sin\theta_a & \cos\theta_a & 0 & DD\ 4 \\ 0 & 0 & -1 & l_3 \\ 0 & 0 & 0 & 1 \end{bmatrix} \\
 &= \begin{bmatrix} \cos\theta_a & -\sin\theta_a & 0 & x_a + DD\ 3 \\ 0 & 0 & -1 & l_3 \\ -\sin\theta_a & -\cos\theta_a & 0 & -DD\ 4 \\ 0 & 0 & 0 & 1 \end{bmatrix}
 \end{aligned} \tag{24}$$

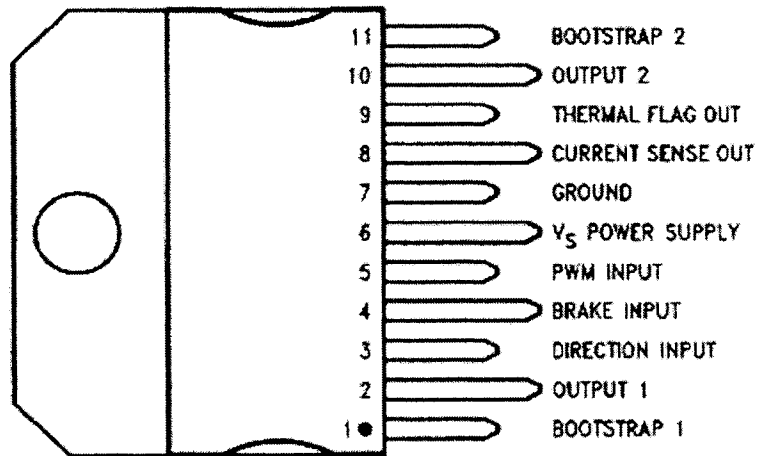
$$\begin{aligned}
 {}^6_rT=0_rT_0^6T &= \begin{bmatrix} 1 & 0 & 0 & x_a \\ 0 & 0 & 1 & 0 \\ 0 & -1 & 0 & 0 \\ 0 & 0 & 0 & 1 \end{bmatrix} \begin{bmatrix} \cos\theta_a & -\sin\theta_a & 0 & DD5 \\ \sin\theta_a & \cos\theta_a & 0 & DD6 \\ 0 & 0 & -1 & l_3 \\ 0 & 0 & 0 & 1 \end{bmatrix} \\
 &= \begin{bmatrix} \cos\theta_a & -\sin\theta_a & 0 & x_a + DD5 \\ 0 & 0 & -1 & l_3 \\ -\sin\theta_a & \cos\theta_a & 0 & -DD6 \\ 0 & 0 & 0 & 1 \end{bmatrix}
 \end{aligned} \tag{25}$$

$$\begin{aligned}
 {}^7_rT=0_rT_0^7T &= \begin{bmatrix} 1 & 0 & 0 & x_a \\ 0 & 0 & 1 & 0 \\ 0 & -1 & 0 & 0 \\ 0 & 0 & 0 & 1 \end{bmatrix} \begin{bmatrix} \cos(\theta_a - \theta_5) & -\sin(\theta_a - \theta_5) & 0 & DD7 \\ \sin(\theta_a - \theta_5) & \cos(\theta_a - \theta_5) & 0 & DD8 \\ 0 & 0 & -1 & l_3 \\ 0 & 0 & 0 & 1 \end{bmatrix} \\
 &= \begin{bmatrix} \cos(\theta_a - \theta_5) & -\sin(\theta_a - \theta_5) & 0 & x_a + DD7 \\ 0 & 0 & -1 & l_3 \\ -\sin(\theta_a - \theta_5) & \cos(\theta_a - \theta_5) & 0 & -DD8 \\ 0 & 0 & 0 & 1 \end{bmatrix}
 \end{aligned} \tag{26}$$

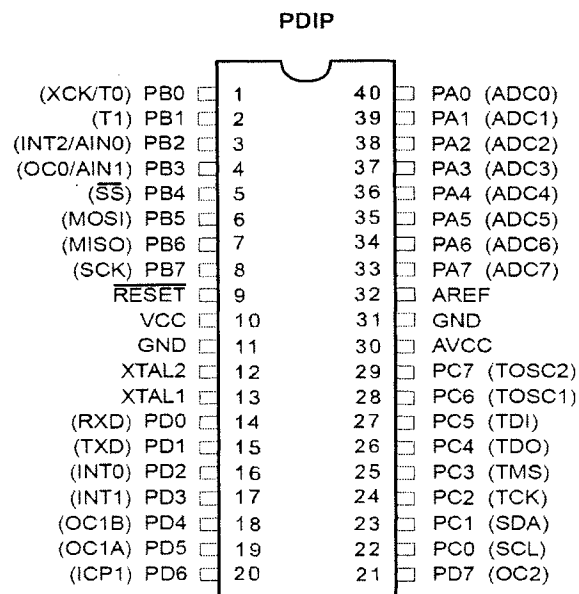
$$\begin{aligned}
 {}^8_rT=0_rT_0^8T &= \begin{bmatrix} 1 & 0 & 0 & x_a \\ 0 & 0 & 1 & 0 \\ 0 & -1 & 0 & 0 \\ 0 & 0 & 0 & 1 \end{bmatrix} \begin{bmatrix} \cos(\theta_a - \theta_5 + \theta_6) & -\sin(\theta_a - \theta_5 + \theta_6) & 0 & DD9 \\ \sin(\theta_a - \theta_5 + \theta_6) & \cos(\theta_a - \theta_5 + \theta_6) & 0 & DD10 \\ 0 & 0 & -1 & l_3 \\ 0 & 0 & 0 & 1 \end{bmatrix} \\
 &= \begin{bmatrix} \cos(\theta_a - \theta_5) & -\sin(\theta_a - \theta_5) & 0 & x_a + DD9 \\ 0 & 0 & -1 & l_3 \\ -\sin(\theta_a - \theta_5) & -\cos(\theta_a - \theta_5) & 0 & -DD10 \\ 0 & 0 & 0 & 1 \end{bmatrix}
 \end{aligned} \tag{27}$$

$$\begin{aligned}
 {}^9_rT=0_rT_0^9T &= \begin{bmatrix} 1 & 0 & 0 & x_a \\ 0 & 0 & 1 & 0 \\ 0 & -1 & 0 & 0 \\ 0 & 0 & 0 & 1 \end{bmatrix} \begin{bmatrix} \cos(\theta_a - \theta_5 + \theta_6 - \theta_7) & -\sin(\theta_a - \theta_5 + \theta_6 - \theta_7) & 0 & DD11 \\ \sin(\theta_a - \theta_5 + \theta_6 - \theta_7) & \cos(\theta_a - \theta_5 + \theta_6 - \theta_7) & 0 & DD12 \\ 0 & 0 & -1 & l_3 \\ 0 & 0 & 0 & 1 \end{bmatrix} \\
 &= \begin{bmatrix} \cos(\theta_a - \theta_5 + \theta_6 - \theta_7) & -\sin(\theta_a - \theta_5 + \theta_6 - \theta_7) & 0 & x_a + DD11 \\ 0 & 0 & -1 & l_3 \\ -\sin(\theta_a - \theta_5 + \theta_6 - \theta_7) & -\cos(\theta_a - \theta_5 + \theta_6 - \theta_7) & 0 & -DD12 \\ 0 & 0 & 0 & 1 \end{bmatrix}
 \end{aligned} \tag{28}$$

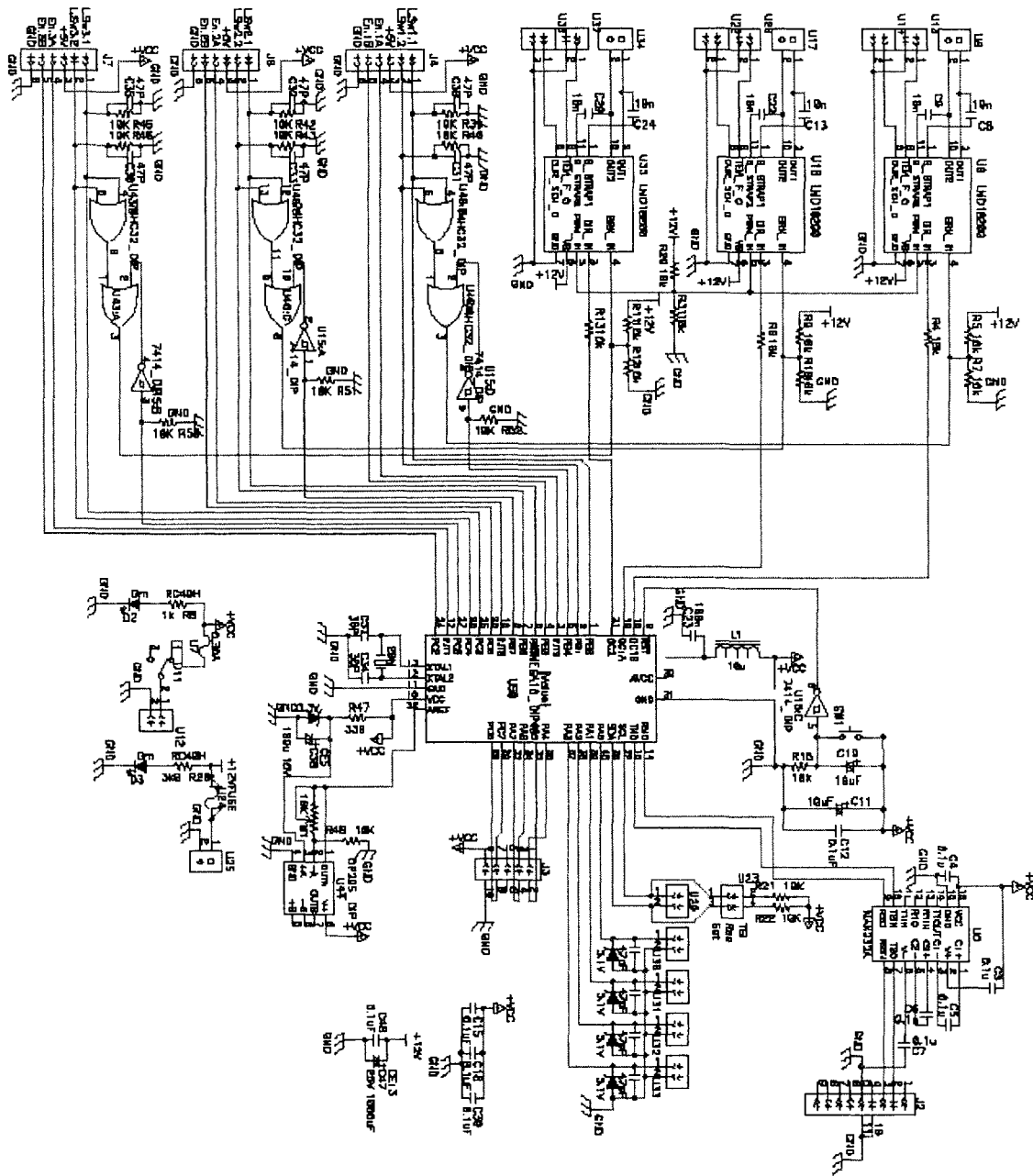
LMD 18200T H-Bridge



Atmega16



Circuit diagram:



Circuit diagram for the control system of the biped robot